HYDROCLIMATE TIME-SERIES ARCHIVED IN A 4300 YEAR OLD STALAGMITE FROM DESOTO CAVERNS (ALABAMA, USA)

by

DAVID E. ALDRIDGE

PAUL AHARON, COMMITTEE CHAIR
FRED ANDRUS
JOHN BLITZ
DELORES ROBINSON

A THESIS

Submitted in partial fulfillment of the requirements
for the degree of Master of Science in the
Department of Geological Sciences
in the Graduate School of
The University of Alabama

TUSCALOOSA, ALABAMA

2014

ABSTRACT

Recently published climate studies have implicated the Atlantic Multidecadal Oscillation (AMO) as the dominant factor modulating the precipitation in the regions adjacent to the Atlantic Ocean and the Gulf of Mexico but long range, land-based paleoclimate proxies, are notably lacking. Here I report the results of a new stalagmite- derived $\delta^{18}O$ and $\delta^{13}C$ (‰ VPDB) time series and petrographic study from DeSoto Caverns, Alabama, spanning the interval from recent to 4025 years BP. The new data document AMO as having a pervasive controlling influence on the Southeastern USA region's hydroclimate during the Late Holocene.

Ten precise $^{230}Th/^{234}U$ age determinations, from an 11.3 cm section of stalagmite, spanning the interval from 1883 to 4025 years BP, were used to construct an age model for the stable isotopes time-series containing 882 determinations. Analysis of the stalagmite's $\delta^{18}O$ time-series in the frequency domain exhibits dominant periodicities of 30.8 ± 1.4 years and 27.4 ± 0.8 years at the Chi Squared 95% confidence interval that match the instrument-derived AMO half cycle periodicity of approximately 30 years. At the Chi Squared 90% confidence interval, the stalagmite's $\delta^{18}O$ time-series frequency analysis reveal a periodicity of 58.0 ± 2.7 years, matching the instrument derived AMO full cycle of approximately 60 years.

Starting about 1883 years BP a series of anomalous black laminations appear in the stalagmite and continue, with short interruptions, until a return to normal deposition at approximately 49 years BP. Petrographic investigations reveal that the section of the stalagmite that contains the black laminations also features intense dissolutional unconformities that are

predominately composed of detrital material. Both the detrital material and dissolutional unconformities, likely resulted from intense landscape modifications by the pre-Columbian Native American and European societies inhabiting the region during the time.

DEDICATION

This thesis is dedicated to all past, present and future Leathernecks, Jarheads, Teufelshunde, to my brothers of 2nd Battalion, 8th Marines, Scout/Sniper Platoon and to all of my compatriots of unpleasant places. *Semper Fidelis*.

LIST OF ABBREVIATIONS AND SYMBOLS

C	Carbon
df	degrees of freedom
O	Oxygen
U	Uranium
DBT	depth below top of stalagmite
DSSG	DeSoto Caverns stalagmite
%	percent
‰	per mil
δ	delta notation
o	standard deviation
M	lags
*u*g	micro-gram: millionth of a gram
*u*m	micron: millionth of a meter
mm	millimeter: thousands of a meter
mL	milliliter: thousands of a liter
m	meter
ppl	plane polarized light
xpl	cross polarized light
GOM	Gulf of Mexico

AWP	Atlantic Warm Pool
AMO	Atlantic Multidecadal Oscillation
Th	Thorium
SEM	Scanning Electron Microscope
CF-IRMS	Continuous Flow – Isotope Ratio Mass Spectrometer
USA	United States of America
A.D.	Anno Domini
BP	Before present relative to 1950 A.D.
Cal.	Calendar
^{18}O	Oxygen atom with atomic mass of 18
^{13}C	Carbon with atomic mass of 13
^{234}U	Uranium atom with atomic mass of 234
^{238}U	Uranium atom with atomic mass of 238
^{230}Th	Thorium atom with atomic mass of 230
$\delta^{18}O$	Oxygen isotopic composition
$\delta^{13}C$	Carbon isotopic composition
°C	Degrees Celsius
et al.	And others (Latin: et alli)
cm	Centimeter: hundredth of a meter
Corr.	Corrected
ka	kilo-annum

km	Kilometer
l	Liter
m	Meter
n	Number of observations
U/Th	Uranium toThorium ratio
VPDB	Vienna Pee Dee Belemnite
B.C.E.	Before Common Era
MC-ICP-MS	Multicollector-Inductively Coupled Plasma Mass Spectrometer

ACKNOWLEDGEMENTS

Foremost on the long list of people whom I owe thanks is my wife, Jenny. She has supported and enriched my life since the day that we met. I owe significant gratitude to my advisor, Dr. Paul Aharon, whose spirited questions, debates and guidance spurred this research beyond a cookie-cutter thesis. Dr. Joe Lambert has always gladly dropped whatever he was doing to assist with my numerous questions and could always be counted on for valuable insight. I'd like to thank my committee for always being available and helpful. To the students whose work that I built upon, Rajesh Dhungana and Hunter Phillips, I am thankful. This research was funded by the Geological Society of America, the Gulf Coast Association of Geological Societies and numerous grants from The University of Alabama, Department of Geological Sciences and the Geological Sciences Advisory Board.

CONTENTS

LIST OF TABLES

LIST OF FIGURES

1. INTRODUCTION

1.1 SCOPE OF STUDY: LONG RANGE REGIONAL CLIMATE RECORDS

Rainfall variability is an important, yet poorly constrained factor of climate change (Schiermeier, 2010). Importantly, the season in which the dominant rainfall occurs at present and in the past, the cyclicity of hydroclimate changes and the effect of anthropogenic activities are largely unknown for the Southeastern USA. Considering the significant economic and agricultural impacts of hydroclimate variability on the agriculturally important and densely populated Southeastern USA region, long-range regional paleoclimate records are of critical importance (Pederson et al., 2012). Tree ring data available from the Southeastern USA do not cover a sufficiently long period of time to reveal long-range climatic oscillations and are biased towards spring rainfall (Stahle and Cleaveland, 1992). Additionally, Late Holocene marine-based isotope records from the Gulf of Mexico (GOM), the primary source of rainfall in the region, may not necessarily reflect the land-based hydroclimate and also suffer from a lack of sufficient length to accurately reveal long-range climate history (Lambert and Aharon, 2009; Poore, 2009).

Speleothem studies, by being free from many of the common controls on isotope fractionation, may circumvent some of the problems faced by dendrochronology and marine climate proxies by continuously incorporating the fractionated stable isotopes of oxygen and carbon derived from the bicarbonate-rich drip waters, along with radionuclides that allow precise

dating of the climate events (Lachniet, 2009; McDermott, 2004). The Atlantic Multidecadal Oscillation (AMO), a 50-70 year oscillation between the warm and cold phases of the North Atlantic SST, is recognized as controlling the hydroclimate of the entire Atlantic, Sahel and Caribbean regions (Knight et al., 2006; Knudsen et al., 2011). Unfortunately, much of the proxy data that reveal AMO cyclicities are not land-based, or do not provide a sufficiently long record to evaluate (Hetzinger et al., 2008; Oglesby et al., 2012). In contrast, during the instrumental era, the effect of AMO variability upon the Southeastern hydroclimate is well documented (Enfield et al., 2001; McCabe et al., 2008; Ortegren et al., 2011). Therefore, acquisition of the notably lacking, highly resolved, long range, land- based hydroclimate proxies is of critical importance for the planning and management of the region's water resources and for understanding how the region's hydroclimate might respond to anthropogenic activities. (Schiermeier, 2010)

1.2 LOCATION AND SUITABILITY FOR LONG-RANGE, LAND-BASED HYDROCLIMATE RECONSTRUCTIONS

DeSoto Caverns, also known as Kymulga Cave in Alabama, USA (33º 18' 26" N, 86º 16' 36" W, Fig. 1) is a ramiform and spongework cave that has been subjected to a long history of anthropogenic activities that included burials by pre-Columbian Native Americans, saltpeter mining and moon-shining and is also currently a popular tourist attraction (Palmer, 1991; Walthall, 1974). Most importantly, DeSoto Caverns' stalagmites consist of nearly monomineralic, botryoidal, primary aragonite that not only archives pristine oxygen and carbon isotopes, but also incorporates and preserves relatively high [U] concentrations in the ppm range thus affording precise $^{230}Th/^{234}U$ dating of 10-20 mg stalagmite samples.

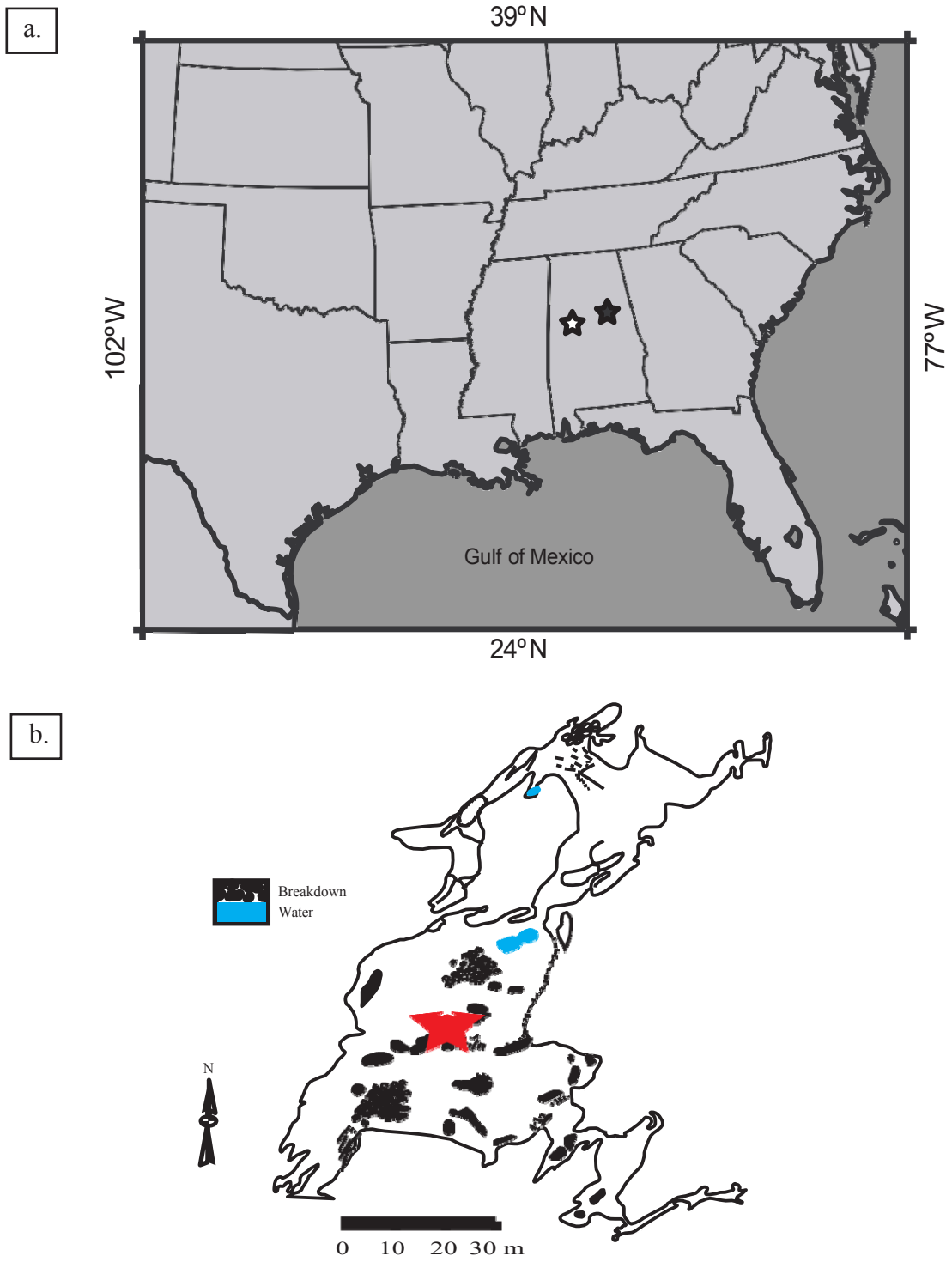

Figure 1. a. Regional map showing Tuscaloosa, AL (open star) and DeSoto Caverns (closed star) b. Plan view map of DeSoto Caverns showing location of DeSoto Caverns Stalagmite # 4 (a. and b. are modified from Lambert and Aharon, 2009, 2011).

According to past and ongoing studies conducted at The University of Alabama, interannual rainfall variability, CO_2 degassing and rainfall seasonality are the primary controls of the O and C isotopes contained in DeSoto Caverns' speleothems (Lambert and Aharon, 2009, 2010). Importantly, Lambert's and Aharon's (2009) study revealed that ^{18}O-enrichments in DeSoto Caverns' stalagmites can be reliably attributed to drought and ^{18}O-depletions can be attributed to an increase in regional inter-annual rainfall (Lambert and Aharon, 2009). Unlike ^{18}O, the ^{13}C values contained in DeSoto Caverns' stalagmites do not reflect the regional inter-annual rainfall, nor do they reflect the changes in vegetation above the cave (Lambert and Aharon, 2010). Rather, the ^{13}C values reflect the intensity of cave air ventilation and CO_2 flux during the time of carbonate deposition, which both in turn reflect the dominating season of stalagmite accretion (Lambert and Aharon, 2010).

Additionally, Lambert's and Aharon's (2009) study reveals that DeSoto Caverns' 10 - 30 meter Upper Ordovician age dolomitic karst over-burden effectively dampens short- lived events, such as storms, ensuring that speleothems prized from DeSoto Caverns faithfully record long-term changes in the region's hydroclimate. Since the overwhelming majority of the moisture that reaches DeSoto Caverns is sourced in the GOM, the stalagmites there are likely to contain reliable inter-annual records of rainfall variability in a land-based setting from largely a single source (GOM).

In addition to O and C isotopes, speleothems incorporate detrital material such as clays, mites, pollen and carbon soot that may also be used to supplement paleoclimate interpretations and to reveal human activities inside and above the cave (Gradziński et al., 2007; Polyak et al., 2001; McGarry and Caseldine, 2004).

1.3 TESTING LINKS BETWEEN CLIMATE CHANGE AND SOCIETY

Although it is known from studies conducted at The University of Alabama that the $\delta^{18}O$ of drip waters that feed DeSoto Caverns' stalagmites reliably reflect the amount of rainfall that the region experiences, the long-range climate mechanisms that influence the region's rainfall amount are not well defined (Lambert and Aharon 2009). Therefore, the primary goal of this study is to obtain and analyze the $\delta^{18}O$ and $\delta^{13}C$ from a Desoto Caverns stalagmite for the purpose of unraveling the long-range hydroclimate mechanisms that govern the amount of rainfall that the region experiences.

Stalagmite #4 (DSSG-4 heretofore), was cored at DeSoto Caverns in 2008 using an electrically-powered drill assemblage. The stalagmite features anomalous black laminations that become dominant approximately 36.8 mm below the top of the stalagmite (Fig. 2). DeSoto Caverns was used as a burial site by pre-Columbian Native Americans known as the Copena, approximately 1950 to 1450 years BP, which coincides with the initiation of limited agriculture in North America during the Woodland Period (Smith, 1989). The black laminations may result from several competing causes (Peacock, et al, 2004; Smith, 1989; Walthall, 1999) such as (i) clay and other detrital material flushed in the cave by drip waters; (ii) carbon soot entrained in the drip waters from natural or anthropogenic forest fires, and/or (iii) carbon film deposited from the smoke produced by the fires/torches used by the cave's prehistoric visitors/inhabitants.

The distinctions among the three competing causes have important paleoclimate and paleoecological implications. For example, (i) has paleoclimate implications suggesting that detrital material was flushed into the cave, possibly because of unusually high rainfall/flooding events whereas (ii) will be compatible with routine forest fires, likely started by the pre-

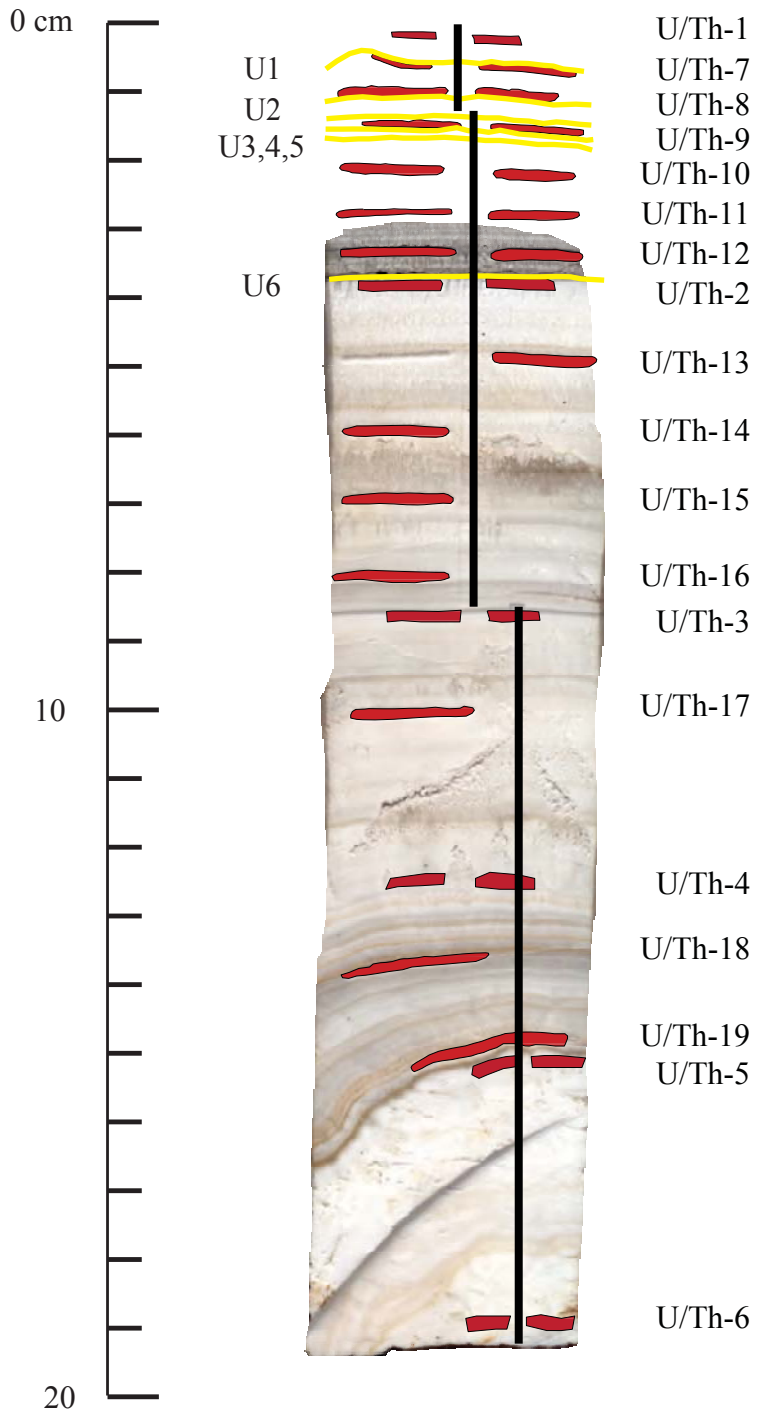

Figure 2. Cored stalagmite DSSG-4. Age date locations are shown in red and samples ID are listed on the right side of the stalagmite section. Micromilling profile is indicated by thick black line. Unconformity locations, revealed by petrographic observations, are indicated by yellow lines and numbered on the left side of the section.

Columbian Native American inhabitants of the region at the time (Delcourt and Delcourt, 1997). A carbon film (iii) will relate to habitation or utilization of the cave by various groups as diverse as Native Americans, saltpeter miners during the Civil War era and moon-shiners during the era of prohibition.

2. METHODS

2.1 MICRO-MILLING AND STABLE ISOTOPES

For the purpose of stable oxygen and carbon isotope analysis, samples between 40 and 90 *u*g in weight were micro-milled from stalagmite DSSG-4 at an interval of 100 *u*m for the first 100 mm below stalagmite top (191.8 mm total stalagmite length). The sampling interval was increased for the bottom 91.8 mm of the stalagmite to an interval of 200 *u*m. The tight sampling intervals were chosen to ensure that a continuous record of the $\delta^{18}O$ and $\delta^{13}C$ for the last 4300 years would be acquired for this study thus mitigating the possibility that changes in the stalagmite's growth rate could adversely affect the fidelity and veracity of the isotope time-series.

The predominantly aragonite samples were dissolved in orthophosphoric acid to obtain CO_2 gas for $\delta^{18}O$ and $\delta^{13}C$ determinations from a Finnigan Delta Plus CF- IRMS equipped with a CTC Analytics Autosampler. A precision, accuracy and reproducibility of ± 0.1‰ was established on the basis of multiple NBS-19 standard repeats. Additionally, any correction that was applied to the NBS-19 standards in order to adjust deviation from the accepted NBS-19 standard values of -2.20 ‰ and 1.95‰ for $\delta^{18}O$ and $\delta^{13}C$, respectively, was also applied to the $\delta^{18}O$ and $\delta^{13}C$ stalagmite-sourced sample results, reported in Appendix 1. Furthermore, to ensure high fidelity isotope results, the top 4.5 mm of the stalagmite was re-sampled and re-analyzed to test the reproducibility of the isotope sampling technique, reported in Appendix 2.

The $\delta^{18}O$ results obtained from aragonite samples were corrected by -0.34 (‰ VPDB) in order to account for the difference in kinetic fractionation between aragonite and the NBS-19 calcite standard at the reaction temperature of 50º C (Appendix 1) (Kim et al., 2007). Additionally, the results of an investigation of equilibrium isotope fractionation conducted at The University of Alabama by Hunter Phillips (2011) revealed that a necessary correction of 0.6 and 2.0 (‰ VPDB) should be applied to the $\delta^{18}O$ and $\delta^{13}C$ results, respectively, obtained from any neomorphic columnar calcite found in DSSG-4 (Appendix 1) (Phillips, 2011).

2.2 DISSOLUTION OF STALAGMITE

In order to investigate the nature of the black laminations prominent in DSSG-4, ten 0.21 to 0.33 gram samples were cut from the dark laminated section that begins 36.8 mm below the top of the stalagmite (Fig. 2). One 0.60 gram sample was cut from a non-laminated section approximately 48 mm below the top of the stalagmite. The samples were then placed in a 150 mL beaker to which 25 mL of room temperature 5% HCl was added. Microscope slides were used in order to enable inspection of any liberated detrital material that adhered to the slides. The samples were allowed to react with the acid until visually completely dissolved, requiring approximately 5 minutes. The acid containing the sample was then immediately filtered through a 24mm Whatman GF/C borosilicate microfiber filter that was attached to two Erlenmeyer flasks hooked in series to a vacuum outlet. Once the entire sample was filtered, the samples and filtering apparatus were flushed with DI water. The filtering apparatus was thoroughly washed between samples.

2.3 IMAGING OF STALAGMITE COMPONENTS

Samples from the laminated section of DSSG-4 were cut, washed in cold 5% HCl for 30 seconds and then immediately washed in DI water in order to identify the nature and origin of DSSG-4's black laminations and to investigate morphology and mineralogy changes. Upon drying, the samples were gold coated and inspected with a Phillips XL30 scanning electron microscope. A Nikon Eclipse LV100 polarizing microscope was used to inspect three 5 cm by 7.5 cm thin sections obtained from DSSG-4, as well as the 24mm Whatman GF/C borosilicate microfiber filters. The thin sections obtained from DSSG-4 enabled the entire stalagmite core to be investigated, excluding the sawing marks between the thin section locations and the top 6 mm section of DSSG-4 that was lost during thin section acquisition.

2.4 AGE DATING

Nineteen 10-20 mg samples were drilled for high precision MC-ICP-MS $^{230}Th/^{234}U$ age dating. All samples met the selection criteria of visual absence of secondary calcite and that growth laminations were thick enough to reliably ensure single growth lamination sampling. Additionally, the age dating samples were removed as close to the central axis of the stalagmite as possible and in a manner that would not interfere with obtaining a continuous isotopic profile along the central growth axis (Fig. 2). Detailed description of the U-series dating techniques used in this study can be found in Hellstrom (2003, 2006).

3. RESULTS

3.1 IMAGING RESULTS

Petrographic investigations reveal that the most prominent black laminations correspond to six unconformities, located 5.5 mm, 10.1 mm, 13.3 mm, 15.6 mm, 17.2 mm and 36.8 mm below the top of the stalagmite (Figure 3a-b) that are predominately composed of detrital material. The unconformable sequences typically begin with a rind of irregularly dissolved and truncated botryoidal aragonite bundles that are partially transformed into calcite. Upon this surface is the detritus-stained physical unconformity featuring differential dissolution, followed by comparatively short and wide competitively growing aragonite botryoides that have a mean length of 513 ± 18 *u*m and a mean width of 253 ± 14 *u*m, as shown in Figure 4a. The morphology of the competitively growing aragonite bundles indicates nucleation and growth of new aragonitic botryoides after a return to equilibrium conditions (Turgeon and Lundberg, 2001). Following a complete return to normal depositional conditions, the aragonite botryoids resume the tall and narrow morphology common in the areas of DSSG-4 not adjacent to unconformities, as is seen in the section of DSSG-4 between unconformities #5 and #6, 17.2 mm and 36.8 mm DBT, respectively (Fig 6a-b). Figure 5 illustrates how the morphology associated with dissolution unconformities develops. The process begins with normal stalagmite deposition of comparatively tall and narrow aragonitic botryoids that result from a slow and steady drip-rate with no detrital input (Fig. 5a). The in-situ detrital material discovered in areas of DSSG-4 that

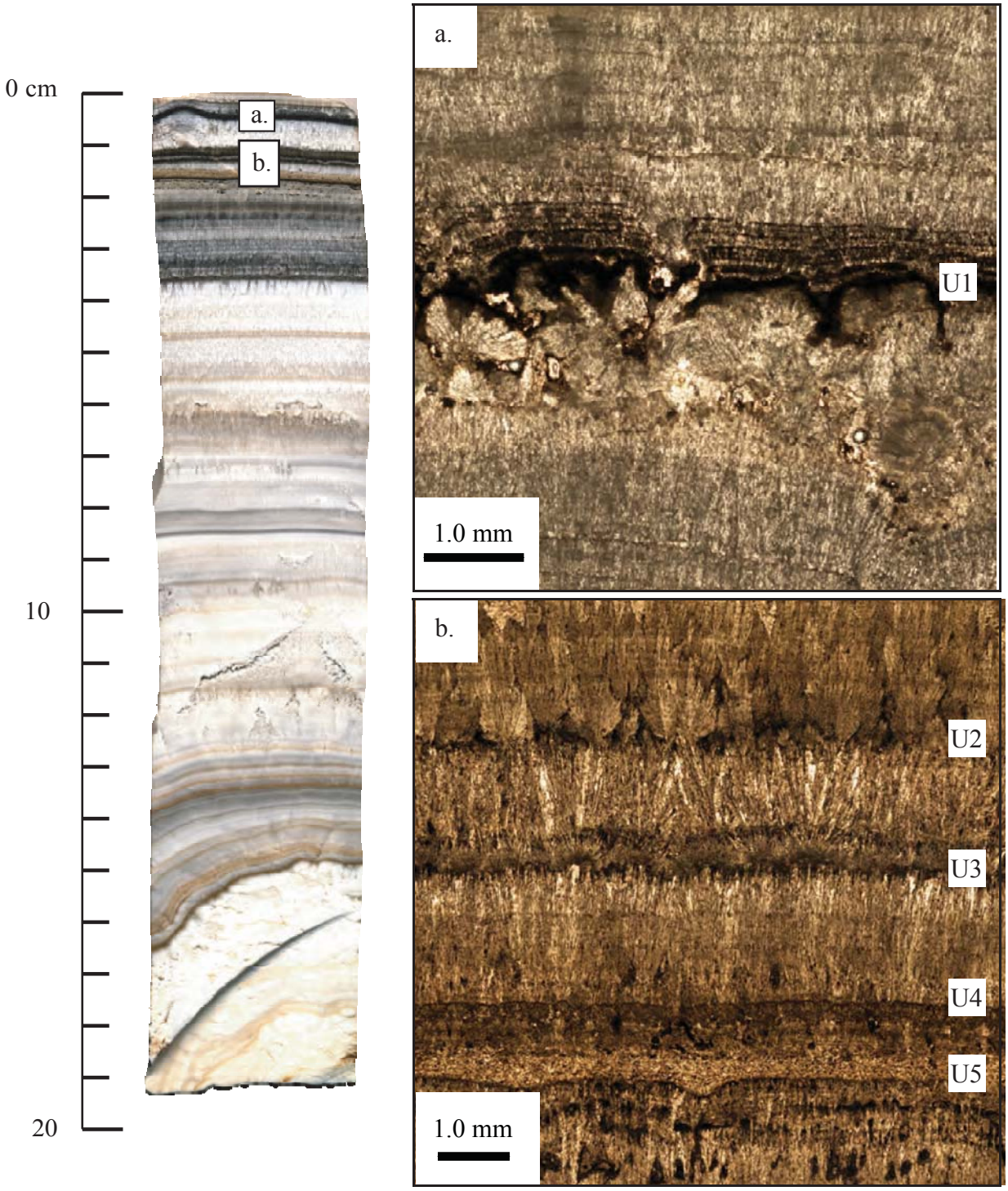

Figure 3. Unconformities 1 through 5. (a) Unconformity 1. Image taken from coeval stalagmite DSSG-5. (b) Unconformities 2 through 5, position indicated by "U" followed by unconformity number. Images from both (a) and (b) are PPL transmitted light.

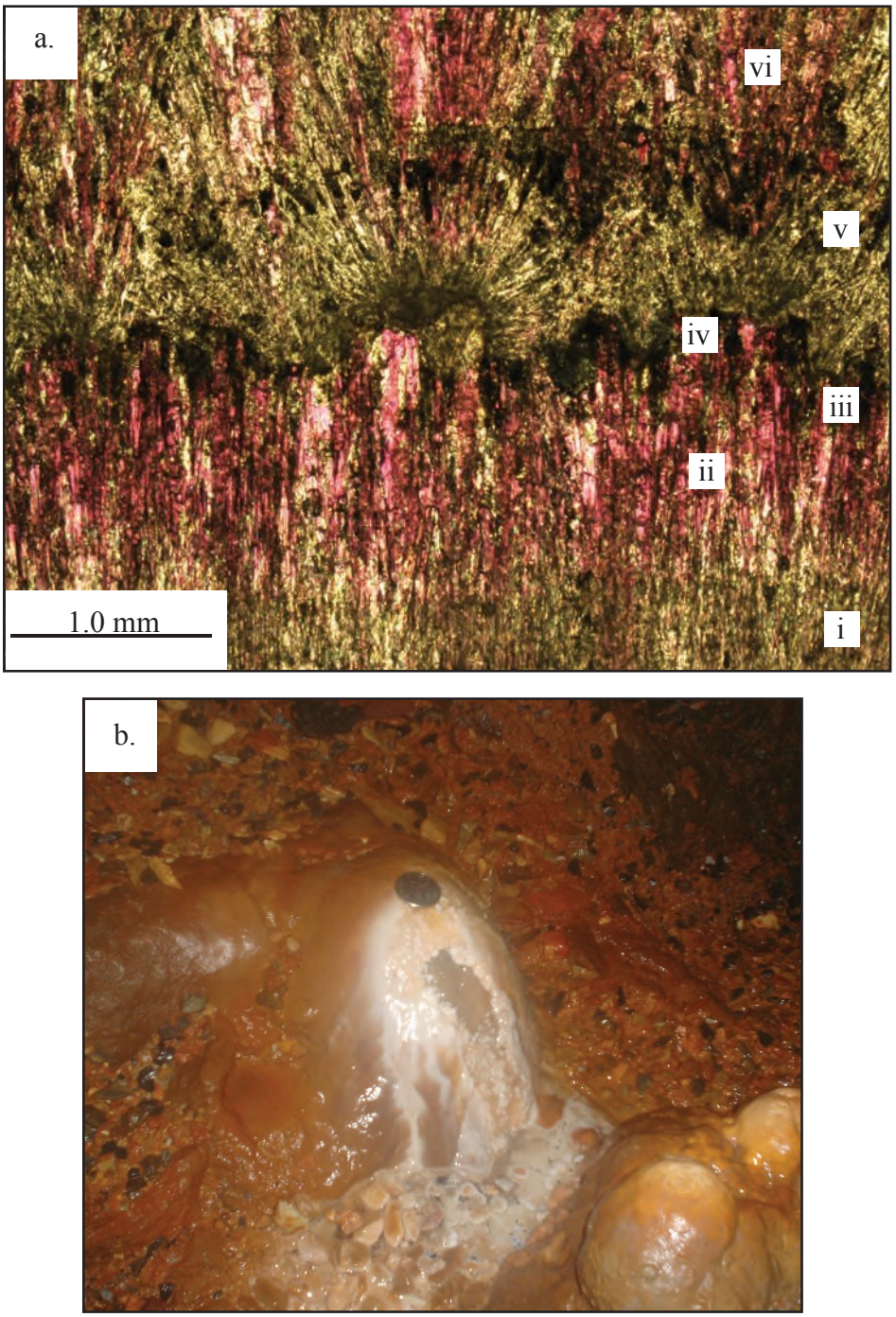

Figure 4. Detail of unconformity #3. (a) An XPL transmitted light, with gypsum wedge showing a sequence of a dissolution likely caused by an increased drip rate and followed by deposition: (i) Normal aragonite deposition. (ii) Aragonite partially transformed to calcite. (iii) Irregular dissolution. (iv) Detrital lag deposit. (v) Unconstrained aragonite nucleation and growth. (vi) Return to normal deposition. (b) A DeSoto Caverns stalagmite whose top is being eroded by an increased drip rate.

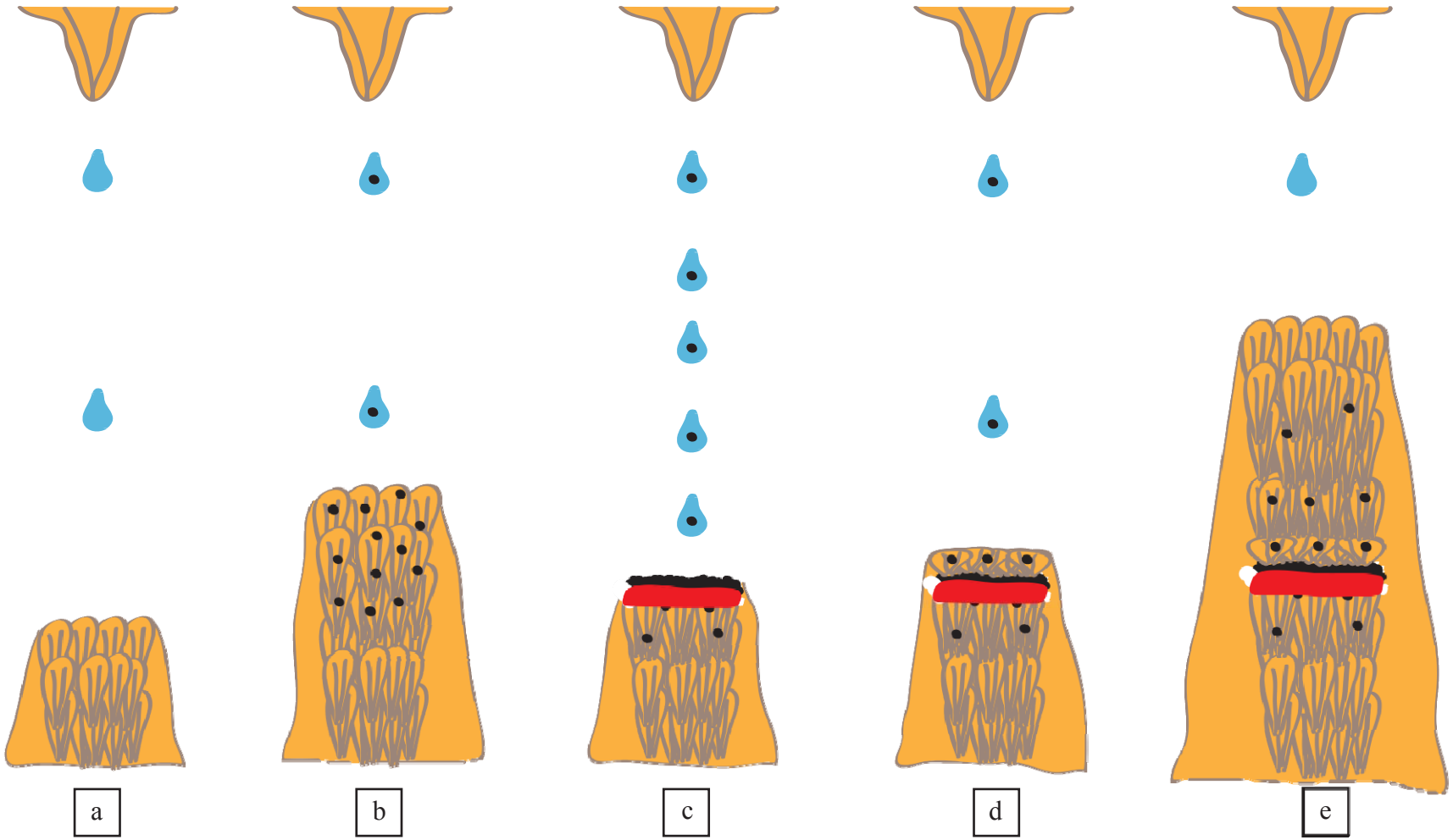

Figure 5. Sequence of events creating an unconformable interval in DSSG-4. (a) Step 1, normal deposition with no detrital input. (b) Step 2, deposition with detrital input creating in-situ detritus. (c) Step 3, increase in drip rate and detrital input creating dissolution of stalgmite and collection of detrital material along the unconformity along with an interval of partial aragonite to calcite transformation. (d) Step 4, growth of unconstrained aragonite botryoids resulting in a short and wide morphology. (e) Step 5, gradual resumption of normal stalagmite deposition and morphology.

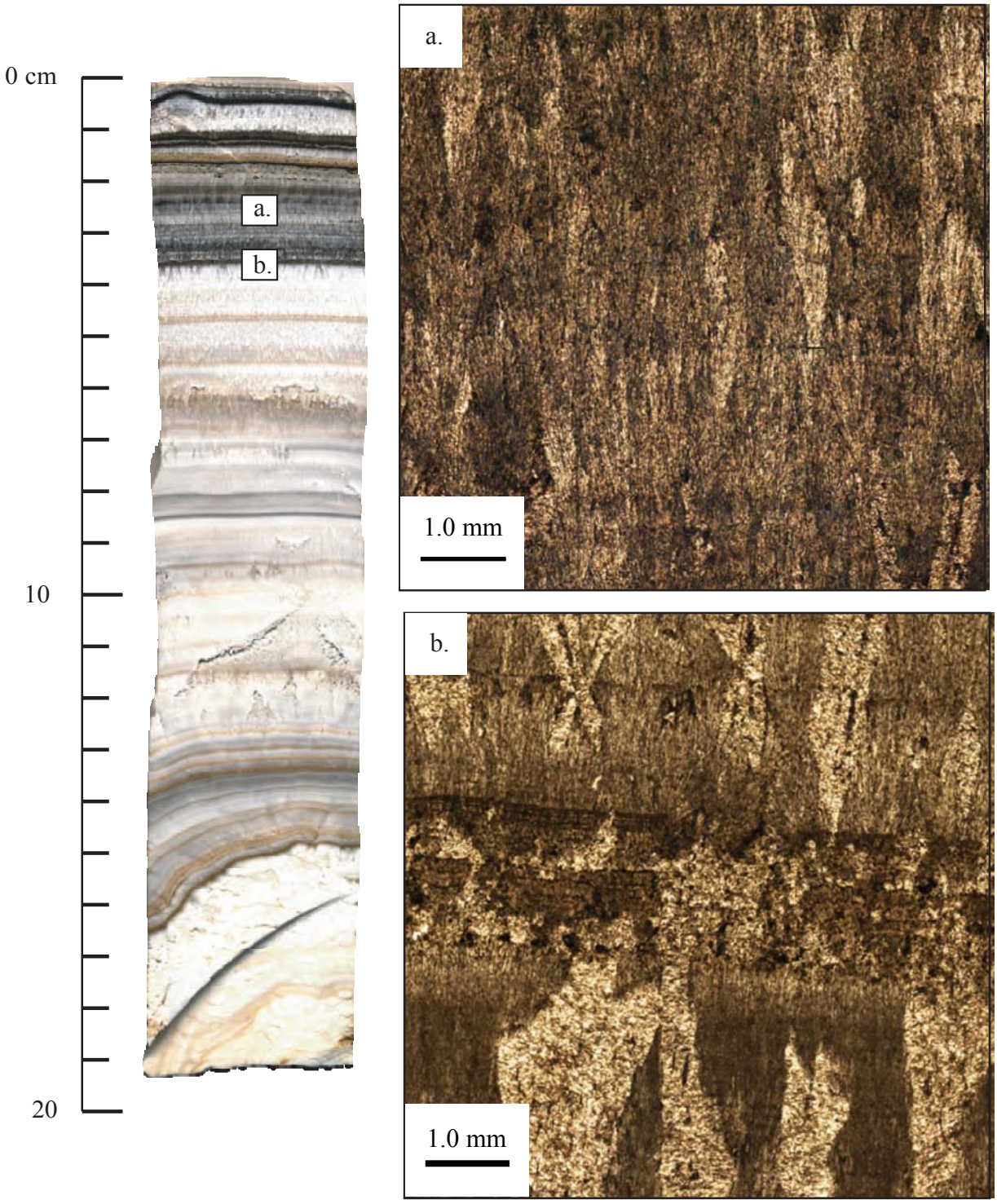

Figure 6. Tall and narrow aragonite botryoids located between unconformity 5 and 6 (a). Unconformity 6 (b). Images from both (a) and (b) are PPL transmitted light.

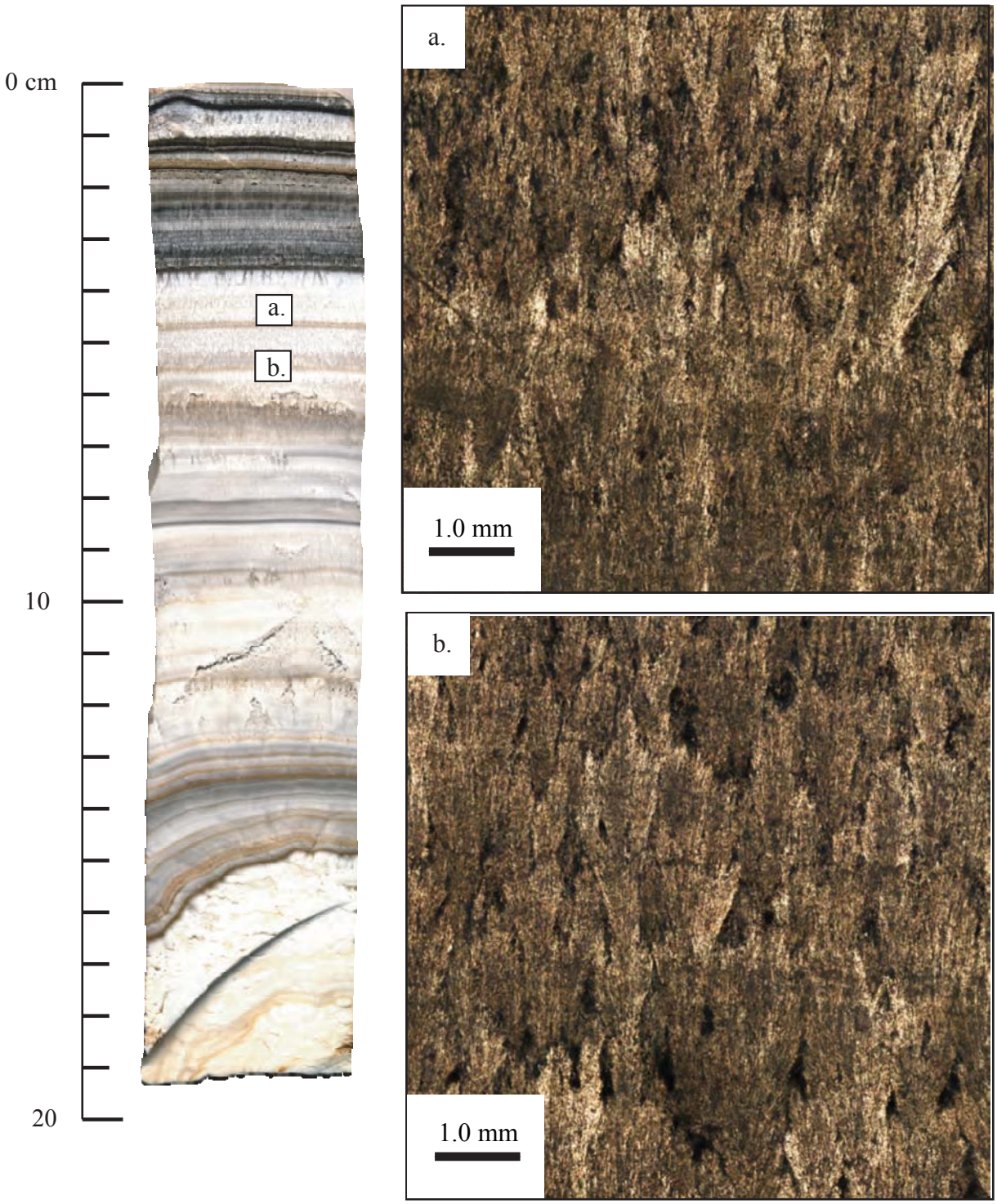

Figure 7. Tall and narrow aragonite botryoids indicative of slow and steady stalagmite growth. Images from both (a) and (b) are PPl transmitted light.

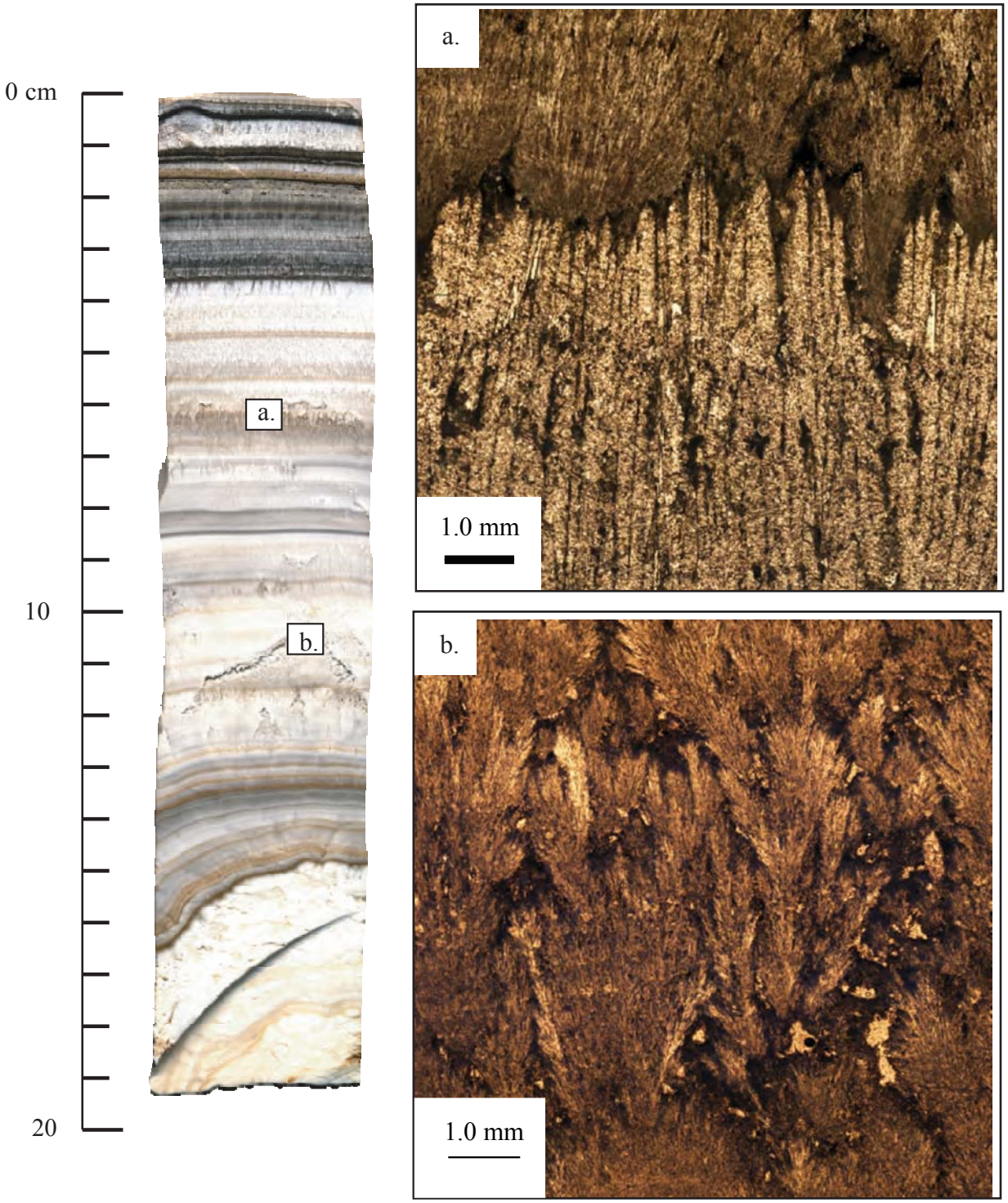

Figure 8. Neomorphic columnar calcite (a). Aragonite botryoids (b). Images from both (a) and (b) are PPL transmitted light.

feature the tall and narrow aragonite botryoidal morphology also result from a slow and steady drip-rate, except that the drip water contains detrital material (Fig. 5b). Upon an increase in drip-rate, the aragonite is eroded and a lag deposit of detrital material collects upon the unconformity (Fig. 5c). When the drip rate slows, new nucleation of aragonitic material begins, except that the aragonite botryoids are not constrained, and feature a comparatively short and wide morphology (Fig. 5d). The final step is the gradual resumption of normal stalagmite deposition and morphology (Fig. 5e).

Below unconformity #6, DSSG-4 features no evidence of unconformities, suggesting that this section of the stalagmite is appropriate for paleoclimate reconstruction, as shown in Figure 7. Except for a region of neomorphic columnar calcite (Fig 8a) located between 62.5 mm and 69.7 mm DBT, the entire section of DSSG-4 from 36.8 mm to 150.0 mm DBT features conformable aragonite botryoids and laminations (Figs. 7a-b, 8b and 9a). Below 150.0 mm to the end of the cored stalagmite at 191.8 mm DBT is the section of the stalagmite core that is interpreted as the flowstone upon which DSSG-4 grew, as shown in Figure 9b.

3.2 DISSOLUTION RESULTS

Two grains of *Pinus* (pine) and 10 grains of *Poaceae* (grass) pollen, ash consistent with ash from *Arundinaria* (common cane) and from unknown species and soil detritus were documented among the insolubles contained in DSSG-4's black laminated sections (Figure 10a-f). None of the pollen or ash appears to have experienced significant weathering, and no detrital soil components were observed inside the cellular structure of the in-situ ashes. However, the overwhelming majority of the detrital material cannot be identified as ash or pollen, and

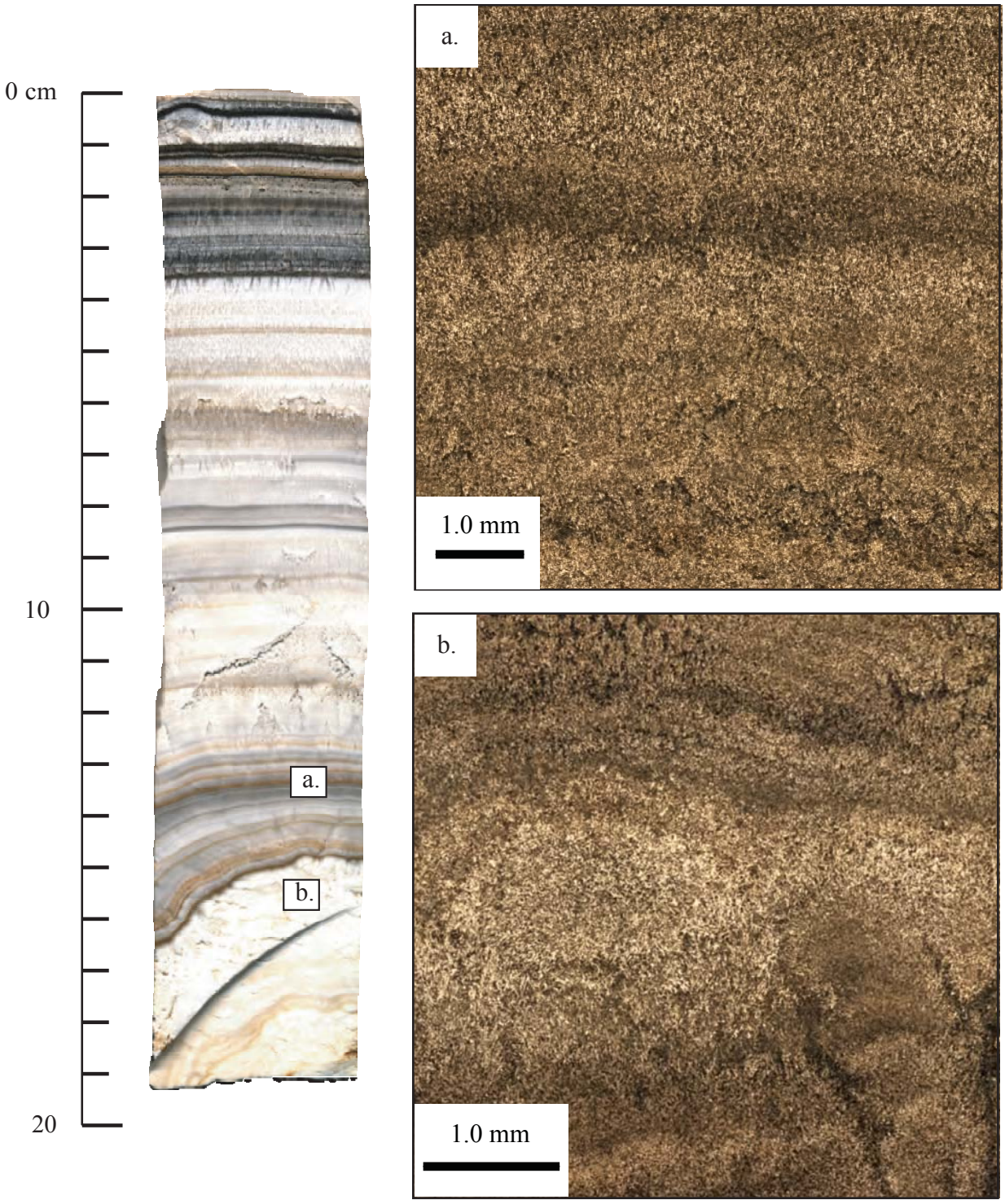

Figure 9. Aragonite laminations that grew quickly, approximately 0.08 mm per year (a). The flowstone upon which DSSG-4 grew (b). Images from both (a) and (b) are PPL transmitted light.

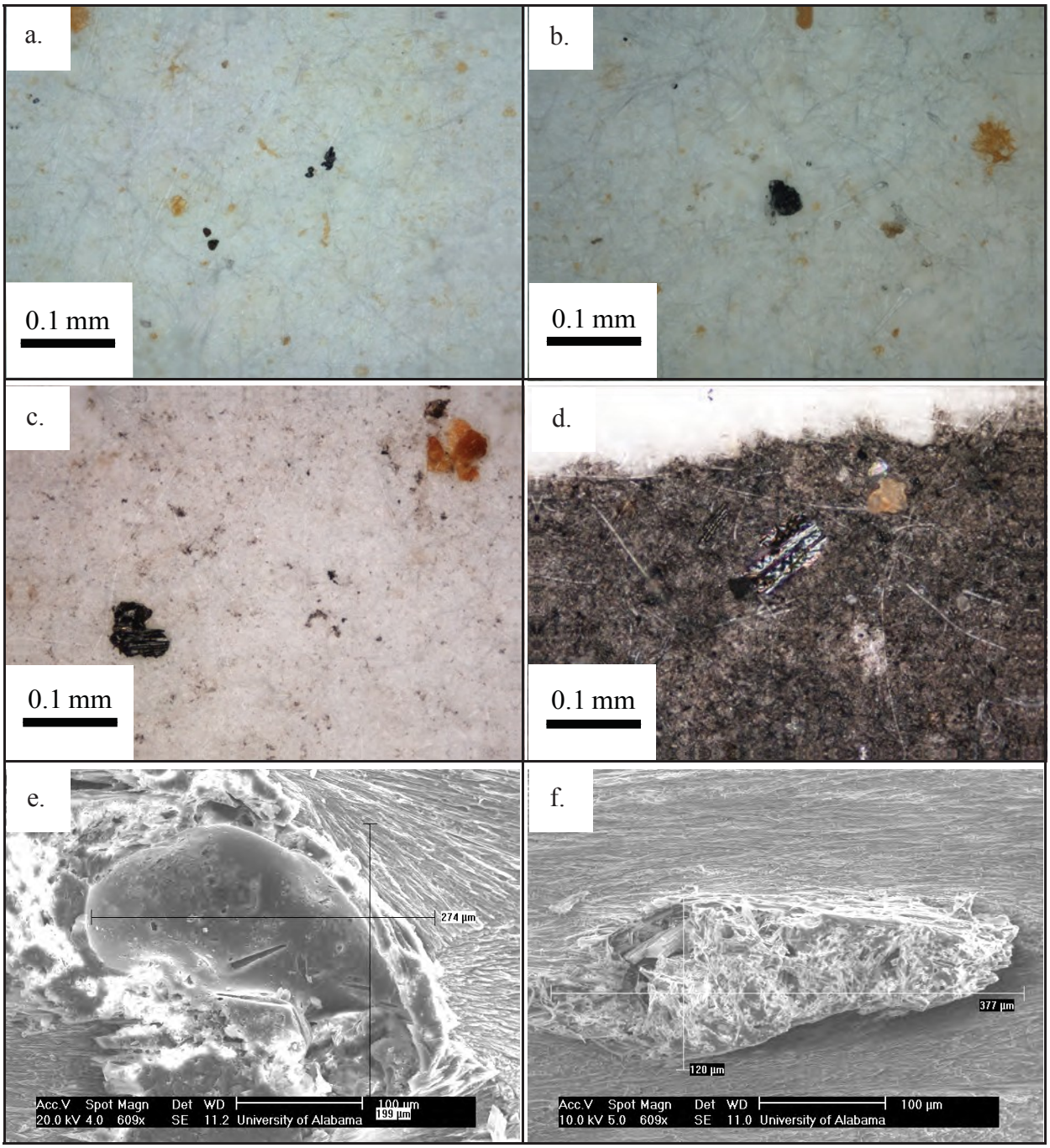

Figure 10. Detrital material collected from a DeSoto Caverns stalagmite and drip. Unknown detrital material and soil collected from an erosive drip in DeSoto Caverns (a and b). Ash, soil and unknown detrital material retained after carbonate removal from DSSG-4 (c and d). In situ unknown detrital material and ash in DSSG-4 (e and f). Images (a), (b), (c), and (d) are PPL reflected light. Images (e) and (f) are scanning electron micrographs.

Table 3.3 U-series data and calculated ages for speleothem DSSG-4 from DeSoto Caverns

Sample Number	Year meas	depth (mm)	U (ppm)	$^{234}U/^{238}U$ activity	$^{234}U/^{238}U$ activity (i)	$^{230}Th/^{238}U$ activity	Uncorrected age	$^{230}Th/^{232}Th$ Activity	U/Th (cal yrs)	Cal yrs BP	U/Th ± 2σ
U/Th-1	2008	2.2	3.2	0.0013	1.6543	0.0013	86	1.2	40	-18	29
U/Th-7	2010	6.4	2.4	0.0031	1.7277	0.0031	198	26.6	191	131	13
U/Th-8	2010	9.9	3.7	0.0039	1.7040	0.0039	250	17.9	241	181	14
U/Th-9	2010	14.8	2.5	0.0153	1.6775	0.0153	1000	134.2	996	936	20
U/Th-10	2010	21.4	1.0	0.0240	1.6437	0.0240	1600	95.9	1597	1537	41
U/Th-11	2010	27.6	0.5	0.0266	1.6296	0.0266	1792	44.8	1773	1713	37
U/Th-12	2010	33.2	3.4	0.0277	1.6352	0.0277	1861	74.1	1851	1791	28
U/Th-2	2008	37.8	2.3	0.0296	1.6198	0.0296	2010	26.6	1960	1902	46
U/Th-13	2010	48.4	1.4	0.0334	1.6318	0.0334	2254	314.8	2257	2197	48
U/Th-14	2010	59.3	1.1	0.0364	1.6295	0.0364	2457	27.0	2413	2353	68
U/Th-15	2010	69.3	2.9	0.0387	1.6122	0.0387	2650	517.8	2654	2594	42
U/Th-16	2010	80.6	3.0	0.0412	1.6424	0.0412	2769	538.4	2775	2715	55
U/Th-3	2008	86.2	3.6	0.0447	1.6460	0.0447	2999	792.4	2997	2939	35
U/Th-17	2010	100.4	2.7	0.0482	1.6417	0.0482	3247	133.5	3245	3185	56
U/Th-4	2008	124.8	1.4	0.0534	1.6748	0.0534	3528	455.6	3526	3468	68
U/Th-18	2010	136.5	0.7	0.0594	1.6913	0.0594	3894	53.1	3867	3807	123
U/Th-19	2010	148.1	0.9	0.0625	1.6999	0.0625	4086	28.1	4006	3946	92
U/Th-5	2008	151.8	1.1	0.0625	1.6662	0.0625	4169	485.4	4162	4104	48
U/Th-6	2008	189.2	0.8	0.0658	1.7190	0.0658	4258	408.4	4256	4198	87

resembles the soil particles that were obtained by filtering drip-water from an aggressively dripping location in DeSoto Caverns (Fig 8a-b). Importantly, no insolubles were documented in the dissolved sections of DSSG-4 where black laminations are absent and upon which stable isotope analysis was conducted (186.3 mm to 150.0 mm DBT).

3.3 AGE DATING AND AGE MODEL CONSTRUCTION

The nineteen MC-ICP-MS $^{230}Th/^{234}U$ age dates exhibit no reversals, or out of range age date determinations. The results of the $^{230}Th/^{234}U$ age determinations are listed in Table 3.3 along with the ages in cal years BP.

Although creation of an age model for the top 36.8 mm of DSSG-4 is complicated, the section of DSSG-4 below 36.8 mm and extending to 150.0 mm DBT is ideal for age model construction. For this persistent and conformable section that includes 10 $^{230}Th/^{234}U$ age dates (1883 to 4025 years BP), DSSG-4 maintains a mean growth rate of 0.06 ± 0.02 mm per year, yielding a mean of 2.43 ± 1.76 years between samples for this entire 113.2 mm section (36.8 mm to 150.0 mm DBT), as shown in Figure 11.

Unlike the section of DSSG-4 that is mineralogically ideal for paleoclimate reconstruction, and features a persistent growth rate (36.8 mm to 150.0 mm DBT), the exact growth rates of DSSG-4 in the areas bounding unconformities #1 to #6 cannot be established with certainty. The simplest approach to estimating the timing and duration of the unconformities followed here is to assume a mean growth rate of the stalagmite between the unconformities and apply it to the age model for each unconformable section. Starting at the DBT of the lower bracketing $^{230}Th/^{234}U$ age date, the estimated growth rate was applied upward in time to the DBT

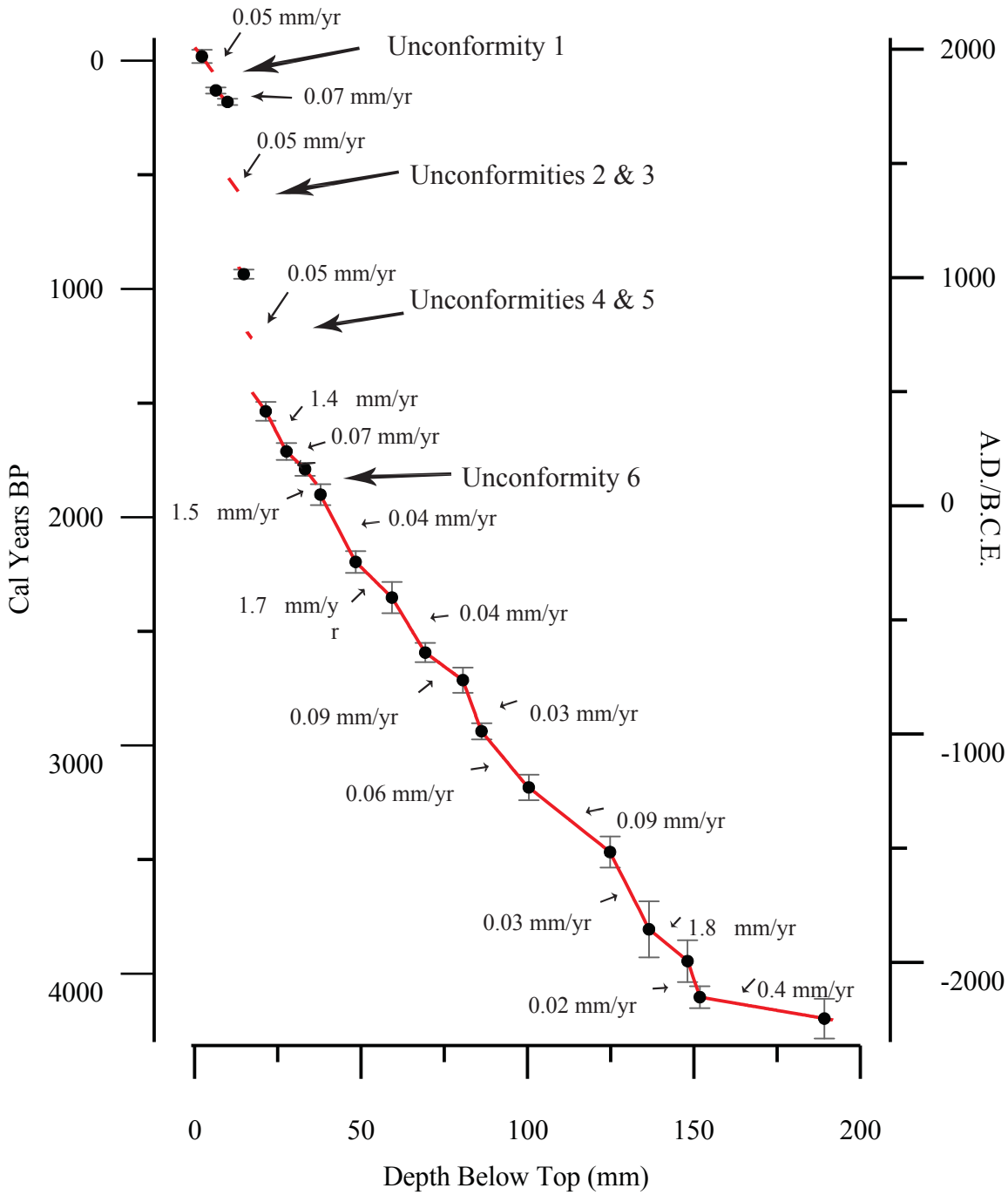

Figure 11. DSSG-4 age model. Depth below top of DSSG-4 (DBT) versus age in cal years BP and A.D./B.C.E. $^{230}Th/^{234}U$ age dates are shown with 2 σ error. Unconformities are shown as discontinuous intervals and annotated. Growth rates are shown in millimeters per year.

of the unconformity, followed by applying the same methodology from the DBT of the top bracketing $^{230}Th/^{234}U$ age date down to the DBT of the unconformity (Fig. 11). By this method of applying the bracketing growth rates to an unconformable section, an estimate of the timing and duration of unconformities #1 and #6 can be obtained. However, when more than one unconformity is located in an area between two $^{230}Th/^{234}U$ age date locations, as is the case with unconformities #2 and #3 (181 to 936 years BP) and unconformities #4 and #5 (936 to 1537 years BP), it is only possible to estimate the total duration of the combined unconformities. Thus, the duration of each unconformity in these sections was divided equally between the unconformities because assessing the amount of time between the unconformities is not possible.

Additionally, since it is unknown if each dissolution event removed evidence of earlier unconformities, the total amount of missing time from these sections may be erroneous. Therefore, stable isotope analysis can only be conducted on the section of DSSG-4 that is contiguous and features a persistent growth rate (186.3 mm to 150.0 mm DBT).

3.4 STABLE ISOTOPE RESULTS

The top 4.5 mm of DSSG-4 that was re-sampled and re-analyzed to test the reproducibility of the isotope sampling technique produced no methodological or instrumentation-induced variability between the original and re-micromilled ^{18}O and ^{13}C samples (Appendix 2), beyond what could be expected from the natural variation produced by two adjacent sampling profiles. A cross- plot and linear plot of the $\delta^{18}O$ (‰ VPDB) from both the original and re-micromilled interval yields an r-squared of 0.81 and good agreement between the original and re-micromilled samples versus DBT, as shown in Figure 12a-b. The cross-plot of the $\delta^{13}C$ (‰ VPDB) yields and

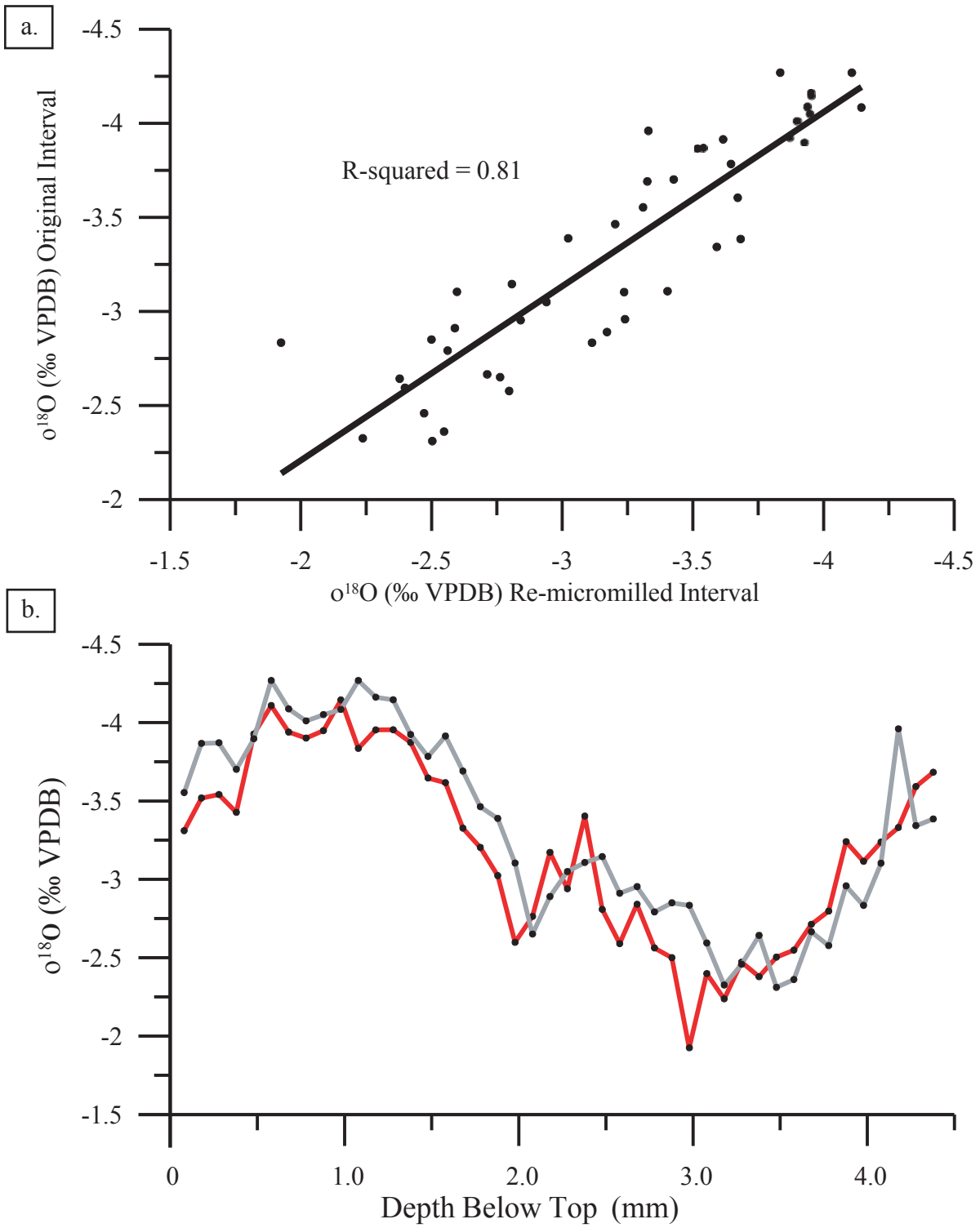

Figure 12. Cross plot (a) and linear plot (b) of the o^{18}O (‰ VPDB) obtained from the first 45 samples of DSSG-4 (100 *u*m sampling interval). R-squared of the cross plot is 0.81 (a). The gray line with black symbols represents the original samples and the red line with black dots is the re-micromilled samples (b). Samples from both sampling passes share the same DBT.

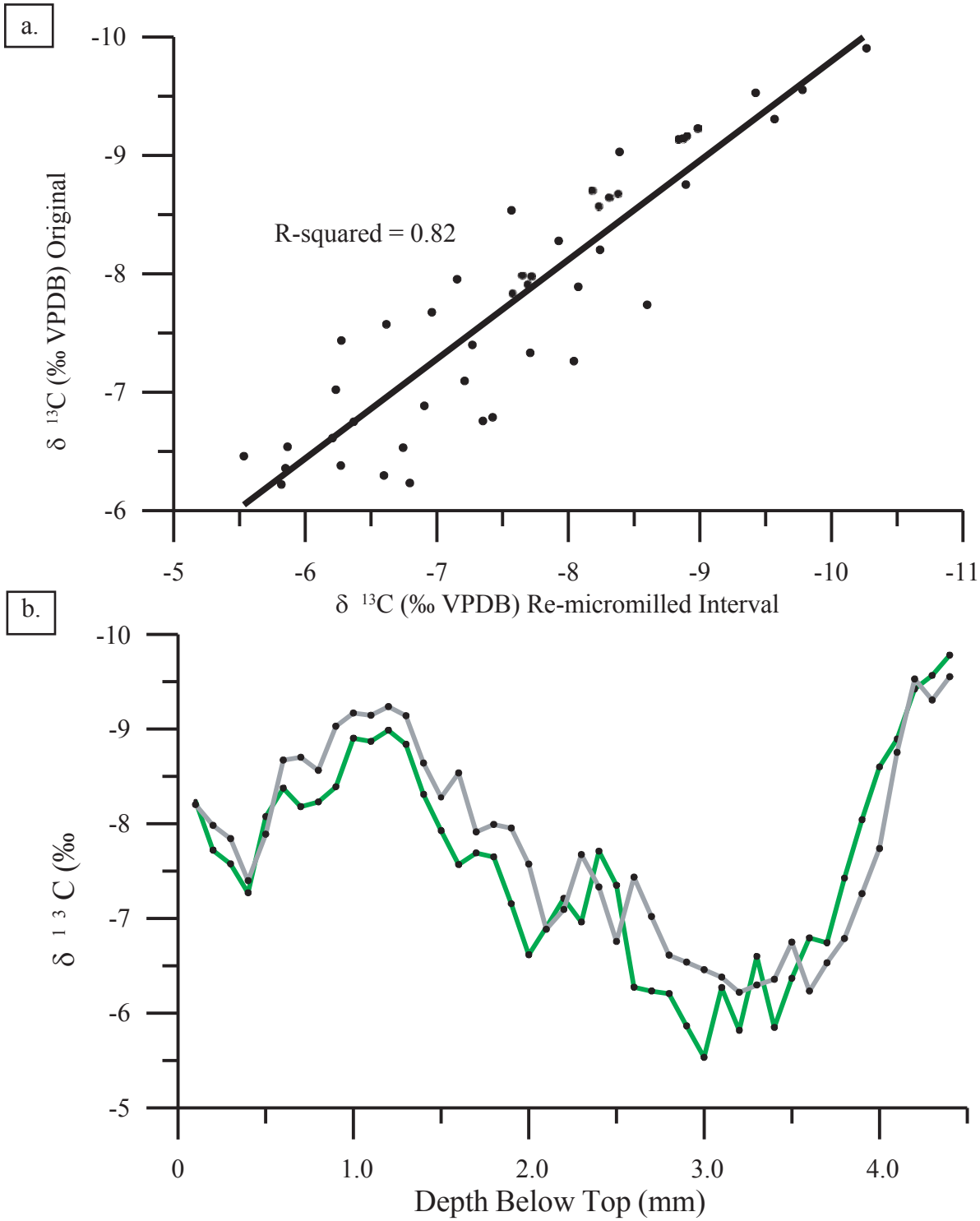

Figure 13. Cross plot (a) and linear plot (b) of the δ 13C (‰ VPDB) obtained from the first 45 samples of DSSG-4 (100 um sampling interval). R-squared of the cross plot is 0.82 (a). The gray line with black symbols represents the original samples and the green line with black dots is the re-micromilled samples (b). Samples from both sampling passes share the same DBT.

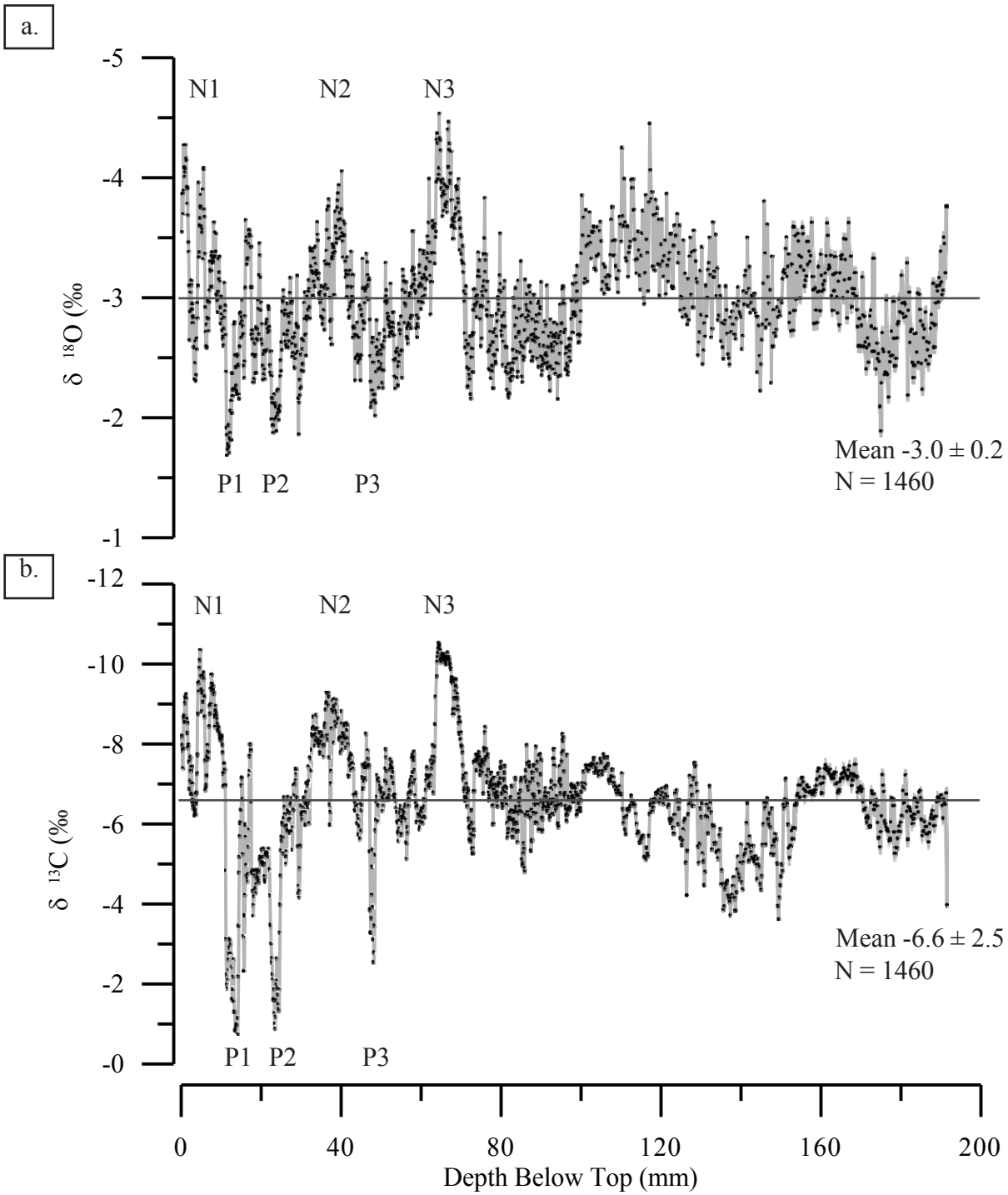

Figure 14. Plot of DSSG-4's $\delta^{18}O$ (a) and $\delta^{13}C$ (b) (‰ VPDB) (black dots), uncorrected for aragonite and columnar calcite (see text), versus Depth Below Top (DBT). Straight gray lines represent mean value. Anomalous positive and negative excursions are indicated by a P and N, respectively.

r-squared of 0.82 and the linear plot of the original and re-micromilled samples versus DBT also reveals good agreement between the two sampling profiles (Fig 13a-b).

A continuous down-core plot of the $\delta^{18}O$ aragonite, plotted versus DBT in Figure 14a, yield a mean $\delta^{18}O$ value of -3.0 ± 0.2‰ (n = 1460) with the most negative and positive excursions from the mean of 1.5‰ and 1.3‰, respectively. The plot of the $\delta^{13}C$ data versus DBT yield a mean $\delta^{13}C$ of -6.6 ± 2.5 (n = 1460) with the most negative and positive excursions from the mean of 5.8‰ and 3.8‰, respectively (Fig. 14b). The only anomalously negative isotope excursion that can be attributed to a change in mineralogy or fabric is the section of columnar calcite from 62.5 mm and 69.7 mm below the top of the stalagmite. The negative excursion caused by this section of columnar calcite is annotated as N1 in Figure 14a-b. To this 7.2 mm section, a correction factor of 0.6 and 2.0 (‰ VPDB) has been applied to the $\delta^{18}O$ and $\delta^{13}C$ results used for time-series analysis, respectively (Phillips, 2011). The remaining positive isotope excursions, annotated as P1, P2 and P3 in Figure 15a-b, occur in the black laminated section of the stalagmite, and do not correspond to any fabric or mineralogy known to require a correction (Phillips, 2011). These excursions occur in the profile between 10.7 mm to 14.8 mm (P1), between 22.3 mm to 25.3 mm (P2) and between 47.2 mm to 48.6 mm (P3), below the top of the stalagmite (Fig. 14a-b). The $\delta^{18}O$ values for these areas (P1, P2, P3), although generally more positive than the mean, do not show such pronounced variation as is found in the $\delta^{13}C$ results.

3.5 STABLE ISOTOPE TIME SERIES

The isotope time-series for DSSG-4's $\delta^{18}O$ and $\delta^{13}C$ (‰ VPDB), created using ARAND Time Series Analysis Software, is shown in Figure 15a-b (Howell, et al, 2006). Because

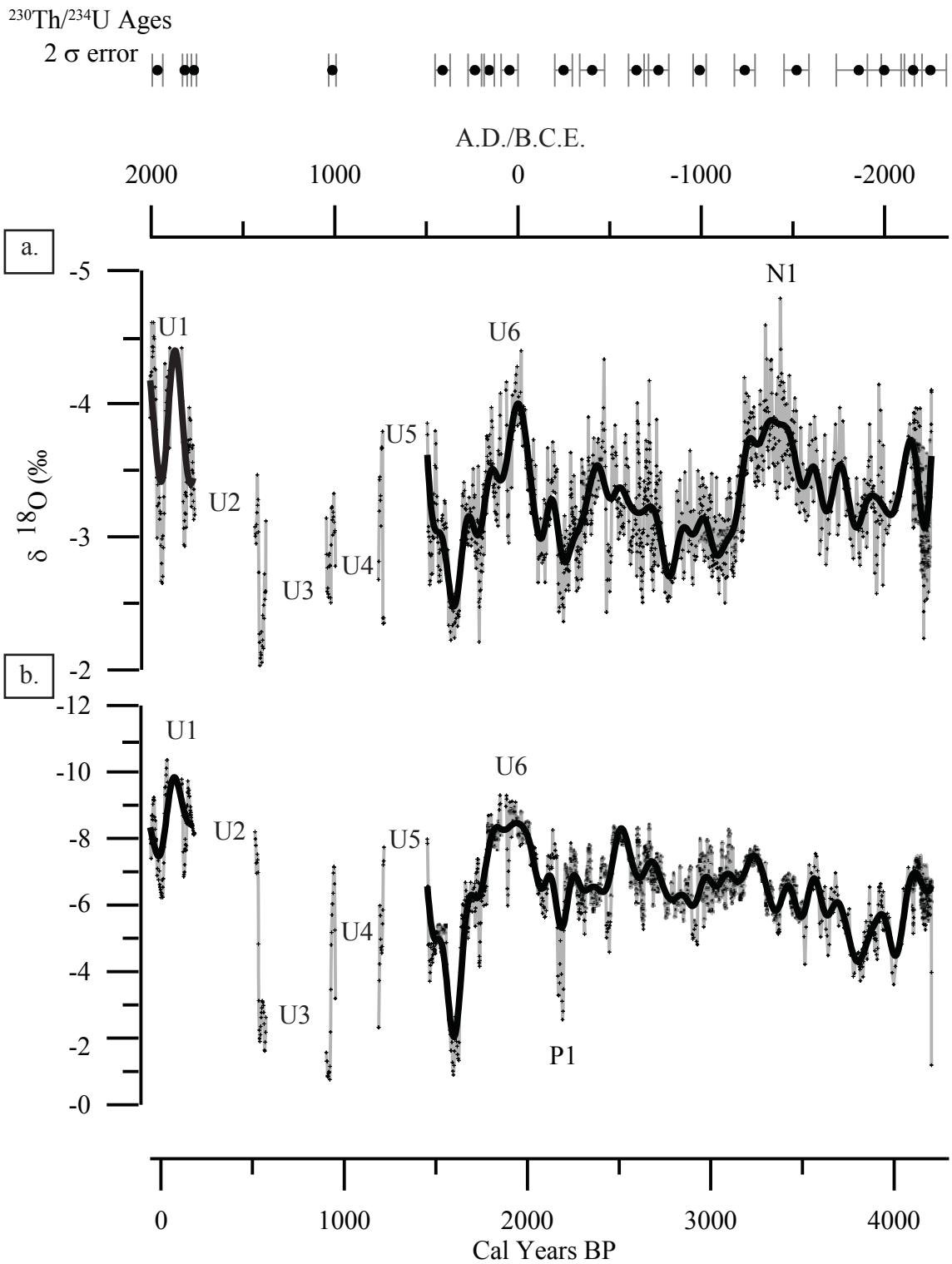

Figure 15. δ 18 O (a) and $\delta^{13}C$ (b) (‰ VPDB) time-series. Unconformities are shown as discontinuous intervals and annotated by "U" and unconformity number. $^{230}Th/^{234}U$ ages, with 2 σ error, are shown on the top axis.

unconformities #1 and #6 are relatively short, in the order of 65 and 27 years, respectively, they were disregarded in the 60-year smoothing interval for illustrative purposes. The interval below 4025 years BP and extending to the end of the cored stalagmite at 4205 years BP (150.0 mm to 191.8 mm DBT) was not included in the frequency analysis as this section of the stalagmite is interpreted as a flowstone upon which DSSG-4 grew. Additionally, no paleoclimate interpretation can be attempted on the $\delta^{18}O$ and $\delta^{13}C$ results contained between unconformities #1 and #6 because of the age model uncertainty in this portion of the stalagmite. Additionally, the repeated isotope excursions found between unconformities #1 and #6 suggest that the isotopes sourced from this region may be erroneous.

The aragonite and columnar calcite-corrected plot of the pre 1883 years BP $\delta^{18}O$ time-series exhibits a noticeable long cycle periodicity of approximately 1400 years and has a mean of -3.3 ± 0.2‰ (n = 882) (Fig 15a). Although the long 1400 year periodicity, which is more noticeable in the $\delta^{18}O$ than in the $\delta^{13}C$ time-series (Fig 14a-b), is suggestive of a Bond Cycle, the time series is not long enough to produce a confident periodicity of such a length (Bond et al., 1997).

Although the $\delta^{18}O$ reaches -4.8 (‰ VPDB) at approximately 3380 years BP (annotated as N1 in Figure 15a), this isotope excursion is interpreted as the peak of a trend and is not considered anomalous. However, the extreme variation in both the $\delta^{18}O$ and $\delta^{13}C$ after approximately 4140 years BP cannot be attributed to any effect known to require a correction and, since this variation occurs in the section interpreted as the flowstone upon which DSSG-4 grew, was not included in frequency analysis.

Unlike the $\delta^{18}O$, DSSG-4's $\delta^{13}C$ exhibits more variability for the interval spanning 1883 to 4025 years BP (36.8 mm to 150.0 mm DBT), up to 6 per mil (VPDB) (Fig 15b). Not only do

the $\delta^{13}C$ results for this interval have a mean of -6.6 ± 1.0‰ (n = 882), but they also display a pronounced negative trend through time (Fig 15b).

Comparing the mean $\delta^{18}O$ and $\delta^{13}C$ of the upper and lower approximate 200 years of the analyzed time series, 1883 to 2083 years BP and 3826 to 4025 years BP, respectively, reveals a 52% negative difference in $\delta^{13}C$ as DSSG-4 youngs. The mean $\delta^{13}C$ of the upper approximate 200 years is -7.9 ± 0.8 (n = 75) (‰ VPDB), whereas the $\delta^{13}C$ for the lower approximate 200 years (3826 to 4025 years BP) is -5.2 ± 0.5 (n = 59) (‰ VPDB). Furthermore, the $\delta^{18}O$ does not show such a pronounced trend. For the same upper and lower sections, the $\delta^{18}O$ has a mean of -3.6 ± 0.2 (n = 75) and a mean of -3.3 ± 0.1 (n = 59) (‰ VPDB), respectively, resulting in a comparatively small 9% negative difference of DSSG-4's $\delta^{18}O$. Such a pronounced negative trend of only the $\delta^{13}C$, as the stalagmite youngs, cannot be attributed to any mineralogy or fabric induced affect and is interpreted as a climate signal.

Although the positive excursion in the $\delta^{13}C$ between 2164 to 2200 years BP, annotated as P1 in Figure 15b, appears anomalous, this excursion also cannot be attributed to any mineralogy or fabric induced affect and is therefore interpreted as a climate signal.

3.6 SPECTRAL ANALYSIS RESULTS

ARAND Time Series Analysis Software was used to produce spectral analysis of the $\delta^{18}O$ time series, shown in Figure 16a, for the uninterrupted stalagmite section between 1883 to 4025 years BP (186.3 mm to 150.0 mm DBT) (Howell, et al, 2006). The analysis was limited to $\delta^{18}O$ because $\delta^{13}C$ is considered to be a poor proxy for regional rainfall (Lambert and Aharon, 2009). The $\delta^{18}O$ time series was first timed at a 5-year interval, followed by applying a Nyquist

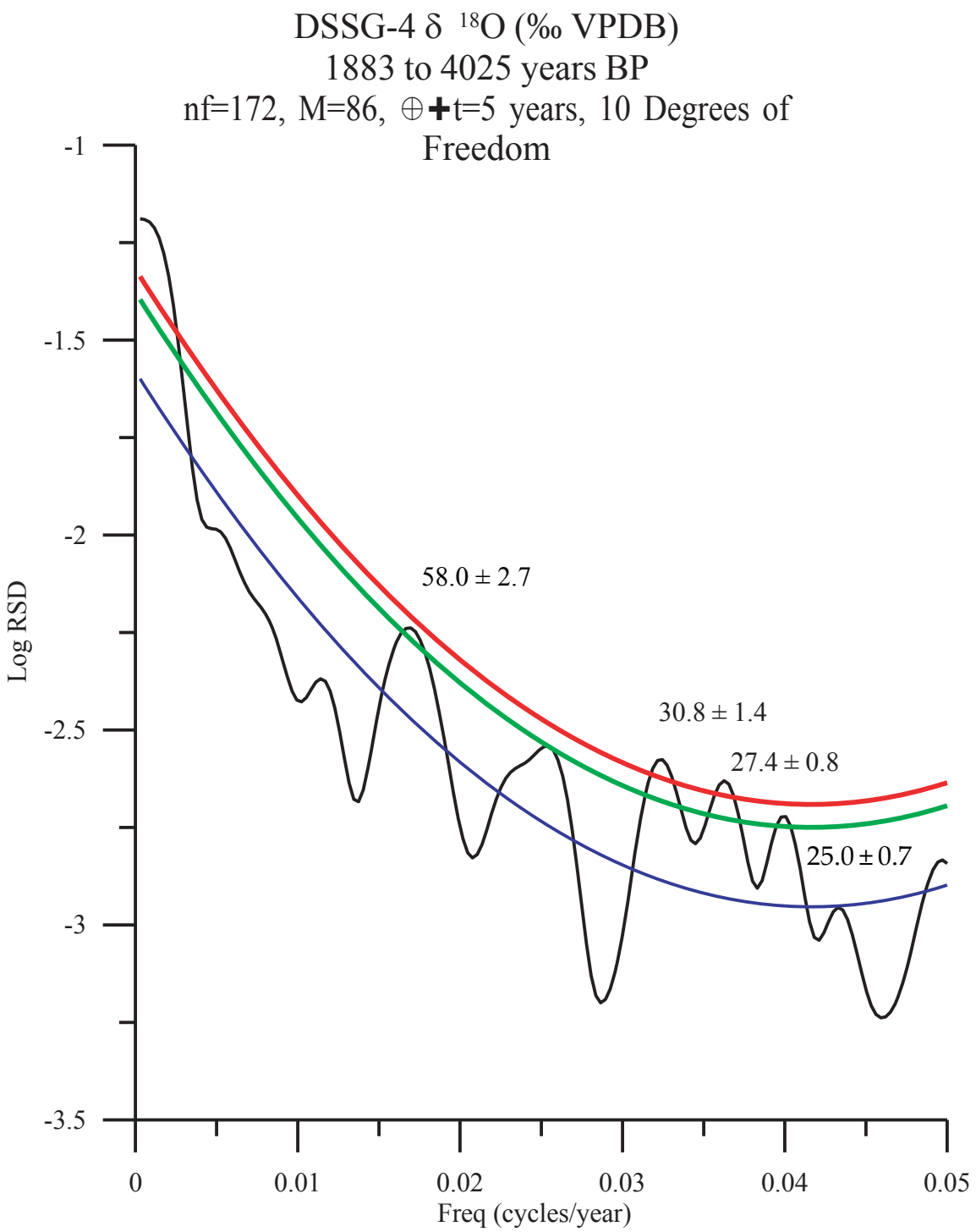

Figure 16. Spectral analysis of DSSG-4's $\delta^{18}O$ (‰ VPDB) when nf = 172, M = 86⊕✚, t= 5 years and 10 degrees of freedom. Red line represents Chi Squared 95% confidence interval and the green line is the Chi Squared 90% confidence interval. The blue line is the polynomial ($Y = 792.57x^2 - 65.98x + 1.58$). Frequency analysis obtained by using ARAND Time Series Analysis Software (Howell, et al, 2006).

frequency of 172 and a lag of 86 with 10 degrees of freedom that resulted in 2 periodicities above the 95% Chi Squared confidence interval of 30.8 ± 1.4 years and 27.4 ±.0.8 years, as shown in Figure 16. Additionally, 2 periodicities above the Chi Squared 90% confidence interval were discovered, at 58.0 ± 2.7 years and 25.0 ± 0.7 years (Fig. 16).

4. DISCUSSION

Since stalagmite dissolution caused by an increased drip-rate has been observed in DeSoto Caverns (Fig. 4b), and the fabrics and mineralogy observed in DSSG-4 match what has been described as dissolutional unconformities in other stalagmites (Fig. 4a), the unconformities observed in DSSG-4 likely resulted from an increased drip-rate (Turgeon and Lundberg, 2001). Additionally, the zone of partial aragonite to calcite transformation immediately below the unconformities (Fig. 4a) suggests that water was present to hasten the calcite to aragonite transformation (Frisia et al., 2002). Unconformities resulting from a lack of deposition, as described by Railsback (2011), are not found in DSSG-4 (Railsback et al., 2011).

Since detrital material entering DeSoto Caverns via entrainment in the cave's drip-waters has also been observed (Fig 10a-b), the detrital material ensconced in DSSG-4 was also likely transported into the cave via drip-waters (Fig. 10c-f). However, even though the unconformities and detrital material are found together in DSSG-4, they may not always result from the same processes, as both have been independently observed. For instance, DSSG-4 deposition appears to be continuous for the 19.8 mm between unconformities #5 and #6, yet this interval is very dark in nature due to detrital contamination (Fig. 6a). Described by Gradziński (2003), it is likely that the detrital material accumulates as a lag deposit on top of the unconformity as a result of the dissolution process, (Gradziński et al., 2003).

It has long been known that the pre-Columbian Native Americans modified their local environments to suit their needs, but it is only recently that the true extent of these modifications has become understood (Denevan, 1992; Woods, 2004; Springer et al., 2010). Their land use practices often resulted in deforestation and soil loss caused by unsustainable farming practices that relied upon slash and burn techniques (Fowler and Konopik, 2007; Peacock et al., 2004). Until the region's pre-Columbian Native Americans began limited agriculture during the Late Woodland period, followed by the initiation of intensive agriculture that was dependant on slash and burn techniques by the Mississippian Chiefdoms, between 1000 and 1150 years BP, no unconformities or detrital material appear in DSSG-4 (Figs. 7-9) (Smith, 1989). However, at approximately the time of the Mississippian chiefdoms, DSSG-4 features intense detrital contamination along with pronounced unconformities (Figs. 4, 6 and 10c-f). Since the ash featured in DSSG-4 appears to not have experienced severe diagenesis before being incorporated in to DSSG- 4 (Fig. 10c-d), nor do the pore spaces in the ash contain other detrital material (Fig. 10e-f), the ash and the unconformities are likely penecontemporaneous (Cohen-Ofri et al., 2006). Furthermore, if the detrital material contained in the unconformable section of DSSG-4 was a purely natural phenomenon, far more pollen and other terrestrial material should be included (McGarry and Caseldine, 2004).

Although the unconformities in DSSG-4 prevent interpretation of the region's hydroclimate from approximately 1883 years BP to the present, the section of DSSG-4 from 1883 to 4025 years BP (36.8 mm to 150.0 mm DBT) features contiguous and conformable aragonite botryoids and laminations (Figs. 6 through 8a), along with consistent growth rate (Fig. 11), suggesting that this section of DSSG-4 is ideal for

hydroclimate reconstructions.

Foremost among the hydroclimate signals are the periodicities revealed by analysis of DSSG-4's $\delta^{18}O$ in the frequency domain between 1883 and 4025 years BP. The dominant periodicities of 30.8 ± 1.4 years and 27.4 ± 0.8 and a minor frequency at 58.0 ± 2.7 years (Fig. 16) agree well with the often reported half and full cycles of the AMO, respectively (Knight et al., 2006; Knudsen et al., 2011). This representation of the AMO periodicities from a land-based record during this period of time and duration, 1883 to 4025 years BP, is unique and suggests that the AMO has manipulated the Southeastern hydroclimate for longer than has been previously reported.

The minor periodicity of DSSG-4's $\delta^{18}O$ at 25 ± 0.7 years is significant at the 90% Chi Squared confidence interval, but bits interpretation is ambiguous. The 25 ± 0.7 periodicity could result from a harmonic of the often reported 11 cyclicity of solar variability (Bard and Frank, 2006; Gray et al., 2010). However, the 25 ± 0.7 periodicity does not precisely match any of the reported solar cyclicities, and is alone in its suggestion of a solar influence of the Southeastern hydroclimate revealed by DSSG-4. Furthermore, it is possible that the minor 25 ± 0.7 periodicity of DSSG-4's $\delta^{18}O$ may result from some variation of AMO's cyclicities during the analyzed time period (1883 to 4025 years BP), even though modern and recent studies of AMO reveal its approximate 30 and 60 year cyclicities (Knudsen et al, 2011).

The steady depletion of the ^{13}C in DSSG-4 between 1883 to 4025 years BP (Fig. 15b) suggests a long-term shift toward a summer/autumn bias in the seasonality of stalagmite accretion in DeSoto Caverns. This shift toward a summer/autumn bias is consistent with the results of Lambert and Aharon's 2011 study of $\delta^{13}C$ in the modern and

recorded past 200 years deposition of aragonite in DeSoto Caverns (Lambert and Aharon, 2011).

5. CONCLUSIONS

(1.) Frequency analysis of DSSG-4's $\delta^{18}O$ suggests that the Atlantic Multidecadal Oscillation was a prevailing influence on the amount of rainfall in the Southeastern USA from 1883 to 4025 years BP.

(2.) Deposition of stalagmite DSSG-4 shifted more from a winter/spring to summer/autumn dominance between 4025 to 1883 years BP.

(3.) Pre-Columbian Native American agricultural practices likely caused local periodic denudation above DeSoto Caverns, and resulted in copious soil detritus being washed into the cave and the dissolutional unconformities in DSSG- 4.

REFERENCES

Bard E., Frank M. (2006), Climate change and solar variability: What's new under the sun? *Earth and Planetary Science Letters*. **248**, 1-14.

Bond G., Showers W., Cheseby M., Lotti R., Almasi P., deMenocal P., Priore P., Cullen H., Hajdas I., Bonani G. (1997), A pervasive millennial-scale cycle in North Atlantic Holocene and glacial climates. *Science*. **278**, 1257-1266.

Cohen-Ofri I., Weiner L., Boaretto E., Mintz G., Weiner S. (2006), Modern and fossil charcoal: aspects of structure and diagenesis. *Journal of Archaeological Science*. **33**, 428-439.

Dai, A., Hu A., Meehl G. A., Washington W. M., Strand W. G. (2005) Atlantic Thermohaline Circulation in a coupled general circulation model: Unforced variations versus forced changes. *Journal of Climate*. **18**, 3270-3293.

Delcourt, H. R., and Delcourt, P. A. (1997), Pre-Columbian Native American use of fire on Southern Appalachian landscapes. *Conservation Biology*. **11**, 1010-1014.

Denevan, W. (1992), The pristine myth: The landscape of the Americas in 1492. *Annals of the Association of American Geographers*. **82**, 369-385.

Dhungana, R. (2010), A high-resolution hydroclimate record of the last three millennia from a cored stalagmite at DeSoto Caverns (Alabama, USA) (Master's thesis). *University of Alabama Libraries*.

Enfield D. B., Mestas-Nunez A. M., Trimble P. J. (2001), The Atlantic multidecadal oscillation and its relation to rainfall and river flows in the continental U.S. *Geophysical Research Letters*. **28(10)**. 2077-2080.

Fowler C., Konopik E. (2007), The history of fire the southern United States. *Human Ecology Review*. **14**, 165-176.

Frisia S., Borsato A., Fairchild I. J., McDermott F., Selmo E. M. (2002), Aragonite-calcite relationships in speleothems (Grotte De Clamouse, France): Environment, fabrics, and carbonate geochemistry. *Journal of Sedimentary Research*. **72**, 687-699.

Gradziński, M., Hercman, H., Nowak, M., and Bella, P. (2007), Age of black coloured laminae within speleothems from Domica Cave and its significance for dating of prehistoric human settlement. *Geochronometria*. **28**, 39-45.

Gradziński, M., Gorny, A., Pazdur, A., and Pazdur, M. F. (2003), Origin of black coloured laminae in speleothems from the Krakow-Wielun Upland, Poland. *Boreas*. **32**, 532-542.

Gray L.J., Beer J., Geller M., Haigh J.D., Lockwood M., Matthes K., Cubasch U., Heitmann D. Harrison G., Hood L., Luterbacher J., Meehl G.A., Shindell D., van Geel B., White W., (2010), Solar Influences on Climate. *Reviews of Geophysics*. **48**, 1-53.

Hellstrom, J. (2003), Rapid and accurate U/Th dating using parallel ion-counting multi-collector ICP-MS, *J. Anal. At. Spectrom*. **18**,1346–1351.

Hellstrom J. (2006), U–Th dating of speleothems with high initial 230Th using stratigraphical constraint. *Quat. Geochronol.* **1**, 289-295.

Hetzinger S., Pfeiffer M., Dullo W-C., Keenlyside N., Latif M., Zinke J. (2008), Caribbean coral tracks Atlantic Mutidecadal Oscillation and past hurricane activity. *GEOLOGY*. **36**, 11 14.

Howell P., Pisias N., Balance J., Baughman J., Ochs L. (2006),Time Series Analysis Software, Brown Univ., Providence, R. I.

Karkanas P., Kyparissi-Apostolika N., Bar-Yosef O., Goldberg P., Weiner S. (1999), Mineral assemblages in Theopetra, Greece: A framework for understanding diagenesis in aprehistoric cave. *Journal of Archaeological Science*. **26**, 1171-1180.

Karkanas P., Bar-Yosef O., Goldberg P., Weiner S. (2000), Diagenesis in prehistoric caves: the use of minerals that form *in situ* to asses the completeness of the archaeological record. *Journal of Archaeological Science*. **27**, 915-929.

Kim S.T., Mucci A., and Taylor B. E. (2007), Phosphoric acid fractionation factors for calcite and aragonite between 25 and 75 °C: Revisited. *Chem. Geol.* **246**, 135-146.

Knight J. R., Folland C. K., Scaife A. A. (2006), Climate impacts of the Atlantic Multidecadal Oscillation. *Geophysical Research Letters.* **33**, 1-4.

Knudesn M.F., Seidenkrantz M-S., Jacobsen B. H., Kuijpers A. (2011), Tracking the Atlantic Multidecadal Oscillation through the last 8,000 years. *Nature Communications.* **2**, 1-8.

Lachniet, M. (2009), Climatic and environmental controls on speleothem oxygen-isotope values. *Quaternary Science Reviews*. **28**, 412-432.

Lambert, W., Aharon, P. (2011), Controls on dissolved inorganic carbon and $\delta^{13}C$ in cave waters from DeSoto Caverns: Implications for speleothem $\delta^{13}C$ assessments. *Geochimica et Cosmochimica Acta.* **75**, 753-768.

Lambert, W., Aharon, P. (2009), Oxygen and hydrogen isotopes of rainfall and dripwater at

DeSoto Caverns (Alabama, USA): Key to understanding past variability of moisture transport from the Gulf of Mexico. *Geochimica et Cosmochimica Acta.* **74**, 846-861.

McGarry S. F., Caseldine C. (2004), Speleothem palynology: an undervalued tool in Quaternary studies. *Quaternary Science*. **23**, 2389-2404.

McCabe G. J., Betancourt J. L., Gray S. T., Palecki M. A., Hidalgo H. G. (2008), Associations of multi-decadal sea-surface temperature variability with US drought. *Quaternary International*. **188**, 31-40.

McDermott, F. (2004), Palaeo-climate reconstruction from stable isotope variations in speleothems: a review. *Quaternary Science Reviews*. **23**, 901-918.

Pederson N., Bell A. R., Knight T. A., Leland C., Malcomb N., Anchukaitis K. J., Tackett K., Scheff J., Brice A., Catron B., Blozan W., Riddle J. (2012), A long-term perspective on a modern drought in the American Southeast. *Environmental Research Letters*. **7**, 1-8.

Poore R. Z., DeLong K. L., Richey J. N., Quinn T. M. (2009), Evidence of multidecadal climate variability and the Atlantic Multidecadal Oscillation from a Gulf of Mexico sea-surface temperature- proxy record. *Geo-Marine Letters*. **29**, 477-484.

Oglesby R., Feng S., Hu Q., Rowe C. (2012), The role of the Atlantic Multidecadal Oscillation on medieval drought in North America: Synthesizing results from proxy data and climate models. *Global and Planetary Change*. **84-85**, 56-65

Ortegren J. T., Knapp P. A., Maxwell J. T., Tyminski W. P., Soule P. T. (2011), Ocean-Atmosphere influences on low-frequency warm-season drought variability in the Gulf Coast and Southeastern United States. *American Meteorological Society*. **50**, 1177-1186.

Palmer A. N. (1991), Origin and morphology of limestone caves. *Geological Society of America Bulletin*. **103**, 1-21.

Peacock E., Haag W. R., Warren M. L. (2004), Prehistoric decline in freshwater mussels coincident with the advent of maize agriculture. *Conservation Biology*. **19**, 547-551.

Phillips J. H. (2011), Insights into aragonite diagenesis as evidenced from spelean carbonate (Master's thesis). *University of Alabama Libraries*.

Polyak V. J., Ckendolpher J. C., Norton R. A., Asmerom Y. (2010), Wetter and cooler late Holocene climate in the southwestern United States from mites preserved in stalagmites. *Geology*. **29**, 643-646.

Railsback L. B., Liang F., Romani J. R. V., Grandal-d'Anglade A., Rodriguez M. V., Fidalgo L. S., Mosquera D. F., Cheng H., Edwards R. L. (2011), Petrographic and isotopic evidence for Holocene long-term climate change and shorter-term environmental shifts from a stalagmite from the Serra do Courel of northwestern Spain, and implications for climatic

history across Europe and the Mediterranean. *Palaeogeography, Palaeoclimatology, Palaeoecology*. **305**, 172-184.

Schiermeier, Q. (2010), The real holes in climate science. *Nature*. **463**, 284-287.

Smith B. D. (1989), Origins of Agriculture in Eastern North America. *Science*. **246**, 1566-1571.

Springer G. S., White D. M., Rowe H. D., Hardt B., Mihimdukulasooriya N., Cheng H., Edwards R. L. (2010), Multiproxy evidence from caves of Native Americans altering the overlying landscape during the late Holocene of east-central North America. *The Holocene*. **20**, 275-283.

Stahle D. W., Cleaveland M. K. (1992), Reconstruction and analysis of spring rainfall over the Southeastern U.S. for the past 1000 years. *Bulletin of the American Meteorological Society*. **73**, 1947-1961.

Turgeon S., Lundberg J. (2001), Chronology of discontinuities and petrology of speleothems as climatic indicators of the Klamath Mountains, Southwest Oregon, USA. *Carbonates and Evaporites*. **16(2)**, 153-167.

Walthall, J.A., and DeJarnette, D.L. (1974), Copena burial caves. *Journal of Alabama Archaeolog.* **XX**, 1-59.

Woods W. I. (2004), Population nucleation, intensive agriculture, and environmental degredation: The Cahokia example. *Agriculture and Human Values*. **21**, 255-261.

APPENDIX 1

DBT with $\delta^{18}O$ and $\delta^{13}C$ data from DSSG-4

DBT (mm)	$\delta^{13}C$ (‰ VPDB)	$\delta^{18}O$ (‰ VPDB)	$\delta^{13}C$ (‰ VPDB) Aragonite and Calcite Corr (*)	$\delta^{18}O$ (‰ VPDB) Aragonite and Calcite Corr (*)
0.1	-8.2	-3.6	-8.2	-3.9
0.2	-8.0	-3.9	-8.0	-4.2
0.3	-7.8	-3.9	-7.8	-4.2
0.4	-7.4	-3.7	-7.4	-4.0
0.5	-7.9	-3.9	-7.9	-4.2
0.6	-8.7	-4.3	-8.7	-4.6
0.7	-8.7	-4.1	-8.7	-4.4
0.8	-8.6	-4.0	-8.6	-4.4
0.9	-9.0	-4.1	-9.0	-4.4
1.0	-9.2	-4.1	-9.2	-4.4
1.1	-9.1	-4.3	-9.1	-4.6
1.2	-9.2	-4.2	-9.2	-4.5
1.3	-9.1	-4.1	-9.1	-4.5
1.4	-8.6	-3.9	-8.6	-4.3
1.5	-8.3	-3.8	-8.3	-4.1
1.6	-8.5	-3.9	-8.5	-4.3
1.7	-7.9	-3.7	-7.9	-4.0
1.8	-8.0	-3.5	-8.0	-3.8
1.9	-8.0	-3.4	-8.0	-3.7
2.0	-7.6	-3.1	-7.6	-3.4
2.1	-6.9	-2.7	-6.9	-3.0
2.2	-7.1	-2.9	-7.1	-3.2
2.3	-7.7	-3.0	-7.7	-3.4
2.4	-7.3	-3.1	-7.3	-3.4
2.5	-6.8	-3.1	-6.8	-3.5
2.6	-7.4	-2.9	-7.4	-3.3
2.7	-7.0	-3.0	-7.0	-3.3
2.8	-6.6	-2.8	-6.6	-3.1
2.9	-6.5	-2.9	-6.5	-3.2
3.0	-6.5	-2.8	-6.5	-3.2
3.1	-6.4	-2.6	-6.4	-2.9
3.2	-6.2	-2.3	-6.2	-2.7
3.3	-6.3	-2.5	-6.3	-2.8
3.4	-6.4	-2.6	-6.4	-3.0
3.5	-6.7	-2.3	-6.7	-2.7
3.6	-6.2	-2.4	-6.2	-2.7
3.7	-6.5	-2.7	-6.5	-3.0

DBT (mm)	$\delta^{13}C$ (‰ VPDB)	$\delta^{18}O$ (‰ VPDB)	$\delta^{13}C$ (‰ VPDB) Aragonite and Calcite Corr (*).	$\delta^{18}O$ (‰ VPDB) Aragonite and Calcite Corr (*).
3.8	-6.8	-2.6	-6.8	-2.9
3.9	-7.3	-3.0	-7.3	-3.3
4.0	-7.7	-2.8	-7.7	-3.2
4.1	-8.8	-3.1	-8.8	-3.4
4.2	-9.5	-4.0	-9.5	-4.3
4.3	-9.3	-3.3	-9.3	-3.7
4.4	-9.6	-3.4	-9.6	-3.7
4.5	-9.9	-3.6	-9.9	-3.9
4.6	-10.1	-3.7	-10.1	-4.0
4.7	-10.3	-3.8	-10.3	-4.1
4.8	-10.4	-3.9	-10.4	-4.2
4.9	-9.7	-3.8	-9.7	-4.1
5.0	-9.4	-3.6	-9.4	-3.9
5.1	-8.8	-3.5	-8.8	-3.9
5.2	-9.2	-3.6	-9.2	-3.9
5.3	-9.3	-3.9	-9.3	-4.2
5.4	-9.1	-3.3	-9.1	-3.7
5.5	-9.7	-4.1	-9.7	-4.4
5.6	-9.8	-4.1	-9.8	-4.4
5.7	-9.6	-3.7	-9.6	-4.1
5.8	-9.2	-3.7	-9.2	-4.0
5.9	-8.7	-3.4	-8.7	-3.7
6.0	-7.6	-2.9	-7.6	-3.3
6.1	-6.9	-2.7	-6.9	-3.1
6.2	-6.9	-2.6	-6.9	-2.9
6.3	-7.0	-2.8	-7.0	-3.1
6.4	-7.2	-2.6	-7.2	-2.9
6.5	-7.7	-2.8	-7.7	-3.2
6.6	-8.0	-3.0	-8.0	-3.3
6.7	-7.8	-3.0	-7.8	-3.3
6.8	-7.6	-2.8	-7.6	-3.2
6.9	-7.7	-2.7	-7.7	-3.1
7.0	-7.8	-3.0	-7.8	-3.3
7.1	-8.4	-3.1	-8.4	-3.4
7.2	-9.0	-3.3	-9.0	-3.6
7.3	-8.8	-3.2	-8.8	-3.6
7.4	-9.0	-3.2	-9.0	-3.6

DBT (mm)	$\delta^{13}C$ (‰ VPDB)	$\delta^{18}O$ (‰ VPDB)	$\delta^{13}C$ (‰ VPDB) Aragonite and Calcite Corr (*).	$\delta^{18}O$ (‰ VPDB) Aragonite and Calcite Corr (*).
7.5	-9.4	-3.1	-9.4	-3.4
7.6	-9.7	-3.4	-9.7	-3.7
7.7	-9.5	-3.4	-9.5	-3.7
7.8	-9.4	-3.3	-9.4	-3.6
7.9	-9.4	-3.3	-9.4	-3.7
8.0	-9.4	-3.3	-9.4	-3.7
8.1	-9.3	-3.6	-9.3	-4.0
8.2	-9.3	-3.3	-9.3	-3.7
8.3	-8.7	-3.5	-8.7	-3.9
8.4	-8.4	-3.3	-8.4	-3.7
8.5	-8.8	-3.4	-8.8	-3.7
8.6	-9.0	-3.5	-9.0	-3.9
8.7	-8.8	-3.0	-8.8	-3.4
8.8	-8.7	-3.0	-8.7	-3.4
8.9	-8.6	-3.0	-8.6	-3.3
9.0	-8.5	-2.9	-8.5	-3.2
9.1	-8.3	-3.1	-8.3	-3.4
9.2	-8.4	-3.3	-8.4	-3.7
9.3	-8.4	-3.2	-8.4	-3.5
9.4	-8.4	-3.2	-8.4	-3.6
9.5	-8.3	-3.3	-8.3	-3.7
9.6	-8.2	-3.1	-8.2	-3.5
9.7	-8.1	-2.9	-8.1	-3.3
9.8	-8.1	-2.8	-8.1	-3.1
9.9	-8.1	-3.0	-8.1	-3.4
10.0	-8.2	-2.9	-8.2	-3.2
10.1	-8.1	-2.8	-8.1	-3.2
10.2	-8.2	-2.7	-8.2	-3.1
10.3	-8.0	-2.7	-8.0	-3.0
10.4	-7.8	-2.7	-7.8	-3.0
10.5	-7.3	-2.6	-7.3	-2.9
10.6	-7.0	-2.8	-7.0	-3.1
10.7	-7.3	-2.8	-7.3	-3.2
10.8	-7.5	-3.1	-7.5	-3.5
10.9	-7.4	-2.9	-7.4	-3.2
11.0	-7.0	-2.9	-7.0	-3.3
11.1	-4.8	-2.7	-4.8	-3.0

DBT (mm)	$\delta^{13}C$ (‰ VPDB)	$\delta^{18}O$ (‰ VPDB)	$\delta^{13}C$ (‰ VPDB) Aragonite and Calcite Corr (*).	$\delta^{18}O$ (‰ VPDB) Aragonite and Calcite Corr (*).
11.2	-3.1	-2.4	-3.1	-2.7
11.3	-2.2	-1.9	-2.2	-2.3
11.4	-2.0	-1.9	-2.0	-2.2
11.5	-1.9	-1.7	-1.9	-2.0
11.6	-2.1	-1.7	-2.1	-2.1
11.7	-2.4	-1.8	-2.4	-2.1
11.8	-2.6	-1.8	-2.6	-2.1
11.9	-2.8	-1.9	-2.8	-2.3
12.0	-2.9	-1.7	-2.9	-2.1
12.1	-3.1	-1.8	-3.1	-2.2
12.2	-3.1	-1.9	-3.1	-2.2
12.3	-3.1	-2.1	-3.1	-2.4
12.4	-3.0	-1.8	-3.0	-2.2
12.5	-2.8	-2.1	-2.8	-2.5
12.6	-2.4	-2.0	-2.4	-2.4
12.7	-1.6	-2.4	-1.6	-2.7
12.8	-1.6	-2.2	-1.6	-2.5
12.9	-1.9	-2.2	-1.9	-2.6
13.0	-2.2	-2.3	-2.2	-2.6
13.1	-2.6	-2.8	-2.6	-3.1
13.2	-1.6	-2.8	-1.6	-3.1
13.3	-1.3	-2.5	-1.3	-2.9
13.4	-1.3	-2.2	-1.3	-2.6
13.5	-0.8	-2.4	-0.8	-2.8
13.6	-0.9	-2.3	-0.9	-2.6
13.7	-0.9	-2.2	-0.9	-2.6
13.8	-0.9	-2.2	-0.9	-2.5
13.9	-1.0	-2.5	-1.0	-2.9
14.0	-1.0	-2.5	-1.0	-2.9
14.1	-0.8	-2.4	-0.8	-2.8
14.2	-1.2	-2.4	-1.2	-2.8
14.3	-2.2	-2.2	-2.2	-2.5
14.4	-3.5	-2.2	-3.5	-2.5
14.5	-4.8	-2.6	-4.8	-2.9
14.6	-5.2	-2.9	-5.2	-3.2
14.7	-5.7	-2.9	-5.7	-3.2
14.8	-6.0	-2.8	-6.0	-3.1

DBT (mm)	$\delta^{13}C$ (‰ VPDB)	$\delta^{18}O$ (‰ VPDB)	$\delta^{13}C$ (‰ VPDB) Aragonite and Calcite Corr (*).	$\delta^{18}O$ (‰ VPDB) Aragonite and Calcite Corr (*).
14.9	-6.0	-2.7	-6.0	-3.0
15.0	-6.4	-2.8	-6.4	-3.2
15.1	-7.0	-2.8	-7.0	-3.1
15.2	-7.2	-3.0	-7.2	-3.3
15.3	-7.1	-2.8	-7.1	-3.1
15.4	-6.6	-2.7	-6.6	-3.0
15.5	-5.2	-2.7	-5.2	-3.0
15.6	-3.2	-2.4	-3.2	-2.8
15.7	-2.3	-2.3	-2.3	-2.7
15.8	-2.3	-2.5	-2.3	-2.8
15.9	-3.7	-2.9	-3.7	-3.2
16.0	-4.2	-3.1	-4.2	-3.4
16.1	-6.0	-3.6	-6.0	-3.4
16.2	-5.7	-3.5	-5.7	-3.3
16.3	-5.0	-3.5	-5.0	-3.3
16.4	-4.7	-3.3	-4.7	-3.1
16.5	-4.6	-3.3	-4.6	-3.7
16.6	-4.6	-3.3	-4.6	-3.7
16.7	-4.8	-3.3	-4.8	-3.7
16.8	-5.4	-3.5	-5.4	-3.8
16.9	-5.9	-2.5	-5.9	-2.8
17.0	-7.2	-2.4	-7.2	-2.8
17.1	-7.3	-2.5	-7.3	-2.8
17.2	-7.7	-2.5	-7.7	-2.8
17.3	-8.0	-3.5	-8.0	-3.9
17.4	-7.8	-3.4	-7.8	-3.8
17.5	-6.6	-3.1	-6.6	-3.4
17.6	-4.8	-2.7	-4.8	-3.0
17.7	-4.8	-2.7	-4.8	-3.1
17.8	-4.8	-2.7	-4.8	-3.0
17.9	-4.3	-2.5	-4.3	-2.9
18.0	-3.7	-2.3	-3.7	-2.6
18.1	-4.0	-2.3	-4.0	-2.7
18.2	-4.2	-2.6	-4.2	-3.0
18.3	-4.7	-2.5	-4.7	-2.9
18.4	-4.8	-2.4	-4.8	-2.7
18.5	-4.4	-2.5	-4.4	-2.9

DBT (mm)	$\delta^{13}C$ (‰ VPDB)	$\delta^{18}O$ (‰ VPDB)	$\delta^{13}C$ (‰ VPDB) Aragonite and Calcite Corr (*).	$\delta^{18}O$ (‰ VPDB) Aragonite and Calcite Corr (*).
18.6	-4.4	-2.8	-4.4	-3.1
18.7	-4.3	-2.4	-4.3	-2.7
18.8	-4.5	-2.7	-4.5	-3.0
18.9	-4.7	-2.7	-4.7	-3.1
19.0	-4.8	-2.6	-4.8	-3.0
19.1	-4.8	-3.0	-4.8	-3.3
19.2	-4.7	-2.9	-4.7	-3.3
19.3	-4.6	-2.7	-4.6	-3.0
19.4	-4.6	-3.2	-4.6	-3.5
19.5	-4.5	-3.5	-4.5	-3.8
19.6	-4.8	-3.4	-4.8	-3.7
19.7	-5.1	-3.2	-5.1	-3.5
19.8	-5.2	-2.9	-5.2	-3.2
19.9	-5.1	-3.0	-5.1	-3.3
20.0	-5.1	-2.7	-5.1	-3.0
20.1	-5.0	-2.8	-5.0	-3.1
20.2	-5.4	-2.6	-5.4	-3.0
20.3	-5.2	-2.4	-5.2	-2.8
20.4	-5.0	-2.3	-5.0	-2.7
20.5	-5.2	-2.5	-5.2	-2.9
20.6	-5.0	-2.4	-5.0	-2.7
20.7	-5.4	-2.6	-5.4	-2.9
20.8	-5.0	-2.4	-5.0	-2.7
20.9	-4.7	-2.3	-4.7	-2.7
21.0	-4.6	-2.6	-4.6	-2.9
21.1	-4.6	-2.6	-4.6	-2.9
21.2	-5.2	-2.8	-5.2	-3.1
21.3	-5.3	-2.8	-5.3	-3.1
21.4	-5.2	-2.8	-5.2	-3.2
21.5	-5.2	-2.6	-5.2	-2.9
21.6	-5.2	-2.7	-5.2	-3.1
21.7	-5.3	-2.7	-5.3	-3.1
21.8	-5.2	-2.9	-5.2	-3.3
21.9	-5.4	-2.9	-5.4	-3.3
22.0	-5.4	-2.8	-5.4	-3.1
22.1	-4.9	-2.7	-4.9	-3.1
22.2	-4.2	-2.4	-4.2	-2.8

DBT (mm)	$\delta^{13}C$ (‰ VPDB)	$\delta^{18}O$ (‰ VPDB)	$\delta^{13}C$ (‰ VPDB) Aragonite and Calcite Corr (*).	$\delta^{18}O$ (‰ VPDB) Aragonite and Calcite Corr (*).
22.3	-3.5	-2.4	-3.5	-2.7
22.4	-3.4	-2.6	-3.4	-2.9
22.5	-3.0	-2.4	-3.0	-2.7
22.6	-2.6	-2.0	-2.6	-2.3
22.7	-2.7	-2.2	-2.7	-2.5
22.8	-2.2	-2.1	-2.2	-2.5
22.9	-2.1	-1.9	-2.1	-2.3
23.0	-1.6	-1.9	-1.6	-2.2
23.1	-1.6	-2.2	-1.6	-2.5
23.2	-1.9	-2.1	-1.9	-2.5
23.3	-1.3	-2.0	-1.3	-2.3
23.4	-1.0	-2.1	-1.0	-2.5
23.5	-0.9	-2.1	-0.9	-2.4
23.6	-1.2	-2.0	-1.2	-2.3
23.7	-1.6	-1.9	-1.6	-2.2
23.8	-2.0	-2.0	-2.0	-2.4
23.9	-2.6	-2.2	-2.6	-2.6
24.0	-2.1	-2.0	-2.1	-2.4
24.1	-1.9	-2.2	-1.9	-2.6
24.2	-1.8	-2.1	-1.8	-2.4
24.3	-1.5	-2.0	-1.5	-2.3
24.4	-1.4	-2.1	-1.4	-2.4
24.5	-1.3	-2.1	-1.3	-2.4
24.6	-1.9	-2.1	-1.9	-2.4
24.7	-3.3	-2.4	-3.3	-2.7
24.8	-4.0	-2.5	-4.0	-2.8
24.9	-4.7	-2.4	-4.7	-2.7
25.0	-5.3	-2.6	-5.3	-3.0
25.1	-5.7	-2.6	-5.7	-2.9
25.2	-5.6	-2.9	-5.6	-3.2
25.3	-6.0	-3.0	-6.0	-3.3
25.4	-6.0	-3.0	-6.0	-3.3
25.5	-5.7	-3.1	-5.7	-3.4
25.6	-5.3	-3.0	-5.3	-3.3
25.7	-6.1	-2.7	-6.1	-3.0
25.8	-6.7	-2.9	-6.7	-3.2
25.9	-6.4	-2.9	-6.4	-3.2

DBT (mm)	$\delta^{13}C$ (‰ VPDB)	$\delta^{18}O$ (‰ VPDB)	$\delta^{13}C$ (‰ VPDB) Aragonite and Calcite Corr (*).	$\delta^{18}O$ (‰ VPDB) Aragonite and Calcite Corr (*).
26.0	-6.2	-2.9	-6.2	-3.2
26.1	-5.9	-2.6	-5.9	-3.0
26.2	-5.2	-2.6	-5.2	-2.9
26.3	-5.0	-2.6	-5.0	-2.9
26.4	-5.3	-2.7	-5.3	-3.0
26.5	-6.0	-3.0	-6.0	-3.3
26.6	-5.8	-2.7	-5.8	-3.1
26.7	-6.3	-2.9	-6.3	-3.2
26.8	-6.7	-2.8	-6.7	-3.2
26.9	-6.3	-2.6	-6.3	-2.9
27.0	-6.1	-2.6	-6.1	-3.0
27.1	-5.8	-2.8	-5.8	-3.1
27.2	-6.3	-3.0	-6.3	-3.4
27.3	-6.5	-3.2	-6.5	-3.5
27.4	-6.1	-2.9	-6.1	-3.2
27.5	-6.5	-3.0	-6.5	-3.3
27.6	-6.7	-3.0	-6.7	-3.3
27.7	-5.8	-2.6	-5.8	-3.0
27.8	-5.4	-2.5	-5.4	-2.9
27.9	-5.9	-2.5	-5.9	-2.9
28.0	-6.3	-2.7	-6.3	-3.0
28.1	-7.0	-2.7	-7.0	-3.0
28.2	-6.4	-2.4	-6.4	-2.8
28.3	-6.7	-2.7	-6.7	-3.0
28.4	-7.0	-2.5	-7.0	-2.8
28.5	-7.0	-2.6	-7.0	-2.9
28.6	-7.4	-2.5	-7.4	-2.9
28.7	-7.1	-2.8	-7.1	-3.1
28.8	-7.2	-2.8	-7.2	-3.1
28.9	-7.4	-3.2	-7.4	-3.5
29.0	-6.7	-2.6	-6.7	-2.9
29.1	-6.7	-2.8	-6.7	-3.1
29.2	-5.4	-2.2	-5.4	-2.5
29.3	-4.3	-1.9	-4.3	-2.2
29.4	-4.5	-2.1	-4.5	-2.5
29.5	-4.2	-2.3	-4.2	-2.7
29.6	-4.3	-2.2	-4.3	-2.5

DBT (mm)	$\delta^{13}C$ (‰ VPDB)	$\delta^{18}O$ (‰ VPDB)	$\delta^{13}C$ (‰ VPDB) Aragonite and Calcite Corr (*).	$\delta^{18}O$ (‰ VPDB) Aragonite and Calcite Corr (*).
29.7	-4.9	-2.3	-4.9	-2.6
29.8	-5.4	-2.5	-5.4	-2.9
29.9	-5.5	-2.3	-5.5	-2.6
30.0	-6.5	-2.4	-6.5	-2.7
30.1	-6.3	-2.7	-6.3	-3.0
30.2	-6.2	-2.6	-6.2	-2.9
30.3	-6.1	-2.5	-6.1	-2.8
30.4	-6.3	-2.4	-6.3	-2.8
30.5	-6.3	-2.4	-6.3	-2.7
30.6	-6.4	-2.6	-6.4	-3.0
30.7	-6.7	-3.0	-6.7	-3.3
30.8	-6.7	-2.8	-6.7	-3.2
30.9	-6.6	-3.1	-6.6	-3.4
31.0	-6.3	-2.7	-6.3	-3.0
31.1	-6.0	-2.7	-6.0	-3.0
31.2	-6.5	-2.5	-6.5	-2.9
31.3	-6.8	-2.8	-6.8	-3.2
31.4	-7.0	-3.0	-7.0	-3.4
31.5	-6.6	-2.8	-6.6	-3.2
31.6	-6.5	-2.8	-6.5	-3.2
31.7	-6.4	-2.9	-6.4	-3.2
31.8	-7.0	-3.1	-7.0	-3.4
31.9	-7.4	-3.1	-7.4	-3.5
32.0	-7.1	-3.1	-7.1	-3.4
32.1	-6.0	-2.9	-6.0	-3.3
32.2	-6.6	-2.8	-6.6	-3.2
32.3	-7.7	-3.4	-7.7	-3.8
32.4	-7.7	-3.4	-7.7	-3.7
32.5	-7.3	-3.3	-7.3	-3.6
32.6	-7.9	-3.4	-7.9	-3.7
32.7	-8.2	-3.2	-8.2	-3.6
32.8	-8.4	-3.4	-8.4	-3.8
32.9	-8.2	-3.0	-8.2	-3.4
33.0	-8.7	-3.2	-8.7	-3.5
33.1	-8.2	-3.1	-8.2	-3.5
33.2	-8.4	-3.3	-8.4	-3.7
33.3	-8.2	-3.1	-8.2	-3.4

DBT (mm)	$\delta^{13}C$ (‰ VPDB)	$\delta^{18}O$ (‰ VPDB)	$\delta^{13}C$ (‰ VPDB) Aragonite and Calcite Corr (*).	$\delta^{18}O$ (‰ VPDB) Aragonite and Calcite Corr (*).
33.4	-8.0	-3.4	-8.0	-3.8
33.5	-8.4	-3.3	-8.4	-3.6
33.6	-8.1	-3.2	-8.1	-3.6
33.7	-8.2	-3.2	-8.2	-3.6
33.8	-8.7	-3.2	-8.7	-3.5
33.9	-8.2	-3.6	-8.2	-4.0
34.0	-8.4	-3.5	-8.4	-3.9
34.1	-8.4	-3.5	-8.4	-3.8
34.2	-8.0	-3.2	-8.0	-3.5
34.3	-8.0	-3.2	-8.0	-3.5
34.4	-8.1	-3.0	-8.1	-3.4
34.5	-8.0	-3.0	-8.0	-3.3
34.6	-8.3	-3.0	-8.3	-3.4
34.7	-7.8	-3.0	-7.8	-3.3
34.8	-8.0	-3.1	-8.0	-3.4
34.9	-7.8	-2.8	-7.8	-3.2
35.0	-8.2	-3.1	-8.2	-3.4
35.1	-8.1	-3.0	-8.1	-3.3
35.2	-8.3	-2.8	-8.3	-3.2
35.3	-8.2	-2.8	-8.2	-3.1
35.4	-8.2	-2.8	-8.2	-3.1
35.5	-8.2	-2.8	-8.2	-3.2
35.6	-7.9	-2.9	-7.9	-3.2
35.7	-7.7	-3.1	-7.7	-3.4
35.8	-8.0	-2.7	-8.0	-3.1
35.9	-8.4	-3.3	-8.4	-3.6
36.0	-8.5	-3.0	-8.5	-3.4
36.1	-8.5	-3.1	-8.5	-3.4
36.2	-8.9	-3.3	-8.9	-3.6
36.3	-9.0	-3.4	-9.0	-3.7
36.4	-9.3	-3.6	-9.3	-3.9
36.5	-9.0	-3.7	-9.0	-4.1
36.6	-8.2	-3.1	-8.2	-3.4
36.7	-8.1	-3.3	-8.1	-3.6
36.8	-9.0	-3.8	-9.0	-4.1
36.9	-9.3	-3.8	-9.3	-4.2
37.0	-9.2	-3.5	-9.2	-3.8

DBT (mm)	$\delta^{13}C$ (‰ VPDB)	$\delta^{18}O$ (‰ VPDB)	$\delta^{13}C$ (‰ VPDB) Aragonite and Calcite Corr (*).	$\delta^{18}O$ (‰ VPDB) Aragonite and Calcite Corr (*).
37.1	-7.7	-3.3	-7.7	-3.6
37.2	-6.5	-3.0	-6.5	-3.3
37.3	-6.0	-2.8	-6.0	-3.1
37.4	-6.3	-2.7	-6.3	-3.0
37.5	-7.0	-2.8	-7.0	-3.2
37.6	-7.3	-2.6	-7.3	-3.0
37.7	-8.4	-3.3	-8.4	-3.7
37.8	-8.8	-3.3	-8.8	-3.7
37.9	-9.1	-3.4	-9.1	-3.8
38.0	-8.8	-3.4	-8.8	-3.7
38.1	-8.9	-3.4	-8.9	-3.8
38.2	-8.0	-3.0	-8.0	-3.4
38.3	-9.1	-3.4	-9.1	-3.7
38.4	-8.9	-3.7	-8.9	-4.1
38.5	-8.6	-3.6	-8.6	-3.9
38.6	-8.4	-3.5	-8.4	-3.9
38.7	-8.8	-3.5	-8.8	-3.8
38.8	-9.0	-3.5	-9.0	-3.8
38.9	-8.8	-3.8	-8.8	-4.1
39.0	-9.1	-3.8	-9.1	-4.2
39.1	-8.5	-3.9	-8.5	-4.2
39.2	-8.6	-3.6	-8.6	-4.0
39.3	-8.6	-3.9	-8.6	-4.3
39.4	-8.7	-3.5	-8.7	-3.8
39.5	-8.1	-3.7	-8.1	-4.0
39.6	-8.1	-3.7	-8.1	-4.1
39.7	-8.1	-3.6	-8.1	-3.9
39.8	-8.2	-3.7	-8.2	-4.0
39.9	-7.8	-3.5	-7.8	-3.9
40.0	-8.2	-3.7	-8.2	-4.1
40.1	-8.8	-4.1	-8.8	-4.4
40.2	-8.5	-3.5	-8.5	-3.9
40.3	-7.8	-3.5	-7.8	-3.8
40.4	-8.0	-3.3	-8.0	-3.7
40.5	-8.3	-3.5	-8.3	-3.9
40.6	-8.3	-3.6	-8.3	-4.0
40.7	-8.2	-3.5	-8.2	-3.9

DBT (mm)	$\delta^{13}C$ (‰ VPDB)	$\delta^{18}O$ (‰ VPDB)	$\delta^{13}C$ (‰ VPDB) Aragonite and Calcite Corr (*).	$\delta^{18}O$ (‰ VPDB) Aragonite and Calcite Corr (*).
40.8	-8.2	-3.5	-8.2	-3.9
40.9	-8.5	-3.6	-8.5	-4.0
41.0	-8.5	-3.3	-8.5	-3.6
41.1	-8.1	-3.2	-8.1	-3.5
41.2	-7.9	-3.2	-7.9	-3.6
41.3	-8.1	-3.2	-8.1	-3.5
41.4	-8.5	-3.0	-8.5	-3.3
41.5	-8.4	-3.3	-8.4	-3.7
41.6	-8.1	-3.1	-8.1	-3.4
41.7	-8.5	-3.0	-8.5	-3.3
41.8	-8.0	-3.2	-8.0	-3.5
41.9	-7.2	-2.9	-7.2	-3.2
42.0	-7.2	-2.8	-7.2	-3.2
42.1	-7.6	-2.8	-7.6	-3.2
42.2	-7.6	-3.2	-7.6	-3.6
42.3	-7.5	-2.9	-7.5	-3.3
42.4	-7.7	-3.0	-7.7	-3.3
42.5	-7.7	-3.4	-7.7	-3.7
42.6	-7.3	-3.1	-7.3	-3.4
42.7	-7.5	-3.0	-7.5	-3.4
42.8	-7.7	-3.0	-7.7	-3.3
42.9	-7.5	-3.2	-7.5	-3.5
43.0	-7.5	-2.7	-7.5	-3.0
43.1	-7.4	-2.8	-7.4	-3.1
43.2	-6.7	-2.7	-6.7	-3.1
43.3	-6.6	-2.7	-6.6	-3.0
43.4	-6.3	-2.3	-6.3	-2.7
43.5	-6.3	-2.5	-6.3	-2.8
43.6	-6.5	-2.5	-6.5	-2.8
43.7	-6.4	-2.7	-6.4	-3.0
43.8	-6.8	-2.7	-6.8	-3.0
43.9	-6.7	-2.8	-6.7	-3.1
44.0	-6.0	-2.5	-6.0	-2.9
44.1	-6.5	-2.5	-6.5	-2.9
44.2	-6.2	-2.5	-6.2	-2.8
44.3	-5.8	-2.7	-5.8	-3.0
44.4	-6.1	-2.5	-6.1	-2.9

DBT (mm)	$\delta^{13}C$ (‰ VPDB)	$\delta^{18}O$ (‰ VPDB)	$\delta^{13}C$ (‰ VPDB) Aragonite and Calcite Corr (*).	$\delta^{18}O$ (‰ VPDB) Aragonite and Calcite Corr (*).
44.5	-6.0	-2.5	-6.0	-2.8
44.6	-5.9	-2.9	-5.9	-3.3
44.7	-5.6	-2.5	-5.6	-2.8
44.8	-5.6	-2.3	-5.6	-2.7
44.9	-6.5	-2.9	-6.5	-3.2
45.0	-5.8	-2.5	-5.8	-2.9
45.1	-6.3	-2.9	-6.3	-3.2
45.2	-6.5	-2.9	-6.5	-3.2
45.3	-7.2	-3.3	-7.2	-3.7
45.4	-7.5	-3.1	-7.5	-3.4
45.5	-6.9	-2.8	-6.9	-3.1
45.6	-6.9	-2.7	-6.9	-3.1
45.7	-7.1	-2.8	-7.1	-3.1
45.8	-7.5	-2.8	-7.5	-3.1
45.9	-7.4	-3.0	-7.4	-3.3
46.0	-7.1	-3.1	-7.1	-3.4
46.1	-7.1	-3.1	-7.1	-3.4
46.2	-7.5	-3.1	-7.5	-3.4
46.3	-8.3	-3.4	-8.3	-3.7
46.4	-7.4	-3.0	-7.4	-3.3
46.5	-7.4	-3.3	-7.4	-3.6
46.6	-7.4	-3.2	-7.4	-3.5
46.7	-7.8	-3.1	-7.8	-3.4
46.8	-7.6	-3.0	-7.6	-3.3
46.9	-7.5	-3.1	-7.5	-3.5
47.0	-7.4	-3.1	-7.4	-3.5
47.1	-7.5	-3.2	-7.5	-3.5
47.2	-5.3	-2.8	-5.3	-3.2
47.3	-3.9	-2.5	-3.9	-2.9
47.4	-3.3	-2.3	-3.3	-2.6
47.5	-3.3	-2.1	-3.3	-2.4
47.6	-3.7	-2.1	-3.7	-2.5
47.7	-4.2	-2.2	-4.2	-2.6
47.8	-4.9	-2.6	-4.9	-3.0
47.9	-5.4	-2.7	-5.4	-3.0
48.0	-3.9	-2.5	-3.9	-2.8
48.1	-3.1	-2.2	-3.1	-2.5

DBT (mm)	$\delta^{13}C$ (‰ VPDB)	$\delta^{18}O$ (‰ VPDB)	$\delta^{13}C$ (‰ VPDB) Aragonite and Calcite Corr (*).	$\delta^{18}O$ (‰ VPDB) Aragonite and Calcite Corr (*).
48.2	-2.6	-2.1	-2.6	-2.5
48.3	-2.8	-2.2	-2.8	-2.5
48.4	-3.5	-2.0	-3.5	-2.4
48.5	-5.2	-2.1	-5.2	-2.5
48.6	-5.8	-2.4	-5.8	-2.7
48.7	-6.1	-2.6	-6.1	-2.9
48.8	-6.6	-2.8	-6.6	-3.2
48.9	-6.7	-2.5	-6.7	-2.9
49.0	-7.2	-2.7	-7.2	-3.0
49.1	-7.1	-2.6	-7.1	-2.9
49.2	-6.5	-2.4	-6.5	-2.8
49.3	-6.1	-2.3	-6.1	-2.6
49.4	-6.5	-2.5	-6.5	-2.8
49.5	-7.1	-2.7	-7.1	-3.0
49.6	-7.0	-2.4	-7.0	-2.8
49.7	-6.9	-2.6	-6.9	-2.9
49.8	-6.8	-2.4	-6.8	-2.8
49.9	-6.9	-2.5	-6.9	-2.9
50.0	-6.8	-2.5	-6.8	-2.8
50.1	-6.8	-2.6	-6.8	-2.9
50.2	-6.9	-2.3	-6.9	-2.6
50.3	-6.7	-2.4	-6.7	-2.7
50.4	-6.3	-2.3	-6.3	-2.6
50.5	-6.6	-2.6	-6.6	-2.9
50.6	-6.5	-2.4	-6.5	-2.7
50.7	-6.6	-2.6	-6.6	-3.0
50.8	-6.7	-2.7	-6.7	-3.1
50.9	-6.8	-2.7	-6.8	-3.0
51.0	-7.1	-3.0	-7.1	-3.3
51.1	-7.4	-3.3	-7.4	-3.6
51.2	-7.9	-3.0	-7.9	-3.4
51.3	-7.7	-3.1	-7.7	-3.4
51.4	-7.3	-3.0	-7.3	-3.3
51.5	-7.0	-3.0	-7.0	-3.3
51.6	-6.6	-2.9	-6.6	-3.2
51.7	-6.6	-2.8	-6.6	-3.2
51.8	-6.6	-2.8	-6.6	-3.2

DBT (mm)	$\delta^{13}C$ (‰ VPDB)	$\delta^{18}O$ (‰ VPDB)	$\delta^{13}C$ (‰ VPDB) Aragonite and Calcite Corr (*).	$\delta^{18}O$ (‰ VPDB) Aragonite and Calcite Corr (*).
51.9	-6.6	-2.8	-6.6	-3.1
52.0	-6.6	-2.8	-6.6	-3.1
52.1	-6.7	-2.7	-6.7	-3.0
52.2	-6.8	-2.8	-6.8	-3.1
52.3	-7.4	-2.7	-7.4	-3.1
52.4	-7.6	-3.1	-7.6	-3.5
52.5	-7.5	-2.7	-7.5	-3.0
52.6	-7.4	-2.8	-7.4	-3.1
52.7	-7.5	-2.7	-7.5	-3.1
52.8	-7.2	-2.8	-7.2	-3.1
52.9	-7.4	-2.8	-7.4	-3.1
53.0	-7.4	-2.9	-7.4	-3.2
53.1	-7.3	-2.7	-7.3	-3.0
53.2	-7.0	-2.5	-7.0	-2.8
53.3	-6.7	-2.4	-6.7	-2.7
53.4	-6.7	-2.3	-6.7	-2.6
53.5	-6.7	-2.5	-6.7	-2.8
53.6	-6.7	-2.6	-6.7	-2.9
53.7	-6.6	-2.3	-6.6	-2.7
53.8	-6.4	-2.5	-6.4	-2.9
53.9	-6.3	-2.6	-6.3	-2.9
54.0	-6.1	-2.6	-6.1	-2.9
54.1	-6.0	-2.3	-6.0	-2.6
54.2	-5.8	-2.4	-5.8	-2.8
54.3	-5.6	-2.5	-5.6	-2.8
54.4	-5.8	-2.8	-5.8	-3.1
54.5	-5.9	-2.5	-5.9	-2.9
54.6	-6.1	-2.7	-6.1	-3.1
54.7	-6.3	-2.7	-6.3	-3.1
54.8	-6.4	-2.7	-6.4	-3.0
54.9	-6.4	-2.8	-6.4	-3.2
55.0	-6.2	-2.6	-6.2	-2.9
55.1	-5.7	-2.6	-5.7	-2.9
55.2	-5.8	-2.3	-5.8	-2.7
55.3	-6.0	-3.1	-6.0	-3.4
55.4	-6.1	-3.2	-6.1	-3.6
55.5	-6.3	-3.2	-6.3	-3.5

DBT (mm)	$\delta^{13}C$ (‰ VPDB)	$\delta^{18}O$ (‰ VPDB)	$\delta^{13}C$ (‰ VPDB) Aragonite and Calcite Corr (*).	$\delta^{18}O$ (‰ VPDB) Aragonite and Calcite Corr (*).
55.6	-6.2	-3.1	-6.2	-3.5
55.7	-6.3	-3.1	-6.3	-3.5
55.8	-6.2	-2.8	-6.2	-3.1
55.9	-6.3	-3.0	-6.3	-3.3
56.0	-6.4	-3.1	-6.4	-3.4
56.1	-6.5	-2.9	-6.5	-3.3
56.2	-6.1	-3.1	-6.1	-3.5
56.3	-5.5	-3.1	-5.5	-3.5
56.4	-5.1	-2.7	-5.1	-3.0
56.5	-5.5	-2.8	-5.5	-3.1
56.6	-5.9	-2.7	-5.9	-3.0
56.7	-5.8	-2.6	-5.8	-3.0
56.8	-6.6	-2.8	-6.6	-3.1
56.9	-6.8	-2.8	-6.8	-3.1
57.0	-6.5	-2.8	-6.5	-3.1
57.1	-6.6	-3.0	-6.6	-3.4
57.2	-6.9	-3.0	-6.9	-3.4
57.3	-7.0	-3.0	-7.0	-3.4
57.4	-7.1	-2.8	-7.1	-3.2
57.5	-6.8	-2.8	-6.8	-3.1
57.6	-6.8	-2.9	-6.8	-3.2
57.7	-7.2	-3.1	-7.2	-3.4
57.8	-7.7	-3.2	-7.7	-3.6
57.9	-7.7	-3.6	-7.7	-3.9
58.0	-7.3	-3.3	-7.3	-3.6
58.1	-7.0	-3.1	-7.0	-3.5
58.2	-7.6	-3.2	-7.6	-3.5
58.3	-7.8	-3.2	-7.8	-3.5
58.4	-7.7	-3.1	-7.7	-3.4
58.5	-7.4	-3.1	-7.4	-3.4
58.6	-7.1	-3.0	-7.1	-3.4
58.7	-6.7	-2.8	-6.7	-3.1
58.8	-6.5	-2.9	-6.5	-3.2
58.9	-6.4	-2.7	-6.4	-3.0
59.0	-6.0	-2.8	-6.0	-3.1
59.1	-6.4	-2.8	-6.4	-3.1
59.2	-6.5	-2.8	-6.5	-3.2

DBT (mm)	$\delta^{13}C$ (‰ VPDB)	$\delta^{18}O$ (‰ VPDB)	$\delta^{13}C$ (‰ VPDB) Aragonite and Calcite Corr (*).	$\delta^{18}O$ (‰ VPDB) Aragonite and Calcite Corr (*).
59.3	-6.2	-3.0	-6.2	-3.3
59.4	-6.2	-3.1	-6.2	-3.4
59.5	-6.2	-3.3	-6.2	-3.6
59.6	-5.9	-3.2	-5.9	-3.5
59.7	-5.9	-3.4	-5.9	-3.7
59.8	-6.1	-3.1	-6.1	-3.5
59.9	-6.2	-2.9	-6.2	-3.3
60.0	-6.3	-3.0	-6.3	-3.3
60.1	-6.4	-3.1	-6.4	-3.4
60.2	-6.3	-3.2	-6.3	-3.5
60.3	-6.1	-3.0	-6.1	-3.3
60.4	-6.0	-3.0	-6.0	-3.3
60.5	-6.0	-3.2	-6.0	-3.5
60.6	-6.4	-3.4	-6.4	-3.7
60.7	-6.6	-3.4	-6.6	-3.7
60.8	-6.4	-3.2	-6.4	-3.5
60.9	-6.2	-3.0	-6.2	-3.4
61.0	-6.2	-3.1	-6.2	-3.4
61.1	-6.6	-3.2	-6.6	-3.5
61.2	-6.8	-3.3	-6.8	-3.6
61.3	-7.1	-3.2	-7.1	-3.6
61.4	-7.2	-3.2	-7.2	-3.5
61.5	-7.4	-3.3	-7.4	-3.7
61.6	-7.4	-3.5	-7.4	-3.9
61.7	-7.2	-3.4	-7.2	-3.7
61.8	-7.1	-3.5	-7.1	-3.8
61.9	-6.9	-3.6	-6.9	-4.0
62.0	-7.0	-4.0	-7.0	-4.3
62.1	-7.2	-3.5	-7.2	-3.8
62.2	-7.2	-3.3	-7.2	-3.6
62.3	-6.9	-3.2	-6.9	-3.5
62.4	-7.0	-2.9	-7.0	-3.2
62.5	-7.4	-3.0	-5.4*	-2.4*
62.6	-7.0	-3.0	-5.0*	-2.4*
62.7	-7.2	-3.3	-5.2*	-2.7*
62.8	-7.3	-3.3	-5.3*	-2.7*
62.9	-7.5	-3.5	-5.5*	-2.9*

DBT (mm)	$\delta^{13}C$ (‰ VPDB)	$\delta^{18}O$ (‰ VPDB)	$\delta^{13}C$ (‰ VPDB) Aragonite and Calcite Corr (*).	$\delta^{18}O$ (‰ VPDB) Aragonite and Calcite Corr (*).
63.0	-7.8	-3.5	-5.8*	-2.9*
63.1	-7.3	-3.5	-5.3*	-2.9*
63.2	-6.6	-3.3	-4.6*	-2.7*
63.3	-7.4	-3.2	-5.4*	-2.6*
63.4	-7.5	-3.5	-5.5*	-2.9*
63.5	-7.7	-3.4	-5.7*	-2.8*
63.6	-8.3	-3.5	-6.3*	-2.9*
63.7	-9.0	-3.9	-7.0*	-3.3*
63.8	-9.5	-4.2	-7.5*	-3.6*
63.9	-9.9	-4.3	-7.9*	-3.7*
64.0	-10.0	-4.2	-8.0*	-3.6*
64.1	-10.1	-3.9	-8.1*	-3.3*
64.2	-10.2	-3.9	-8.2*	-3.3*
64.3	-10.3	-3.9	-8.3*	-3.3*
64.4	-10.3	-4.0	-8.3*	-3.4*
64.5	-10.3	-4.4	-8.3*	-3.8*
64.6	-10.2	-4.2	-8.2*	-3.6*
64.7	-10.2	-4.2	-8.2*	-3.6*
64.8	-9.9	-4.1	-7.9*	-3.5*
64.9	-9.9	-3.9	-7.9*	-3.3*
65.0	-9.9	-3.8	-7.9*	-3.2*
65.1	-10.0	-3.9	-8.0*	-3.3*
65.2	-10.1	-3.7	-8.1*	-3.1*
65.3	-10.0	-3.6	-8.0*	-3.0*
65.4	-10.0	-3.9	-8.0*	-3.3*
65.5	-10.0	-3.8	-8.0*	-3.2*
65.6	-9.9	-3.6	-7.9*	-3.0*
65.7	-10.1	-3.8	-8.1*	-3.2*
65.8	-9.9	-3.8	-7.9*	-3.2*
65.9	-10.0	-3.8	-8.0*	-3.2*
66.0	-9.9	-3.7	-7.9*	-3.1*
66.1	-9.8	-3.8	-7.8*	-3.2*
66.2	-9.9	-3.7	-7.9*	-3.1*
66.3	-9.8	-3.7	-7.8*	-3.1*
66.4	-9.9	-3.7	-7.9*	-3.1*
66.5	-10.0	-3.6	-8.0*	-3.0*
66.6	-10.1	-3.8	-8.1*	-3.2*

DBT (mm)	$\delta^{13}C$ (‰ VPDB)	$\delta^{18}O$ (‰ VPDB)	$\delta^{13}C$ (‰ VPDB) Aragonite and Calcite Corr (*).	$\delta^{18}O$ (‰ VPDB) Aragonite and Calcite Corr (*).
66.7	-9.9	-4.3	-7.9*	-3.7*
66.8	-9.9	-4.0	-7.9*	-3.4*
66.9	-10.0	-4.4	-8.0*	-3.8*
67.0	-10.0	-4.1	-8.0*	-3.5*
67.1	-9.9	-4.2	-7.9*	-3.6*
67.2	-9.8	-3.9	-7.8*	-3.3*
67.3	-9.8	-3.9	-7.8*	-3.3*
67.4	-9.7	-3.9	-7.7*	-3.3*
67.5	-9.7	-4.1	-7.7*	-3.5*
67.6	-9.4	-3.7	-7.4*	-3.1*
67.7	-9.5	-3.5	-7.5*	-2.9*
67.8	-9.4	-3.5	-7.4*	-2.9*
67.9	-9.4	-3.6	-7.4*	-3.0*
68.0	-8.5	-3.4	-6.5*	-2.8*
68.1	-8.7	-3.6	-6.7*	-3.0*
68.2	-8.7	-3.5	-6.7*	-2.9*
68.3	-9.0	-3.5	-7.0*	-2.9*
68.4	-9.1	-3.6	-7.1*	-3.0*
68.5	-9.3	-3.6	-7.3*	-3.0*
68.6	-9.4	-3.7	-7.4*	-3.1*
68.7	-9.2	-3.8	-7.2*	-3.2*
68.8	-9.0	-3.8	-7.0*	-3.2*
68.9	-9.1	-3.8	-7.1*	-3.2*
69.0	-8.9	-3.8	-6.9*	-3.2*
69.1	-8.7	-3.7	-6.7*	-3.1*
69.2	-8.7	-3.7	-6.7*	-3.1*
69.3	-8.4	-3.9	-6.4*	-3.3*
69.4	-8.1	-3.6	-6.1*	-3.0*
69.5	-8.5	-3.5	-6.5*	-2.9*
69.6	-8.1	-3.3	-6.1*	-2.7*
69.7	-8.4	-3.5	-6.4*	-2.9*
69.8	-8.1	-3.7	-8.1	-4.0
69.9	-8.3	-3.5	-8.3	-3.9
70.0	-8.0	-3.4	-8.0	-3.7
70.1	-7.9	-3.5	-7.9	-3.8
70.2	-7.9	-3.3	-7.9	-3.7
70.3	-7.8	-3.3	-7.8	-3.6

DBT (mm)	$\delta^{13}C$ (‰ VPDB)	$\delta^{18}O$ (‰ VPDB)	$\delta^{13}C$ (‰ VPDB) Aragonite and Calcite Corr (*).	$\delta^{18}O$ (‰ VPDB) Aragonite and Calcite Corr (*).
70.4	-7.5	-3.4	-7.5	-3.8
70.5	-7.1	-3.2	-7.1	-3.6
70.6	-7.2	-3.3	-7.2	-3.6
70.7	-6.8	-3.1	-6.8	-3.4
70.8	-6.9	-3.0	-6.9	-3.3
70.9	-6.7	-2.7	-6.7	-3.0
71.0	-6.6	-2.6	-6.6	-2.9
71.1	-6.6	-3.0	-6.6	-3.4
71.2	-7.3	-3.1	-7.3	-3.4
71.3	-7.0	-2.6	-7.0	-3.0
71.4	-6.7	-2.5	-6.7	-2.9
71.5	-6.5	-2.4	-6.5	-2.8
71.6	-6.8	-2.3	-6.8	-2.6
71.7	-6.9	-2.6	-6.9	-2.9
71.8	-6.8	-2.6	-6.8	-3.0
71.9	-6.1	-2.3	-6.1	-2.6
72.0	-5.9	-2.4	-5.9	-2.8
72.1	-5.6	-2.4	-5.6	-2.7
72.2	-5.9	-2.3	-5.9	-2.7
72.3	-6.0	-2.7	-6.0	-3.0
72.4	-5.6	-2.2	-5.6	-2.5
72.5	-5.7	-2.2	-5.7	-2.5
72.6	-6.4	-2.5	-6.4	-2.8
72.7	-6.0	-2.6	-6.0	-2.9
72.8	-5.4	-2.7	-5.4	-3.0
72.9	-5.3	-2.4	-5.3	-2.7
73.0	-5.7	-2.7	-5.7	-3.1
73.1	-5.9	-2.9	-5.9	-3.2
73.2	-6.8	-3.1	-6.8	-3.4
73.3	-7.6	-2.9	-7.6	-3.3
73.4	-7.6	-3.1	-7.6	-3.4
73.5	-7.6	-2.9	-7.6	-3.3
73.6	-7.7	-3.0	-7.7	-3.3
73.7	-7.4	-3.0	-7.4	-3.3
73.8	-7.6	-2.8	-7.6	-3.2
73.9	-7.7	-3.0	-7.7	-3.4
74.0	-7.6	-3.0	-7.6	-3.3

DBT (mm)	$\delta^{13}C$ (‰ VPDB)	$\delta^{18}O$ (‰ VPDB)	$\delta^{13}C$ (‰ VPDB) Aragonite and Calcite Corr (*).	$\delta^{18}O$ (‰ VPDB) Aragonite and Calcite Corr (*).
74.1	-7.7	-3.2	-7.7	-3.5
74.2	-7.7	-3.4	-7.7	-3.7
74.3	-7.6	-3.2	-7.6	-3.6
74.4	-7.8	-3.2	-7.8	-3.6
74.5	-7.7	-3.2	-7.7	-3.5
74.6	-7.5	-3.3	-7.5	-3.7
74.7	-7.2	-2.8	-7.2	-3.2
74.8	-7.3	-2.9	-7.3	-3.3
74.9	-7.4	-2.6	-7.4	-2.9
75.0	-7.5	-2.9	-7.5	-3.3
75.1	-7.6	-2.7	-7.6	-3.0
75.2	-7.6	-3.1	-7.6	-3.4
75.3	-7.6	-2.9	-7.6	-3.3
75.4	-7.3	-3.0	-7.3	-3.4
75.5	-6.8	-3.1	-6.8	-3.4
75.6	-7.5	-3.4	-7.5	-3.7
75.7	-7.9	-3.1	-7.9	-3.5
75.8	-7.9	-3.5	-7.9	-3.8
75.9	-8.3	-3.8	-8.3	-4.2
76.0	-8.4	-3.2	-8.4	-3.6
76.1	-7.6	-3.3	-7.6	-3.7
76.2	-7.7	-3.1	-7.7	-3.4
76.3	-7.9	-3.4	-7.9	-3.7
76.4	-7.2	-2.9	-7.2	-3.2
76.5	-7.1	-2.9	-7.1	-3.2
76.6	-7.7	-3.1	-7.7	-3.5
76.7	-7.8	-2.8	-7.8	-3.2
76.8	-7.4	-2.6	-7.4	-2.9
76.9	-6.8	-3.0	-6.8	-3.3
77.0	-6.6	-2.4	-6.6	-2.8
77.1	-6.7	-2.6	-6.7	-2.9
77.2	-6.9	-2.4	-6.9	-2.7
77.3	-7.0	-2.7	-7.0	-3.1
77.4	-7.0	-2.6	-7.0	-2.9
77.5	-7.3	-2.3	-7.3	-2.7
77.6	-7.3	-2.9	-7.3	-3.2
77.7	-7.1	-2.4	-7.1	-2.7

DBT (mm)	$\delta^{13}C$ (‰ VPDB)	$\delta^{18}O$ (‰ VPDB)	$\delta^{13}C$ (‰ VPDB) Aragonite and Calcite Corr (*).	$\delta^{18}O$ (‰ VPDB) Aragonite and Calcite Corr (*).
77.8	-7.0	-2.4	-7.0	-2.8
77.9	-6.5	-2.6	-6.5	-3.0
78.0	-6.0	-2.3	-6.0	-2.6
78.1	-6.9	-2.7	-6.9	-3.1
78.2	-7.2	-2.5	-7.2	-2.9
78.3	-7.0	-2.5	-7.0	-2.9
78.4	-6.8	-2.7	-6.8	-3.1
78.5	-6.7	-2.5	-6.7	-2.8
78.6	-6.7	-2.5	-6.7	-2.8
78.7	-6.6	-2.7	-6.6	-3.0
78.8	-7.0	-2.9	-7.0	-3.2
78.9	-6.8	-2.6	-6.8	-2.9
79.0	-6.5	-2.8	-6.5	-3.1
79.1	-6.7	-3.0	-6.7	-3.4
79.2	-7.3	-3.0	-7.3	-3.3
79.3	-7.0	-2.9	-7.0	-3.3
79.4	-7.0	-2.9	-7.0	-3.2
79.5	-7.0	-3.1	-7.0	-3.4
79.6	-7.0	-3.2	-7.0	-3.5
79.7	-7.1	-3.5	-7.1	-3.9
79.8	-7.4	-3.1	-7.4	-3.5
79.9	-7.6	-3.1	-7.6	-3.4
80.0	-7.4	-2.7	-7.4	-3.1
80.1	-6.8	-2.7	-6.8	-3.0
80.2	-6.5	-2.8	-6.5	-3.2
80.3	-6.4	-2.8	-6.4	-3.1
80.4	-6.5	-2.4	-6.5	-2.8
80.5	-6.9	-2.6	-6.9	-3.0
80.6	-6.8	-2.9	-6.8	-3.2
80.7	-7.1	-3.1	-7.1	-3.4
80.8	-7.3	-2.9	-7.3	-3.2
80.9	-7.5	-3.1	-7.5	-3.5
81.0	-6.9	-2.8	-6.9	-3.1
81.1	-6.6	-2.6	-6.6	-2.9
81.2	-6.8	-2.4	-6.8	-2.7
81.3	-6.9	-2.4	-6.9	-2.8
81.4	-6.5	-2.6	-6.5	-2.9

DBT (mm)	$\delta^{13}C$ (‰ VPDB)	$\delta^{18}O$ (‰ VPDB)	$\delta^{13}C$ (‰ VPDB) Aragonite and Calcite Corr (*).	$\delta^{18}O$ (‰ VPDB) Aragonite and Calcite Corr (*).
81.5	-6.0	-2.2	-6.0	-2.6
81.6	-5.7	-2.4	-5.7	-2.7
81.7	-5.8	-2.4	-5.8	-2.8
81.8	-5.9	-2.2	-5.9	-2.5
81.9	-5.8	-2.2	-5.8	-2.5
82.0	-6.2	-2.2	-6.2	-2.6
82.1	-6.1	-2.5	-6.1	-2.8
82.2	-6.3	-2.2	-6.3	-2.5
82.3	-6.2	-2.3	-6.2	-2.7
82.4	-6.7	-2.4	-6.7	-2.7
82.5	-6.3	-2.3	-6.3	-2.7
82.6	-6.3	-2.4	-6.3	-2.8
82.7	-7.0	-2.4	-7.0	-2.7
82.8	-6.1	-2.3	-6.1	-2.7
82.9	-5.7	-2.5	-5.7	-2.8
83.0	-5.9	-2.6	-5.9	-2.9
83.1	-6.1	-3.0	-6.1	-3.3
83.2	-6.3	-2.5	-6.3	-2.8
83.3	-6.0	-2.9	-6.0	-3.3
83.4	-6.3	-2.8	-6.3	-3.1
83.5	-7.2	-3.1	-7.2	-3.4
83.6	-6.4	-2.7	-6.4	-3.0
83.7	-5.8	-2.5	-5.8	-2.8
83.8	-6.3	-2.8	-6.3	-3.2
83.9	-6.0	-2.6	-6.0	-2.9
84.0	-5.6	-2.3	-5.6	-2.7
84.1	-5.8	-2.4	-5.8	-2.7
84.2	-6.3	-3.1	-6.3	-3.5
84.3	-6.7	-2.7	-6.7	-3.1
84.4	-6.6	-2.7	-6.6	-3.0
84.5	-6.6	-2.9	-6.6	-3.3
84.6	-6.4	-2.7	-6.4	-3.1
84.7	-6.3	-2.5	-6.3	-2.9
84.8	-6.8	-2.6	-6.8	-3.0
84.9	-7.1	-3.3	-7.1	-3.6
85.0	-7.1	-2.8	-7.1	-3.2
85.1	-6.3	-2.6	-6.3	-2.9

DBT (mm)	$\delta^{13}C$ (‰ VPDB)	$\delta^{18}O$ (‰ VPDB)	$\delta^{13}C$ (‰ VPDB) Aragonite and Calcite Corr (*).	$\delta^{18}O$ (‰ VPDB) Aragonite and Calcite Corr (*).
85.2	-5.1	-2.4	-5.1	-2.7
85.3	-5.0	-2.3	-5.0	-2.6
85.4	-5.0	-2.9	-5.0	-3.2
85.5	-5.3	-2.5	-5.3	-2.9
85.6	-5.5	-2.5	-5.5	-2.8
85.7	-5.4	-2.6	-5.4	-2.9
85.8	-4.9	-2.5	-4.9	-2.8
85.9	-4.8	-2.7	-4.8	-3.1
86.0	-7.2	-3.2	-7.2	-3.5
86.1	-6.2	-2.6	-6.2	-3.0
86.2	-7.4	-2.8	-7.4	-3.2
86.3	-7.1	-2.9	-7.1	-3.3
86.4	-8.0	-3.0	-8.0	-3.4
86.5	-7.5	-2.9	-7.5	-3.2
86.6	-6.3	-2.6	-6.3	-3.0
86.7	-6.9	-2.8	-6.9	-3.1
86.8	-6.2	-2.7	-6.2	-3.0
86.9	-6.8	-2.9	-6.8	-3.2
87.0	-7.6	-3.1	-7.6	-3.4
87.1	-7.5	-2.9	-7.5	-3.2
87.2	-7.1	-3.1	-7.1	-3.4
87.3	-7.5	-3.0	-7.5	-3.4
87.4	-6.2	-2.6	-6.2	-2.9
87.5	-5.3	-3.0	-5.3	-3.3
87.6	-6.4	-2.7	-6.4	-3.0
87.7	-5.6	-2.5	-5.6	-2.8
87.8	-7.3	-2.8	-7.3	-3.2
87.9	-7.1	-2.7	-7.1	-3.0
88.0	-6.7	-2.5	-6.7	-2.9
88.1	-6.3	-2.7	-6.3	-3.0
88.2	-7.5	-3.0	-7.5	-3.4
88.3	-6.7	-2.7	-6.7	-3.0
88.4	-6.5	-2.6	-6.5	-3.0
88.5	-6.1	-2.7	-6.1	-3.1
88.6	-7.9	-2.8	-7.9	-3.1
88.7	-6.3	-2.7	-6.3	-3.0
88.8	-7.4	-2.9	-7.4	-3.2

DBT (mm)	$\delta^{13}C$ (‰ VPDB)	$\delta^{18}O$ (‰ VPDB)	$\delta^{13}C$ (‰ VPDB) Aragonite and Calcite Corr (*).	$\delta^{18}O$ (‰ VPDB) Aragonite and Calcite Corr (*).
88.9	-6.0	-2.5	-6.0	-2.8
89.0	-7.6	-2.8	-7.6	-3.1
89.1	-6.5	-2.7	-6.5	-3.0
89.2	-7.0	-3.0	-7.0	-3.3
89.3	-5.9	-2.4	-5.9	-2.8
89.4	-7.7	-3.0	-7.7	-3.3
89.5	-6.8	-2.9	-6.8	-3.2
89.6	-5.9	-2.6	-5.9	-2.9
89.7	-7.8	-2.9	-7.8	-3.3
89.8	-7.3	-2.9	-7.3	-3.3
89.9	-6.6	-2.5	-6.6	-2.9
90.0	-7.6	-3.1	-7.6	-3.5
90.1	-6.2	-2.4	-6.2	-2.7
90.2	-5.8	-2.4	-5.8	-2.8
90.3	-5.9	-2.4	-5.9	-2.7
90.4	-6.1	-2.5	-6.1	-2.8
90.5	-6.4	-2.5	-6.4	-2.8
90.6	-6.5	-2.7	-6.5	-3.1
90.7	-6.5	-2.6	-6.5	-2.9
90.8	-6.4	-2.5	-6.4	-2.8
90.9	-6.7	-2.8	-6.7	-3.1
91.0	-6.8	-2.5	-6.8	-2.9
91.1	-6.9	-2.5	-6.9	-2.8
91.2	-6.7	-2.8	-6.7	-3.1
91.3	-6.7	-2.5	-6.7	-2.9
91.4	-6.4	-2.5	-6.4	-2.9
91.5	-6.3	-3.1	-6.3	-3.4
91.6	-6.3	-2.4	-6.3	-2.8
91.7	-6.6	-2.5	-6.6	-2.8
91.8	-6.8	-2.6	-6.8	-2.9
91.9	-6.5	-2.4	-6.5	-2.8
92.0	-6.5	-2.7	-6.5	-3.0
92.1	-6.4	-2.3	-6.4	-2.7
92.2	-6.1	-2.3	-6.1	-2.7
92.3	-6.2	-2.2	-6.2	-2.6
92.4	-6.6	-2.8	-6.6	-3.2
92.5	-6.9	-2.4	-6.9	-2.8

DBT (mm)	$\delta^{13}C$ (‰ VPDB)	$\delta^{18}O$ (‰ VPDB)	$\delta^{13}C$ (‰ VPDB) Aragonite and Calcite Corr (*).	$\delta^{18}O$ (‰ VPDB) Aragonite and Calcite Corr (*).
92.6	-7.1	-2.7	-7.1	-3.1
92.7	-6.9	-2.6	-6.9	-3.0
92.8	-6.5	-2.6	-6.5	-2.9
92.9	-6.3	-2.6	-6.3	-2.9
93.0	-6.6	-2.4	-6.6	-2.8
93.1	-7.6	-2.7	-7.6	-3.0
93.2	-7.9	-2.7	-7.9	-3.0
93.3	-7.5	-2.8	-7.5	-3.1
93.4	-7.0	-2.6	-7.0	-3.0
93.5	-6.4	-2.4	-6.4	-2.7
93.6	-6.4	-2.7	-6.4	-3.0
93.7	-6.5	-2.5	-6.5	-2.8
93.8	-6.7	-2.7	-6.7	-3.0
93.9	-6.6	-2.6	-6.6	-3.0
94.0	-6.5	-2.8	-6.5	-3.1
94.1	-6.0	-2.2	-6.0	-2.5
94.2	-6.0	-2.5	-6.0	-2.8
94.3	-5.9	-2.3	-5.9	-2.7
94.4	-6.5	-2.7	-6.5	-3.0
94.5	-7.1	-2.7	-7.1	-3.0
94.6	-7.5	-2.5	-7.5	-2.9
94.7	-7.1	-2.9	-7.1	-3.3
94.8	-6.8	-2.4	-6.8	-2.7
94.9	-7.0	-2.7	-7.0	-3.1
95.0	-6.5	-2.6	-6.5	-3.0
95.1	-7.6	-2.8	-7.6	-3.1
95.2	-7.8	-2.8	-7.8	-3.1
95.3	-8.3	-3.1	-8.3	-3.4
95.4	-8.1	-3.1	-8.1	-3.4
95.5	-7.8	-3.0	-7.8	-3.3
95.6	-8.2	-3.1	-8.2	-3.4
95.7	-7.3	-3.0	-7.3	-3.3
95.8	-6.7	-2.7	-6.7	-3.1
95.9	-6.7	-3.0	-6.7	-3.3
96.0	-6.8	-2.7	-6.8	-3.1
96.1	-6.5	-2.4	-6.5	-2.8
96.2	-6.4	-2.5	-6.4	-2.9

DBT (mm)	$\delta^{13}C$ (‰ VPDB)	$\delta^{18}O$ (‰ VPDB)	$\delta^{13}C$ (‰ VPDB) Aragonite and Calcite Corr (*).	$\delta^{18}O$ (‰ VPDB) Aragonite and Calcite Corr (*).
96.3	-6.2	-2.6	-6.2	-2.9
96.4	-6.1	-2.4	-6.1	-2.7
96.5	-7.7	-2.5	-7.7	-2.8
96.6	-6.2	-2.4	-6.2	-2.8
96.7	-6.3	-2.4	-6.3	-2.7
96.8	-6.4	-2.4	-6.4	-2.7
96.9	-6.7	-2.6	-6.7	-2.9
97.0	-6.6	-2.5	-6.6	-2.8
97.1	-6.4	-2.7	-6.4	-3.0
97.2	-6.4	-2.6	-6.4	-2.9
97.3	-6.4	-2.6	-6.4	-2.9
97.4	-6.4	-2.5	-6.4	-2.8
97.5	-6.8	-2.7	-6.8	-3.0
97.6	-7.0	-2.8	-7.0	-3.2
97.7	-7.0	-3.0	-7.0	-3.3
97.8	-6.7	-3.0	-6.7	-3.3
97.9	-6.7	-2.7	-6.7	-3.1
98.0	-6.9	-3.1	-6.9	-3.5
98.1	-6.6	-2.9	-6.6	-3.2
98.2	-6.6	-2.9	-6.6	-3.2
98.3	-7.0	-2.9	-7.0	-3.2
98.4	-6.9	-2.9	-6.9	-3.2
98.5	-6.9	-3.2	-6.9	-3.5
98.6	-6.8	-2.8	-6.8	-3.2
98.7	-6.7	-3.0	-6.7	-3.3
98.8	-6.2	-3.1	-6.2	-3.5
98.9	-6.2	-3.1	-6.2	-3.4
99.0	-6.3	-3.3	-6.3	-3.6
99.1	-7.0	-2.7	-7.0	-3.0
99.2	-6.7	-3.0	-6.7	-3.3
99.3	-6.5	-2.6	-6.5	-3.0
99.4	-6.7	-2.7	-6.7	-3.0
99.5	-6.4	-2.6	-6.4	-3.0
99.6	-6.4	-2.7	-6.4	-3.0
99.7	-6.4	-2.7	-6.4	-3.0
99.8	-6.3	-2.8	-6.3	-3.1
99.9	-6.6	-2.9	-6.6	-3.2

DBT (mm)	$\delta^{13}C$ (‰ VPDB)	$\delta^{18}O$ (‰ VPDB)	$\delta^{13}C$ (‰ VPDB) Aragonite and Calcite Corr (*).	$\delta^{18}O$ (‰ VPDB) Aragonite and Calcite Corr (*).
100.0	-6.8	-3.4	-6.8	-3.7
100.2	-7.0	-3.9	-7.0	-4.2
100.4	-6.9	-3.5	-6.9	-3.9
100.6	-7.3	-3.7	-7.3	-4.0
100.8	-6.9	-3.1	-6.9	-3.5
101.0	-7.0	-3.2	-7.0	-3.5
101.2	-7.5	-3.7	-7.5	-4.1
101.4	-7.4	-3.4	-7.4	-3.8
101.6	-7.4	-3.1	-7.4	-3.5
101.8	-7.5	-3.4	-7.5	-3.8
102.0	-7.3	-3.5	-7.3	-3.9
102.2	-7.5	-3.7	-7.5	-4.1
102.4	-7.5	-3.5	-7.5	-3.8
102.6	-7.4	-3.3	-7.4	-3.7
102.8	-7.5	-3.6	-7.5	-3.9
103.0	-7.5	-3.5	-7.5	-3.9
103.2	-7.6	-3.6	-7.6	-3.9
103.4	-7.3	-3.3	-7.3	-3.6
103.6	-7.4	-3.2	-7.4	-3.6
103.8	-7.3	-3.3	-7.3	-3.7
104.0	-7.5	-3.6	-7.5	-3.9
104.2	-7.3	-3.4	-7.3	-3.7
104.4	-7.2	-3.4	-7.2	-3.7
104.6	-7.3	-3.6	-7.3	-3.9
104.8	-7.6	-3.6	-7.6	-4.0
105.0	-7.6	-3.5	-7.6	-3.8
105.2	-7.3	-3.1	-7.3	-3.4
105.4	-7.3	-3.1	-7.3	-3.5
105.6	-7.7	-3.3	-7.7	-3.6
105.8	-7.7	-3.0	-7.7	-3.4
106.0	-7.4	-3.3	-7.4	-3.6
106.2	-7.4	-3.2	-7.4	-3.5
106.4	-7.5	-3.1	-7.5	-3.4
106.6	-7.7	-3.1	-7.7	-3.4
106.8	-7.5	-3.2	-7.5	-3.5
107.0	-7.1	-3.1	-7.1	-3.4
107.2	-7.1	-3.2	-7.1	-3.5

DBT (mm)	$\delta^{13}C$ (‰ VPDB)	$\delta^{18}O$ (‰ VPDB)	$\delta^{13}C$ (‰ VPDB) Aragonite and Calcite Corr (*).	$\delta^{18}O$ (‰ VPDB) Aragonite and Calcite Corr (*).
107.4	-7.1	-3.4	-7.1	-3.7
107.6	-7.2	-3.7	-7.2	-4.0
107.8	-7.4	-3.8	-7.4	-4.1
108.0	-7.2	-3.5	-7.2	-3.8
108.2	-7.0	-3.4	-7.0	-3.7
108.4	-7.0	-3.5	-7.0	-3.8
108.6	-6.9	-3.3	-6.9	-3.6
108.8	-6.8	-3.2	-6.8	-3.5
109.0	-6.9	-3.2	-6.9	-3.5
109.2	-6.8	-3.0	-6.8	-3.4
109.4	-6.8	-3.2	-6.8	-3.6
109.6	-7.0	-3.7	-7.0	-4.0
109.8	-6.8	-3.6	-6.8	-3.9
110.0	-6.8	-3.5	-6.8	-3.8
110.2	-7.3	-4.2	-7.3	-4.6
110.4	-6.4	-3.7	-6.4	-4.0
110.6	-6.0	-3.6	-6.0	-3.9
110.8	-6.2	-4.0	-6.2	-4.3
111.0	-5.9	-3.6	-5.9	-4.0
111.2	-5.8	-3.3	-5.8	-3.7
111.4	-6.2	-3.3	-6.2	-3.6
111.6	-6.4	-3.6	-6.4	-3.9
111.8	-6.4	-3.2	-6.4	-3.5
112.0	-6.3	-3.4	-6.3	-3.7
112.2	-6.4	-3.4	-6.4	-3.8
112.4	-6.5	-3.5	-6.5	-3.8
112.6	-6.7	-4.0	-6.7	-4.3
112.8	-6.6	-3.9	-6.6	-4.3
113.0	-6.6	-4.0	-6.6	-4.3
113.2	-6.5	-3.7	-6.5	-4.1
113.4	-6.5	-3.5	-6.5	-3.8
113.6	-6.2	-3.3	-6.2	-3.7
113.8	-6.0	-3.2	-6.0	-3.5
114.0	-5.7	-3.3	-5.7	-3.7
114.2	-5.8	-3.6	-5.8	-3.9
114.4	-5.8	-3.4	-5.8	-3.7
114.6	-5.5	-3.2	-5.5	-3.5

DBT (mm)	$\delta^{13}C$ (‰ VPDB)	$\delta^{18}O$ (‰ VPDB)	$\delta^{13}C$ (‰ VPDB) Aragonite and Calcite Corr (*).	$\delta^{18}O$ (‰ VPDB) Aragonite and Calcite Corr (*).
114.8	-5.6	-3.1	-5.6	-3.4
115.0	-5.6	-3.4	-5.6	-3.7
115.2	-5.7	-3.5	-5.7	-3.9
115.4	-5.7	-3.7	-5.7	-4.1
115.6	-5.7	-3.0	-5.7	-3.3
115.8	-5.2	-2.9	-5.2	-3.3
116.0	-5.2	-3.2	-5.2	-3.6
116.2	-5.1	-3.9	-5.1	-4.2
116.4	-5.4	-3.5	-5.4	-3.8
116.6	-5.3	-3.4	-5.3	-3.7
116.8	-5.2	-3.1	-5.2	-3.4
117.0	-5.7	-3.8	-5.7	-4.1
117.2	-6.3	-4.5	-6.3	-4.8
117.4	-6.5	-4.1	-6.5	-4.4
117.6	-6.6	-3.8	-6.6	-4.2
117.8	-6.3	-3.9	-6.3	-4.2
118.0	-6.4	-3.3	-6.4	-3.6
118.2	-6.6	-3.7	-6.6	-4.0
118.4	-6.6	-3.2	-6.6	-3.6
118.6	-6.8	-3.8	-6.8	-4.2
118.8	-6.6	-3.7	-6.6	-4.0
119.0	-6.8	-3.8	-6.8	-4.1
119.2	-6.7	-3.3	-6.7	-3.6
119.4	-6.9	-3.7	-6.9	-4.0
119.6	-6.5	-3.0	-6.5	-3.4
119.8	-6.6	-3.3	-6.6	-3.6
120.0	-6.7	-3.4	-6.7	-3.8
120.2	-6.9	-3.7	-6.9	-4.0
120.4	-6.8	-3.3	-6.8	-3.6
120.6	-6.5	-3.2	-6.5	-3.5
120.8	-6.7	-3.4	-6.7	-3.7
121.0	-6.9	-3.5	-6.9	-3.8
121.2	-6.7	-3.0	-6.7	-3.4
121.4	-7.0	-3.9	-7.0	-4.2
121.6	-6.7	-3.3	-6.7	-3.6
121.8	-6.4	-3.1	-6.4	-3.5
122.0	-6.5	-3.3	-6.5	-3.7

DBT (mm)	$\delta^{13}C$ (‰ VPDB)	$\delta^{18}O$ (‰ VPDB)	$\delta^{13}C$ (‰ VPDB) Aragonite and Calcite Corr (*).	$\delta^{18}O$ (‰ VPDB) Aragonite and Calcite Corr (*).
122.2	-6.1	-3.4	-6.1	-3.7
122.4	-6.0	-3.5	-6.0	-3.9
122.6	-6.1	-3.5	-6.1	-3.9
122.8	-6.1	-3.1	-6.1	-3.4
123.0	-5.9	-3.1	-5.9	-3.4
123.2	-5.8	-3.4	-5.8	-3.8
123.4	-6.2	-3.6	-6.2	-3.9
123.6	-6.8	-3.5	-6.8	-3.9
123.8	-6.8	-3.5	-6.8	-3.9
124.0	-6.6	-3.7	-6.6	-4.0
124.2	-6.0	-3.3	-6.0	-3.6
124.4	-6.4	-3.4	-6.4	-3.7
124.6	-6.6	-3.6	-6.6	-3.9
124.8	-5.6	-2.9	-5.6	-3.2
125.0	-5.6	-3.0	-5.6	-3.4
125.2	-5.5	-3.0	-5.5	-3.3
125.4	-5.6	-2.8	-5.6	-3.2
125.6	-5.9	-3.5	-5.9	-3.8
125.8	-6.1	-2.9	-6.1	-3.3
126.0	-6.1	-3.2	-6.1	-3.5
126.2	-5.1	-2.9	-5.1	-3.2
126.4	-4.2	-2.8	-4.2	-3.2
126.6	-5.3	-2.8	-5.3	-3.1
126.8	-6.3	-3.2	-6.3	-3.5
127.0	-6.5	-2.8	-6.5	-3.2
127.2	-7.2	-3.3	-7.2	-3.7
127.4	-6.6	-3.5	-6.6	-3.8
127.6	-7.0	-3.0	-7.0	-3.4
127.8	-6.7	-3.4	-6.7	-3.7
128.0	-6.5	-2.9	-6.5	-3.3
128.2	-7.2	-3.6	-7.2	-3.9
128.4	-7.5	-3.4	-7.5	-3.7
128.6	-7.5	-3.3	-7.5	-3.6
128.8	-7.0	-3.2	-7.0	-3.5
129.0	-6.8	-3.1	-6.8	-3.5
129.2	-5.4	-2.5	-5.4	-2.9
129.4	-5.0	-2.6	-5.0	-3.0

DBT (mm)	$\delta^{13}C$ (‰ VPDB)	$\delta^{18}O$ (‰ VPDB)	$\delta^{13}C$ (‰ VPDB) Aragonite and Calcite Corr (*).	$\delta^{18}O$ (‰ VPDB) Aragonite and Calcite Corr (*).
129.6	-5.5	-2.7	-5.5	-3.1
129.8	-6.4	-3.2	-6.4	-3.6
130.0	-6.2	-2.9	-6.2	-3.2
130.2	-6.5	-3.4	-6.5	-3.8
130.4	-5.3	-2.4	-5.3	-2.8
130.6	-5.1	-2.6	-5.1	-2.9
130.8	-4.5	-2.8	-4.5	-3.1
131.0	-4.8	-2.7	-4.8	-3.0
131.2	-6.2	-3.1	-6.2	-3.4
131.4	-6.5	-2.8	-6.5	-3.2
131.6	-6.2	-3.0	-6.2	-3.3
131.8	-5.8	-3.2	-5.8	-3.6
132.0	-6.4	-3.3	-6.4	-3.6
132.2	-7.0	-3.5	-7.0	-3.8
132.4	-6.5	-3.2	-6.5	-3.5
132.6	-6.3	-2.7	-6.3	-3.0
132.8	-5.4	-2.7	-5.4	-3.1
133.0	-6.0	-3.6	-6.0	-4.0
133.2	-5.9	-3.2	-5.9	-3.5
133.4	-5.5	-3.2	-5.5	-3.6
133.6	-5.5	-3.5	-5.5	-3.9
133.8	-5.3	-3.0	-5.3	-3.4
134.0	-5.3	-3.3	-5.3	-3.6
134.2	-5.1	-2.8	-5.1	-3.2
134.4	-5.3	-2.9	-5.3	-3.2
134.6	-5.7	-3.1	-5.7	-3.4
134.8	-5.9	-3.0	-5.9	-3.4
135.0	-4.5	-2.6	-4.5	-3.0
135.2	-4.8	-2.8	-4.8	-3.1
135.4	-4.5	-2.6	-4.5	-2.9
135.6	-3.9	-2.5	-3.9	-2.8
135.8	-3.9	-2.8	-3.9	-3.1
136.0	-4.4	-2.8	-4.4	-3.2
136.2	-4.5	-3.1	-4.5	-3.4
136.4	-4.5	-2.9	-4.5	-3.2
136.6	-4.6	-2.7	-4.6	-3.0
136.8	-4.2	-2.5	-4.2	-2.9

DBT (mm)	$\delta^{13}C$ (‰ VPDB)	$\delta^{18}O$ (‰ VPDB)	$\delta^{13}C$ (‰ VPDB) Aragonite and Calcite Corr (*).	$\delta^{18}O$ (‰ VPDB) Aragonite and Calcite Corr (*).
137.0	-4.1	-2.5	-4.1	-2.8
137.2	-4.1	-2.4	-4.1	-2.8
137.4	-3.7	-2.8	-3.7	-3.2
137.6	-4.1	-2.7	-4.1	-3.1
137.8	-4.2	-2.9	-4.2	-3.2
138.0	-4.5	-2.8	-4.5	-3.1
138.2	-4.7	-3.0	-4.7	-3.3
138.4	-4.1	-2.7	-4.1	-3.0
138.6	-3.8	-2.7	-3.8	-3.0
138.8	-4.3	-2.8	-4.3	-3.2
139.0	-4.9	-2.9	-4.9	-3.3
139.2	-5.2	-3.1	-5.2	-3.4
139.4	-4.7	-3.0	-4.7	-3.3
139.6	-4.6	-2.9	-4.6	-3.2
139.8	-5.0	-2.9	-5.0	-3.2
140.0	-5.5	-2.8	-5.5	-3.2
140.2	-4.6	-2.6	-4.6	-2.9
140.4	-4.4	-2.7	-4.4	-3.0
140.6	-5.1	-3.1	-5.1	-3.4
140.8	-5.2	-2.9	-5.2	-3.3
141.0	-5.3	-3.2	-5.3	-3.5
141.2	-5.4	-3.2	-5.4	-3.6
141.4	-6.0	-3.0	-6.0	-3.4
141.6	-6.5	-3.5	-6.5	-3.8
141.8	-5.5	-2.9	-5.5	-3.3
142.0	-5.1	-3.1	-5.1	-3.4
142.2	-5.7	-3.3	-5.7	-3.6
142.4	-5.4	-2.9	-5.4	-3.2
142.6	-5.3	-3.0	-5.3	-3.3
142.8	-5.2	-3.0	-5.2	-3.4
143.0	-5.5	-3.0	-5.5	-3.3
143.2	-5.1	-2.9	-5.1	-3.2
143.4	-5.1	-3.0	-5.1	-3.4
143.6	-5.2	-2.9	-5.2	-3.2
143.8	-5.0	-2.8	-5.0	-3.2
144.0	-4.6	-2.4	-4.6	-2.7
144.2	-5.1	-2.8	-5.1	-3.2

DBT (mm)	$\delta^{13}C$ (‰ VPDB)	$\delta^{18}O$ (‰ VPDB)	$\delta^{13}C$ (‰ VPDB) Aragonite and Calcite Corr (*).	$\delta^{18}O$ (‰ VPDB) Aragonite and Calcite Corr (*).
144.4	-5.0	-2.8	-5.0	-3.1
144.6	-4.9	-2.5	-4.9	-2.9
144.8	-4.5	-2.2	-4.5	-2.6
145.0	-4.4	-2.4	-4.4	-2.8
145.2	-4.7	-2.7	-4.7	-3.0
145.4	-5.5	-2.8	-5.5	-3.1
145.6	-6.0	-3.1	-6.0	-3.5
145.8	-6.5	-3.8	-6.5	-4.1
146.0	-6.4	-3.4	-6.4	-3.7
146.2	-5.5	-2.8	-5.5	-3.1
146.4	-6.5	-2.8	-6.5	-3.2
146.6	-6.6	-3.6	-6.6	-4.0
146.8	-6.1	-3.2	-6.1	-3.5
147.0	-6.0	-3.0	-6.0	-3.3
147.2	-6.3	-2.8	-6.3	-3.1
147.4	-5.9	-3.1	-5.9	-3.4
147.6	-5.2	-2.3	-5.2	-2.6
147.8	-6.4	-3.3	-6.4	-3.7
148.0	-5.5	-2.6	-5.5	-2.9
148.2	-5.2	-2.9	-5.2	-3.2
148.4	-5.6	-2.7	-5.6	-3.1
148.6	-5.7	-2.7	-5.7	-3.0
148.8	-5.6	-2.7	-5.6	-3.1
149.0	-5.0	-2.9	-5.0	-3.3
149.2	-4.0	-2.8	-4.0	-3.2
149.4	-3.6	-3.0	-3.6	-3.3
149.6	-4.2	-2.9	-4.2	-3.2
149.8	-4.5	-2.9	-4.5	-3.2
150.0	-4.7	-3.0	-4.7	-3.3
150.2	-5.0	-3.0	-5.0	-3.3
150.4	-4.8	-3.2	-4.8	-3.5
150.6	-6.5	-3.2	-6.5	-3.6
150.8	-6.4	-3.2	-6.4	-3.6
151.0	-6.6	-3.2	-6.6	-3.5
151.2	-7.1	-3.4	-7.1	-3.8
151.4	-6.6	-3.5	-6.6	-3.8
151.6	-6.5	-3.2	-6.5	-3.5

DBT (mm)	$\delta^{13}C$ (‰ VPDB)	$\delta^{18}O$ (‰ VPDB)	$\delta^{13}C$ (‰ VPDB) Aragonite and Calcite Corr (*).	$\delta^{18}O$ (‰ VPDB) Aragonite and Calcite Corr (*).
151.8	-6.0	-3.3	-6.0	-3.6
152.0	-5.4	-3.4	-5.4	-3.7
152.2	-5.1	-2.8	-5.1	-3.1
152.4	-5.5	-2.9	-5.5	-3.2
152.6	-5.5	-2.7	-5.5	-3.1
152.8	-5.8	-3.3	-5.8	-3.6
153.0	-5.6	-2.7	-5.6	-3.1
153.2	-5.9	-3.6	-5.9	-3.9
153.4	-5.9	-2.9	-5.9	-3.2
153.6	-6.5	-3.5	-6.5	-3.9
153.8	-6.5	-3.0	-6.5	-3.3
154.0	-6.7	-3.2	-6.7	-3.6
154.2	-6.8	-3.5	-6.8	-3.9
154.4	-7.0	-3.5	-7.0	-3.8
154.6	-6.7	-3.4	-6.7	-3.7
154.8	-6.7	-3.0	-6.7	-3.3
155.0	-7.0	-3.3	-7.0	-3.6
155.2	-7.1	-3.3	-7.1	-3.7
155.4	-7.1	-3.6	-7.1	-3.9
155.6	-7.1	-3.5	-7.1	-3.9
155.8	-6.9	-3.2	-6.9	-3.6
156.0	-6.7	-3.1	-6.7	-3.4
156.2	-6.8	-3.1	-6.8	-3.5
156.4	-6.8	-3.2	-6.8	-3.5
156.6	-7.0	-3.5	-7.0	-3.8
156.8	-6.9	-3.3	-6.9	-3.6
157.0	-6.9	-3.5	-6.9	-3.8
157.2	-6.8	-3.4	-6.8	-3.7
157.4	-6.8	-3.3	-6.8	-3.6
157.6	-6.8	-3.4	-6.8	-3.7
157.8	-6.8	-3.6	-6.8	-4.0
158.0	-6.7	-3.2	-6.7	-3.5
158.2	-6.8	-3.1	-6.8	-3.4
158.4	-6.8	-2.8	-6.8	-3.1
158.6	-6.8	-3.1	-6.8	-3.4
158.8	-7.0	-2.9	-7.0	-3.2
159.0	-7.1	-2.8	-7.1	-3.1

DBT (mm)	$\delta^{13}C$ (‰ VPDB)	$\delta^{18}O$ (‰ VPDB)	$\delta^{13}C$ (‰ VPDB) Aragonite and Calcite Corr (*).	$\delta^{18}O$ (‰ VPDB) Aragonite and Calcite Corr (*).
159.2	-7.3	-3.1	-7.3	-3.4
159.4	-7.4	-3.3	-7.4	-3.6
159.6	-7.4	-3.1	-7.4	-3.4
159.8	-7.2	-2.9	-7.2	-3.2
160.0	-7.0	-3.4	-7.0	-3.7
160.2	-6.8	-3.2	-6.8	-3.5
160.4	-6.8	-3.1	-6.8	-3.4
160.6	-7.0	-3.1	-7.0	-3.4
160.8	-7.2	-3.1	-7.2	-3.4
161.0	-7.4	-3.1	-7.4	-3.5
161.2	-7.5	-3.2	-7.5	-3.5
161.4	-7.4	-3.3	-7.4	-3.7
161.6	-7.4	-3.6	-7.4	-4.0
161.8	-7.3	-3.5	-7.3	-3.9
162.0	-7.3	-3.2	-7.3	-3.6
162.2	-7.3	-3.3	-7.3	-3.6
162.4	-7.4	-3.3	-7.4	-3.6
162.6	-7.2	-3.4	-7.2	-3.7
162.8	-7.1	-3.0	-7.1	-3.4
163.0	-7.2	-2.9	-7.2	-3.2
163.2	-7.1	-3.2	-7.1	-3.5
163.4	-7.2	-3.1	-7.2	-3.4
163.6	-7.3	-3.3	-7.3	-3.7
163.8	-7.0	-3.2	-7.0	-3.5
164.0	-7.0	-3.0	-7.0	-3.3
164.2	-6.8	-2.9	-6.8	-3.2
164.4	-6.8	-3.1	-6.8	-3.5
164.6	-6.8	-2.8	-6.8	-3.1
164.8	-7.1	-3.2	-7.1	-3.5
165.0	-7.1	-3.3	-7.1	-3.7
165.2	-7.2	-3.3	-7.2	-3.7
165.4	-7.3	-3.4	-7.3	-3.7
165.6	-7.2	-3.0	-7.2	-3.3
165.8	-7.4	-3.5	-7.4	-3.8
166.0	-7.3	-3.1	-7.3	-3.5
166.2	-7.3	-3.3	-7.3	-3.7
166.4	-7.2	-3.5	-7.2	-3.8

DBT (mm)	$\delta^{13}C$ (‰ VPDB)	$\delta^{18}O$ (‰ VPDB)	$\delta^{13}C$ (‰ VPDB) Aragonite and Calcite Corr (*).	$\delta^{18}O$ (‰ VPDB) Aragonite and Calcite Corr (*).
166.6	-7.2	-2.8	-7.2	-3.2
166.8	-7.1	-3.1	-7.1	-3.4
167.0	-7.3	-3.6	-7.3	-4.0
167.2	-7.5	-3.2	-7.5	-3.5
167.4	-7.2	-3.2	-7.2	-3.5
167.6	-7.3	-3.3	-7.3	-3.7
167.8	-7.0	-2.9	-7.0	-3.3
168.0	-7.1	-3.1	-7.1	-3.4
168.2	-7.2	-3.0	-7.2	-3.4
168.4	-7.2	-3.1	-7.2	-3.4
168.6	-7.5	-3.2	-7.5	-3.6
168.8	-7.2	-3.0	-7.2	-3.4
169.0	-7.2	-2.9	-7.2	-3.2
169.2	-6.8	-2.8	-6.8	-3.1
169.4	-6.9	-2.6	-6.9	-2.9
169.6	-6.9	-2.8	-6.9	-3.2
169.8	-6.9	-2.8	-6.9	-3.2
170.0	-6.9	-2.6	-6.9	-2.9
170.2	-6.8	-2.8	-6.8	-3.1
170.4	-6.9	-3.2	-6.9	-3.5
170.6	-6.6	-2.9	-6.6	-3.2
170.8	-6.4	-2.6	-6.4	-2.9
171.0	-6.3	-2.8	-6.3	-3.2
171.2	-6.4	-2.6	-6.4	-3.0
171.4	-6.1	-2.4	-6.1	-2.8
171.6	-6.0	-2.6	-6.0	-2.9
171.8	-6.2	-2.7	-6.2	-3.0
172.0	-6.1	-2.5	-6.1	-2.8
172.2	-5.9	-2.6	-5.9	-2.9
172.4	-6.0	-2.8	-6.0	-3.2
172.6	-6.5	-2.9	-6.5	-3.2
172.8	-6.8	-2.8	-6.8	-3.1
173.0	-6.8	-2.6	-6.8	-2.9
173.2	-6.7	-3.3	-6.7	-3.7
173.4	-6.4	-2.6	-6.4	-2.9
173.6	-6.5	-2.7	-6.5	-3.1
173.8	-6.6	-2.4	-6.6	-2.8

DBT (mm)	$\delta^{13}C$ (‰ VPDB)	$\delta^{18}O$ (‰ VPDB)	$\delta^{13}C$ (‰ VPDB) Aragonite and Calcite Corr (*).	$\delta^{18}O$ (‰ VPDB) Aragonite and Calcite Corr (*).
174.0	-6.5	-2.6	-6.5	-3.0
174.2	-6.0	-2.5	-6.0	-2.8
174.4	-5.6	-2.5	-5.6	-2.9
174.6	-5.6	-2.5	-5.6	-2.8
174.8	-5.4	-2.1	-5.4	-2.4
175.0	-5.8	-1.9	-5.8	-2.2
175.2	-6.2	-2.3	-6.2	-2.6
175.4	-7.2	-2.7	-7.2	-3.1
175.6	-7.0	-2.6	-7.0	-2.9
175.8	-6.8	-2.6	-6.8	-2.9
176.0	-6.1	-2.4	-6.1	-2.7
176.2	-6.0	-2.4	-6.0	-2.7
176.4	-5.9	-3.0	-5.9	-3.3
176.6	-5.8	-2.4	-5.8	-2.7
176.8	-5.9	-2.4	-5.9	-2.7
177.0	-5.8	-2.2	-5.8	-2.5
177.2	-5.6	-2.5	-5.6	-2.9
177.4	-5.6	-2.5	-5.6	-2.8
177.6	-6.1	-2.5	-6.1	-2.9
177.8	-6.6	-2.7	-6.6	-3.1
178.0	-6.6	-2.5	-6.6	-2.9
178.2	-6.5	-3.0	-6.5	-3.3
178.4	-5.8	-2.7	-5.8	-3.0
178.6	-5.3	-2.4	-5.3	-2.8
178.8	-5.4	-2.5	-5.4	-2.8
179.0	-5.4	-2.7	-5.4	-3.0
179.2	-5.6	-2.8	-5.6	-3.1
179.4	-5.8	-2.8	-5.8	-3.1
179.6	-5.9	-3.0	-5.9	-3.3
179.8	-5.8	-2.9	-5.8	-3.2
180.0	-6.0	-2.9	-6.0	-3.2
180.2	-6.2	-3.2	-6.2	-3.5
180.4	-6.2	-3.0	-6.2	-3.3
180.6	-6.8	-2.9	-6.8	-3.2
180.8	-6.5	-2.8	-6.5	-3.2
181.0	-6.5	-3.0	-6.5	-3.3
181.2	-7.2	-2.9	-7.2	-3.3

DBT (mm)	$\delta^{13}C$ (‰ VPDB)	$\delta^{18}O$ (‰ VPDB)	$\delta^{13}C$ (‰ VPDB) Aragonite and Calcite Corr (*).	$\delta^{18}O$ (‰ VPDB) Aragonite and Calcite Corr (*).
181.4	-6.7	-2.8	-6.7	-3.2
181.6	-6.3	-3.3	-6.3	-3.6
181.8	-5.6	-2.2	-5.6	-2.5
182.0	-6.4	-2.9	-6.4	-3.2
182.2	-6.4	-3.0	-6.4	-3.4
182.4	-6.4	-2.6	-6.4	-3.0
182.6	-6.3	-2.7	-6.3	-3.1
182.8	-6.2	-2.7	-6.2	-3.1
183.0	-6.0	-2.5	-6.0	-2.8
183.2	-6.1	-2.3	-6.1	-2.7
183.4	-6.2	-2.4	-6.2	-2.8
183.6	-6.6	-2.7	-6.6	-3.0
183.8	-6.6	-2.7	-6.6	-3.0
184.0	-6.4	-2.6	-6.4	-2.9
184.2	-6.5	-3.0	-6.5	-3.4
184.4	-6.3	-2.5	-6.3	-2.8
184.6	-6.8	-3.0	-6.8	-3.4
184.8	-6.8	-2.9	-6.8	-3.2
185.0	-6.6	-2.8	-6.6	-3.1
185.2	-6.1	-2.5	-6.1	-2.8
185.4	-5.7	-2.2	-5.7	-2.6
185.6	-5.8	-2.8	-5.8	-3.1
185.8	-5.8	-2.7	-5.8	-3.0
186.0	-6.1	-2.7	-6.1	-3.1
186.2	-5.9	-2.9	-5.9	-3.2
186.4	-5.7	-2.5	-5.7	-2.8
186.6	-5.9	-2.6	-5.9	-3.0
186.8	-5.7	-2.6	-5.7	-2.9
187.0	-5.5	-2.4	-5.5	-2.8
187.2	-5.8	-2.6	-5.8	-3.0
187.4	-6.0	-2.5	-6.0	-2.9
187.6	-6.1	-2.7	-6.1	-3.1
187.8	-6.2	-2.9	-6.2	-3.2
188.0	-6.3	-2.8	-6.3	-3.1
188.2	-6.1	-3.1	-6.1	-3.5
188.4	-6.0	-2.6	-6.0	-2.9
188.6	-6.2	-2.8	-6.2	-3.1

DBT (mm)	$\delta^{13}C$ (‰ VPDB)	$\delta^{18}O$ (‰ VPDB)	$\delta^{13}C$ (‰ VPDB) Aragonite and Calcite Corr (*).	$\delta^{18}O$ (‰ VPDB) Aragonite and Calcite Corr (*).
188.8	-6.2	-3.0	-6.2	-3.3
189.0	-6.6	-3.1	-6.6	-3.4
189.2	-6.7	-3.1	-6.7	-3.4
189.4	-6.6	-3.0	-6.6	-3.3
189.6	-6.6	-3.2	-6.6	-3.5
189.8	-6.6	-3.1	-6.6	-3.4
190.0	-6.7	-3.4	-6.7	-3.7
190.2	-6.7	-3.1	-6.7	-3.5
190.4	-6.5	-3.0	-6.5	-3.4
190.6	-6.1	-3.1	-6.1	-3.4
190.8	-6.6	-3.5	-6.6	-3.8
191.0	-6.5	-3.4	-6.5	-3.8
191.2	-6.5	-3.2	-6.5	-3.5
191.4	-6.8	-3.8	-6.8	-4.1
191.6	-4.0	-3.8	-4.0	-4.1
191.8	-1.2	-3.7	-1.2	-4.1

APPENDIX 2

DBT with original and re-micromilled $\delta^{18}O$

and $\delta^{13}C$ data from DSSG-4

DBT (mm)	$\delta^{13}C$ (‰ VPDB) Original Pass	$\delta^{18}O$ (‰ VPDB) Original Pass	$\delta^{13}C$ (‰ VPDB) Re-micromilled	$\delta^{18}O$ (‰ VPDB) Re-micromilled
0.1	-8.2	-3.6	-8.2	-3.3
0.2	-8.0	-3.9	-7.7	-3.5
0.3	-7.8	-3.9	-7.6	-3.5
0.4	-7.4	-3.7	-7.3	-3.4
0.5	-7.9	-3.9	-8.1	-3.9
0.6	-8.7	-4.3	-8.4	-4.1
0.7	-8.7	-4.1	-8.2	-3.9
0.8	-8.6	-4.0	-8.2	-3.9
0.9	-9.0	-4.1	-8.4	-3.9
1.0	-9.2	-4.1	-8.9	-4.1
1.1	-9.1	-4.3	-8.9	-3.8
1.2	-9.2	-4.2	-9.0	-4.0
1.3	-9.1	-4.1	-8.8	-4.0
1.4	-8.6	-3.9	-8.3	-3.9
1.5	-8.3	-3.8	-7.9	-3.6
1.6	-8.5	-3.9	-7.6	-3.6
1.7	-7.9	-3.7	-7.7	-3.3
1.8	-8.0	-3.5	-7.7	-3.2
1.9	-8.0	-3.4	-7.2	-3.0
2.0	-7.6	-3.1	-6.6	-2.6
2.1	-6.9	-2.7	-6.9	-2.8
2.2	-7.1	-2.9	-7.2	-3.2
2.3	-7.7	-3.0	-7.0	-2.9
2.4	-7.3	-3.1	-7.7	-3.4
2.5	-6.8	-3.1	-7.4	-2.8
2.6	-7.4	-2.9	-6.3	-2.6
2.7	-7.0	-3.0	-6.2	-2.8
2.8	-6.6	-2.8	-6.2	-2.6
2.9	-6.5	-2.9	-5.9	-2.5
3.0	-6.5	-2.8	-5.5	-1.9
3.1	-6.4	-2.6	-6.3	-2.4
3.2	-6.2	-2.3	-5.8	-2.2
3.3	-6.3	-2.5	-6.6	-2.5
3.4	-6.4	-2.6	-5.8	-2.4
3.5	-6.7	-2.3	-6.4	-2.5
3.6	-6.2	-2.4	-6.8	-2.5
3.7	-6.5	-2.7	-6.7	-2.7

3.8	-6.8	-2.6	-7.4	-2.8
3.9	-7.3	-3.0	-8.0	-3.2
4.0	-7.7	-2.8	-8.6	-3.1
4.1	-8.8	-3.1	-8.9	-3.2
4.2	-9.5	-4.0	-9.4	-3.3
4.3	-9.3	-3.3	-9.6	-3.6
4.4	-9.6	-3.4	-9.8	-3.7
4.5	-9.9	-3.6	-10.3	-3.7